University of Alberta

Environmental and Performance Analysis of a 5kW Horizontal Axis Wind Turbine in East Central Alberta

by

Braden Rooke

A thesis submitted to the Faculty of Graduate Studies and Research in partial fulfillment of the requirements for the degree of

Master of Science

Mechanical Engineering

Abstract

This thesis investigates the environmental and performance results of a 5kW horizontal axis wind turbine installed in east-central Alberta. Life cycle assessment (LCA) methodology was utilized to perform a comparative environmental impact study on three sizes of small wind turbines installed in east-central Alberta for the production of 100kW of nameplate power. Field data collected over 17 months from tower mounted instruments were used to assess the performance of a grid connected 5kW wind turbine.

Comparative LCA findings revealed that although 5kW and 20kW options were a vast improvement over current Alberta grid performance, a 100kW turbine had the fastest environmental, energy, and financial payback period and the lowest impact per kilowatt-hour in terms of global warming, ozone depletion, and acidification emission factors.

In-situ power performance analysis demonstrated that the turbine performs at a high-level and the manufacturer's published power curve was accurate. Annual energy production (AEP) estimates made from the measured power curve were slightly low compared to manufacturer's published data. Tower-mounted instruments were found to be an excellent option for in-situ power performance analysis.

Acknowledgements

I would like to thank my graduate supervisor, Dr. Brian Fleck, for the opportunity to pursue my Master's of Science degree in wind energy studies. I would like to thank my co-supervisor Dr. Mel Tyree for the support and knowledge he provided in the assembly of the Halkirk data acquisition system.

I would like to express my gratitude to Steve and Patty McKnight for opening their home and property to me. Without their cooperation this project would not have been possible. Thanks to Derek Brown for his knowledge and assistance in completing the data collection.

Thanks to my lab mates for their camaraderie and listening ear: Mathew Bussiere, Miguel Balzan, Mohammad Mahmoudi, Kevin Breton, Graeme Comyn, and Johana Gonzalez. Md. Ruhul Kabir and Malinga Dassanayake – your hard work and friendship greatly improved my grad school experience. Many thanks to my friends and siblings who commiserated and cheered me on along the way - I am a lucky guy to have the support team I have.

Words cannot describe how thankful and lucky I am for my parents' continuous love and support in everything that I am involved in. Mom and Dad, your constant encouragement kept me pushing myself even when I did not think things would work out.

Lastly, to Jessie: your comfort and affection have been there for me through the trials and tribulations of school and life. Love always.

Table of Contents

1 Introduction 1

1.1 Background and Literature Review 5

1.1.1 Life cycle assessment of several small wind turbines 5

1.1.2 Wind resource assessment 9

1.1.2.1 Vertical Wind Shear 10

1.1.2.2 Turbulence 11

1.1.2.3 Acceleration 13

1.1.3 Methods of data analysis 14

1.1.4 In-situ wind turbine performance testing 15

1.2 Objectives 26

1.3 Format 26

1.4 References 28

2 Life Cycle Assessment 34

2.1 Introduction 34

2.2 Methodology 36

2.3 Goal definition 37

2.4 System boundary 37

2.4.1 Turbine production 39

2.4.2 Transportation and installation 39

2.4.3 Generate power 41

2.4.4 Turbine maintenance 41

2.4.5 Decommissioning, recycling and disposal 41

2.4.6 Environmental stressors 42

2.4.7 Functional unit 43

2.5 Inventory assessment 43

2.5.1 Material inventory data 43
2.5.2 Material embodied energy and emission 43
2.5.3 Transportation data 44
2.5.4 Assumptions and limitations 45
2.6 Energy and Environmental impact analysis 46
2.6.1 Energy impact 46
2.6.2 Environmental impact 47
2.7 Uncertainty analysis 49
2.8 Economic analysis 51
2.9 Conclusion 53
2.10 References 55
3 Wind Conditions Assessment and Turbine Performance Evaluation 60
3.1 Introduction 60
3.1.1 Research Approach 60
3.1.1.1 Research Questions 60
3.1.1.2 Experimental Set up 61
3.1.1.3 Deviation from IEC Standard Procedures 66
3.1.1.4 Data Collection and Processing 67
3.1.1.5 Site Description 71
3.2 Wind Conditions Assessment 76
3.2.1 Introduction and Methodology 76
3.2.2 Results and Discussion 77
3.2.2.1 Yearly Wind Behavior 77
3.2.2.2 Monthly Wind Behavior 84
3.2.2.3 Daily Wind Behavior 86
3.2.3 Summary and Conclusions 91
3.3 Power Curve Development and Turbine Performance 92

3.3.1 Introduction and Methodology 92
3.3.1.1 Data Normalizations 92
3.3.1.2 Power Curve 93
3.3.1.3 Productive Capacity 93
3.3.1.4 Power Coefficient Curves 94
3.3.1.5 Correlation Coefficient 96
3.3.1.6 Uncertainty 97
3.3.2 Results and Discussion 98
3.3.2.1 Monthly Turbine Production 98
3.3.2.2 Power Curve during Turbine Performance Campaign 100
3.3.2.3 Productive Capacity 104
3.3.2.4 Power Coefficient Curve 108
3.3.2.5 Site Turbulence Intensity during Turbine Performance Campaign 111
3.3.2.6 Comparison of undisturbed and disturbed sector power curves . 113
3.3.2.7 Temperature Performance 116
3.3.2.8 Time averaged sampling interval 123
3.3.3 Summary and Conclusions 126
3.4 Use of Vertical Extrapolation for Power Performance Testing 127
3.4.1 Introduction and Methodology 127
3.4.1.1 Uncertainty 127
3.4.2 Vertical Extrapolation Methods 128
3.5 Results and Discussion 129
3.6 Summary and Conclusions 140
4 Conclusion 142
4.1 Summary 142
4.2 Recommendations for Future Research and Development 144

4.3 References 146

Appendix A : Electrical Diagram of System A-1

Appendix B : Instrument Details B-1

Appendix C : Additional Uncertainty Considerations C-1

Appendix D : Cup Anemometer Calibration Sheets D-1

Appendix E : Power Transducer Calibration E-1

Appendix F : Drawings of turbine and instrument arrangement F-1

Appendix G : Wind velocity distributions of datasets G-1

Appendix H : Measured Power Curve Table H-1

Appendix I : Power Curves from Using Different Averaging Schemes I-1

Appendix J : Pictures of the Turbine Site with Direction and Disturbance Annotations J-1

List of Tables

Table 2-1: Inventory data for 100kWe nameplate wind power production facility.. 40
Table 2-2: Recycling and Waste Disposal (Martinez et al. 2009) 42
Table 2-3: Environmental Stressors and weighting factors (Intergovernmental Panel on Climate Change 2007; Stranddorf & Hoffmann 2003)..... 42
Table 2-4: Embodied energy and emission inventory data (Martinez et al. 2009; Schleisner 2000; GHK 2006; Rieradevall et al. 1997; ICF Consulting 2005; White 2007; Athena Institute 2006; Athena Institute 2002)..... 44
Table 2-5: Turbine transportation inventory data (Coleman & Lessard 2011) 45
Table 2-6: Transportation embodied energy and emission inventory data (Transport Canada n.d.; The Railway Association of Canada 2002; H. Mahmudi, P.C. Flynn 2005) 45
Table 2-7: Uncertainty determination matrix of inventory data 50
Table 2-8: Uncertainties for unit processes of all turbine configurations 50
Table 2-9: Input data and assumptions for economic analysis 52
Table 2-10: Findings from economic analysis 53
Table 3-1: Turbine Configuration and Operational Data 64
Table 3-2: Disturbed sectors from nearby obstacles 74
Table 3-3: IEC 61400-12-1 test site requirements - topographical variations..... 75
Table 3-4: 10m Wind Dataset Statistics 80
Table 3-5: Comparison of Mesoscale Statisitcs and Measured Data, Halkirk..... 82
Table 3-6: Estimated annual energy production..... 106
Table 3-7: AEP estimates using binned power curve from undisturbed and disturbed sectors 114
Table 3-8: Averaging case study for AEP estimation..... 124
Table 3-9: Tower-Mounted Anemometer Measurement Errors and Vertical Extrapolation Prediction Errors when compared with U_1 Data at 33.8m (Test Sector Data Only) 134
Table 3-10: Tower-Mounted Anemometer Measurement Errors and Vertical Extrapolation Prediction Errors when compared with Sonic Data at 31.5m (Test Sector Data Only) 134
Table 3-11: Directional Case Studies for Vertical Extrapolation – U_1 at 33.8m 134
Table 3-12: Directional Case Studies for Vertical Extrapolation - U_{son} at 31.5m 135

Table B-1: Field instrument details B-1
Table C-1: Uncertainty values used in analysis C-5
Table C-2: Expanded uncertainties (IEC 2005a) C-6
Table H-1: Measured power curve table (standardized to sea level air density, 1.225kg/m^3) H-1

List of Figures

Figure 1-1: Wind turbine highlighting major components 1
Figure 1-2: Models of wind development - adapted from (Gipe 2004)........ 3
Figure 1-3: Typical wind data measured at 1Hz at Halkirk, Alberta 13
Figure 1-4: A typical SWT power curve, highlighting important features (cut-out velocity not shown – located at 25m/s) 17
Figure 1-5: Power curve biasing (Burton et al. 2001) 19
Figure 1-6: Methods for estimating hub height wind velocity for small wind turbines 25
Figure 2-1: System boundary of the study 38
Figure 2-2: Breakdown of energy use by unit process for different configurations.. 47
Figure 2-3: Environmental impact from three configurations 48
Figure 2-4: Relative environmental impacts by unit process........ 49
Figure 2-5: Comparison of impacts from configurations' under 95% confidence range uncertainties 51
Figure 3-1: Endurance S-343 Cross-section (Endurance Wind Power 2011)........ 63
Figure 3-2: Instrument locations and accompanying variable definitions........ 63
Figure 3-3: Experimental setup with instrument and turbine heights 65
Figure 3-4: Overview of Data Acquisition System........ 68
Figure 3-5: Turbine and wind direction instrument availability........ 69
Figure 3-6: Turbine Location Overview with 50m Scale (Google Maps 2011)........ 71
Figure 3-7: Overview with approximate distances to local obstacles and measurement sector (Google Maps 2011) 73
Figure 3-8: Site overview displaying disturbed and undisturbed direction sectors (Google Maps 2011) 74
Figure 3-9: Yearly turbine site air density 78
Figure 3-10: Year turbine site air temperature........ 78
Figure 3-11: Synthesized Halkirk 10m (a) and Stettler Airport 10m (b) Frequency Distributions........ 79
Figure 3-12: (a) Halkirk hourly averaged wind rose, synthesized 10 m wind velocity, (b) Stettler Airport hourly averaged wind rose, 10 m wind velocity........ 81
Figure 3-13: Comparison of frequency distributions and Weibull statistics, Canada Wind Energy Atlas and Halkirk ten-minute averaged data........ 83

Figure 3-14: Halkirk turbine site (a) Monthly wind velocity at 10m; (b) Monthly air density; (c) Monthly air temperature ... 85
Figure 3-15: Halkirk turbine site (a) Hourly wind velocities at various heights; (b) Hourly air temperature; (c) Hourly air density ... 87
Figure 3-16: Seasonal diurnal variation in (a) turbulence intensity and (b) wind shear ... 88
Figure 3-17: Hourly variation in shear factors between anemometer heights ... 89
Figure 3-18: U_2 to U_3 shear factors, binned for direction and hour ... 90
Figure 3-19: Non-dimensional power curves for constant velocity turbine operation - from (Burton et al. 2001) ... 95
Figure 3-20: Monthly energy production and system availability at Halkirk over 17months ... 98
Figure 3-21: Monthly power variation ... 99
Figure 3-22: Scatter plot of mean, standard deviation, minimum and maximum power data. 1 Hz samples with 1 minute averaging ... 100
Figure 3-23: Measured power curve, raw and binned data at sea level density, showing manufacturer power data. Open circles represent bins with insufficient data ... 101
Figure 3-24: Sea level normalized power curve with 95% uncertainty bars along with manufacturer power curve. Uncertainty determined from IEC 61400-12-1 recommendations ... 103
Figure 3-25: Estimated Annual Energy Production, Manufacturer and Measured. 104
Figure 3-26: Estimated Annual Energy Production, Measured and Estimated from Manufacturer Power Curve ... 105
Figure 3-27: Coefficient of performance, raw and binned data at sea level density versus hub height wind velocity, showing Betz limit. Open circle represents insufficient data. ... 108
Figure 3-28: Coefficient of performance versus tip velocity ratio ... 108
Figure 3-29: Coefficient of performance with error bars indicating a 68.27% confidence interval created from Category A and B uncertainty ... 109
Figure 3-30: Non-dimensional stall regulated and typical performance curves ... 110
Figure 3-31: Wind turbulence intensity as a function of wind velocity ... 111

Figure 3-32: Extrapolated hub height wind velocity and estimated turbulence intensity 112
Figure 3-33: One-minute averaged measured power curve, undisturbed and disturbed raw data, binned by. Open circles denote bins with less than 10 minutes of data. 113
Figure 3-34: Data binned from direction and temperature (a) Energy production binned by temperature (b) Estimated average hub height wind velocity (c) Average power output 117
Figure 3-35: Turbulence intensity versus temperature during turbine performance study 119
Figure 3-36: Data binned by temperature (a) Energy production binned by temperature (b) Estimated average hub height wind velocity (c) Average power output 121
Figure 3-37: Turbulence intensity binned by temperature over the 11 month turbine non-direction study 122
Figure 3-38: U_1 mean estimation error resulting from tower mounted anemometers and different vertical extrapolation methods. The vertical dashed line indicates the instrument boom direction. 131
Figure 3-39: U_1 mean absolute estimation error resulting from tower mounted anemometers and different vertical extrapolation methods 131
Figure 3-40: Sonic horizontal component mean estimation error resulting from tower mounted anemometers and different vertical extrapolation methods 132
Figure 3-41: Sonic horizontal component mean absolute error resulting from tower mounted anemometers and different vertical extrapolation methods 132
Figure 3-42: U_1 mean wind velocity prediction error, binned by U_1 wind velocity 136
Figure 3-43: Sonic mean wind velocity prediction error, binned by sonic wind velocity 136
Figure 3-44: U_1 mean wind velocity prediction error, binned by sonic elevation angle 138
Figure 3-45: U_1 Mean absolute wind velocity prediction error, binned by sonic elevation angle 138
Figure 3-46: 2-D sonic mean wind velocity prediction error, binned by sonic elevation angle 139

Figure 3-47: 2-D sonic mean wind velocity prediction error, binned by sonic elevation angle 139
Figure 4-1: Sea level normalized power curve with 68.27% uncertainty bars along with manufacturer power curve. Uncertainty determined from IEC 61400-12-1 recommendations H-2
Figure A-1: Detailed Electrical Diagram of Enclosure Data Acquisition System A-1
Figure A-2: Detailed Electrical Diagram of Enclosure Door and Bottom A-2
Figure D-1: Anemometer wind velocities plotted against reference pitot tube wind velocities during wind tunnel verification of calibration curves, 4-6 July 2011 .... D-2
Figure D-2: Results of linear regression to sonic anemometer measurements obtained in wind tunnel with correction factor applied D-3
Figure E-1: Power transducer plotted against reference power during verification of power calibration curve, 12 July 2011 .... E-2
Figure F-1: (a) Instrument heights (b) Hub height to instrument distances (c) Rotor detail (d) Cup anemometer and boom (e) Sonic Anemometer and boom F-5
Figure G-1: Wind velocity frequency distribution, Halkirk U_1 (33.8m) G-1
Figure G-2: Wind velocity frequency distribution, Halkirk U_2 (27.4m) G-1
Figure G-3: Wind velocity frequency distribution, Halkirk U_3 (20.8m) G-2
Figure G-4: Wind velocity frequency distribution, Halkirk 2-D sonic (31.5m) G-2
Figure G-5: Wind velocity frequency distribution, Halkirk U_{hub} (38.7m) estimated from U_2 and U_3 values and power law in each time step G-3
Figure G-6: Frequency distributions, Canada Wind Atlas and Halkirk Synthesized 30m data, winter season (December/January/February) G-4
Figure G-7: Frequency distributions, Canada Wind Atlas and Halkirk Synthesized 30m data, spring season (March/April/May) G-4
Figure G-8: Frequency distributions, Canada Wind Atlas and Halkirk Synthesized 30m data, summer season (June/July/August) G-5
Figure G-9: Frequency distributions, Canada Wind Atlas and Halkirk Synthesized 30m data, fall season (September/October/November) G-5
Figure I-1: Ten-second averaged test sector power curve, raw and binned data at sea level density, showing manufacturer power data. Open circles represent bins with less than 10 minutes of data I-1

Figure I-2: One-minute averaged test sector power curve, raw and binned data at sea level density, showing manufacturer power data. Open circles represent bins with insufficient data. I-1
Figure I-3: Ten-minute averaged test sector power curve, raw and binned data at sea level density, showing manufacturer power data. Open circles represent bins with insufficient data. I-2
Figure I-4: Hourly averaged test sector power curve, raw and binned data at sea level density, showing manufacturer power data. Open circles represent bins with insufficient data. I-2
Figure J-1: Winter View to the South J-1
Figure J-2: Summer View to the South J-1
Figure J-3: Winter View to the West J-2
Figure J-4: : Summer View to the West J-2
Figure J-5: Winter View to the North J-3
Figure J-6: Summer View to the North J-3
Figure J-7: Winter View to the East J-4
Figure J-8: Summer View to the East J-4

Nomenclature

Variables

α	Wind shear factor
β_o	Slope of a line
β_1	Intercept of a line
κ	von Karman's constant
λ	Tip velocity ratio
μ	Uncertainty
ρ	Air density (kg m^{-3})
ρ_{avg}	Air density averaged for time step (kg m^{-3})
ρ_o	Reference air density (kg m^{-3})
σ	Standard deviation of wind velocity over averaging period (m s^{-2})
σ_x	Sample standard deviation of *x*
σ_y	Sample standard deviation of *y*
$\sigma_{P,i}$	Standard deviation of normalized power in bin *i* (W)
Ω	Rotational velocity of the rotor (radians s^{-1})
A_d	Swept area of the rotor (m^2)
C_p	Coefficient of performance
c	Scale factor of Weibull distribution
$c_{B,i}$	Sensitivity factor for pressure measurement in bin *i*
c_M	Hub height wind velocity measurement sensitivity factor
$c_{T,i}$	Sensitivity factor for temperature measurement in bin *i*
$c_{V,i}$	Sensitivity factor for wind velocity measurement in bin *i*
$C(U)$	Cumulative probability
D_e	Equivalent rotor diameter (m)
D_{rotor}	Rotor diameter (m)
E_i	Error associated with each point *i*
E_{net}	Net energy input to a unit process (j)
E_{out}	Total energy output from a unit process (j)
E_{net}	Total non-renewable primary energy input to a unit process (j)
$F(U)$	Rayleigh cumulative probability density function

f_{i}	Average probability of wind velocity in bin *i*
g	Acceleration due to gravity (9.807 m s-2),
h	Hub height (m)
h_0	Reference height (m)
h_1	Top cup anemometer height, 33.8m
h_2	Middle cup anemometer height, 27.5m
h_3	Bottom cup anemometer height, 20.8m
h_{son}	Sonic anemometer height, 31.5m
I	Measured current (amperes)
k	Shape factor of Weibull distribution
kJ	Kilojoules
K_p	Stall regulated coefficient of performance
kwh	Kilowatt-hour
L	Litres
L_e	Distance from site obstacle to base of turbine tower (m)
l_h	Site object height (m)
l_w	Site object width (m)
N	Number of averaged data sets in bin *i*
N_h	Number of hours in a year (8760)
n	Number of samples
n_{amp}	Number of ampere turns through current transformer window
P_{avg}	Measured power averaged for the time step (W)
$P_{calculated}$	Calculated power from voltage and current measurements (W)
P_i	Normalized and averaged power output in bin *i* (W)
$P_{n,i,j}$	Normalized power output of dataset *j* in bin *i* (W)
P_n	Normalized power output (W)
$p(U)$	Probability density function
p_{avg}	Measured air pressure average for time step (Pa)
p_b	Measured pressure (Pa)
p_{hub}	Pressure corrected to hub height (Pa)
R	Ideal gas constant of dry air (287.05 J $kg^{-1}K^{-1}$)
R_{tip}	Blade tip radius (m)

r	Linear correlation coefficient
$s_{P,i}$	Category A uncertainty of power in bin i (W)
S_{xx}	Variance of the independent variable x
S_{xy}	Covariance between the variables x and y
S_{yy}	Variance of the dependent variable y
T_{avg}	Measured absolute air temperature averaged for the time step (K)
U	Wind velocity (m s^{-1})
$\overline{U}$	Short term mean of component U (m s^{-1})
U_*	Friction velocity (m s^{-1})
U_∞	Free stream velocity at turbine hub height (m s^{-1})
U_0	Wind velocity at reference height (m s^{-1})
U_1	Wind velocity from top tower cup anemometer, 33.8m (m s^{-1})
U_2	Wind velocity from middle tower cup anemometer, 27.5m (m s^{-1})
$\overline{U}_2$	Mean wind velocity from middle tower cup anemometer, 27.5 (m s^{-1})
U_3	Wind velocity from bottom tower cup anemometer, 20.8m (m s^{-1})
$\overline{U}_3$	Mean wind velocity from middle tower cup anemometer, 20.5 (m s^{-1})
U_{ave}	Annual averaged wind velocity (m s^{-1})
U_{hub}	Hub wind velocity (m s^{-1})
$\overline{U}_{hub}$	Predicted mean wind velocity (m s^{-1})
$U_{est,i}$	Wind velocity estimate of data point i (m s^{-1})
$\overline{U}_i$	Mean wind velocity during averaging period (m s^{-1})
$U_{n,i,j}$	Normalized wind velocity of data set j in bin i (m s^{-1})
U_{ref}	Measured wind velocity at reference height z_{ref} (m s^{-1})
U_{son}	Sonic anemometer 2-D wind velocity (m s^{-1})
$U_{true,i}$	Wind velocity measurement of estimate i (m s^{-1})
u	Fluctuating component of U (m s^{-1})
u_{AEP}	Combined standard uncertainty of AEP calculation (kwh)
$u_{c,i}$	Combined standard uncertainty of power corresponding with each WS bin (W)
$u_{C_p,c,i}$	Combined standard uncertainty of C_p corresponding with each WS bin
u_{hub}	Wind velocity hub height wind velocity uncertainty (m s^{-1})
u_i	Category B wind velocity uncertainty values (m s^{-1})
$u_{DA,i}$	Wind velocity data acquisition uncertainty for bin i (m s^{-1})

u_M	Wind velocity measurement uncertainty (m s^{-1})
$u_{ME,i}$	Wind velocity mounting effect uncertainty for bin *i* (m s^{-1})
$u_{P,i}$	Category B measured power uncertainty for bin *i* (W)
$u_{TE,i}$	Wind velocity terrain effect uncertainty for bin *i* (m s^{-1})
$u_{WS,i}$	Wind velocity instrument uncertainty for bin *i* (m s^{-1})
V	Measured voltage (Volts)
W	Watt
$\overline{\overline{x}}$	Mean value of variable *x*
$\overline{\overline{y}}$	Mean value of variable *y*
z	Height of wind velocity *U* (m)
z_o	Surface roughness of the surrounding terrain (m)
z_{ref}	Height of reference wind velocity U_{ref} (m)

Abbreviations

AEP	Annual Energy Production
AESO	Alberta Electric Systems Operator
AWEA	American Wind Energy Association
CanWEA	Canadian Wind Energy Association
CN	Canadian National Railway
CO_{2eq}	Carbon dioxide equivalent emissions
DOE	Department of Energy
EC	Environment Canada
EN	Endurance (5kW rated)
FU	Functional unit
GHG	Greenhouse gas
HAWT	Horizontal Axis Wind Turbine
HDV	Heavy duty vehicle
Hz	Hertz (s^{-1})
IEC	International Electrotechnical Commission
ISO	International Organization for Standardization
JA	Jacobs (20kW rated)
LLAC	Low-level alternating current
LCA	Life cycle assessment
LIDAR	Light Detection and Ranging
LDV	Light duty vehicle

MAE	Mean average error
MC	Monte Carlo analysis
ME	Mean error
NIST	National Institute of Standards and Technology
NREL	National Renewable Energy Lab
NO_x	Mono nitrogen oxides
NWTC	National Wind Technolgy Center
NP	Northern Power (100kW rated)
RPM	Revolutions per minute of rotor
RSS	Root-sum-square
SO_{2eq}	SO_2 equivalent emissions
SODAR	Sound Detection and Ranging
SWCC	Small Wind Certification Council
SWT	Small wind turbine
TI	Turbulence intensity
Tkm	Tonne-kilometre
TSR	Tip velocity ratio
TTL	Transistor-transistor logic
VOC	Volatile organic compound
WPD	Wind power density

1 Introduction

Wind energy conversion systems come in many designs and sizes and are used for a variety of purposes. The primary purpose of a modern wind turbine machine is to convert the kinetic energy of the wind into electricity (Wood 2011). The most prevalent modern wind turbine design is the horizontal axis wind turbine (HAWT), comprised of a two or three bladed rotor mounted on an axis parallel with the ground and oriented into the wind using some type of yaw system such as a tail. The rotor extracts energy from the wind by transferring the wind's kinetic energy to mechanical energy, which is then converted to electrical energy. This conversion of mechanical energy to electrical energy occurs within the nacelle, which is oriented either downwind or upwind of the rotor and is connected to the blades with a hub. The nacelle houses the drive train, comprised of rotating parts, which transfers the mechanical energy to the electrical system. Also housed within the nacelle, the electrical system in the form of a synchronous or induction generator completes the conversion of kinetic energy to electrical energy. This electrical energy is then fed into the grid or a form of energy storage (J. F. Manwell et al. 2010).

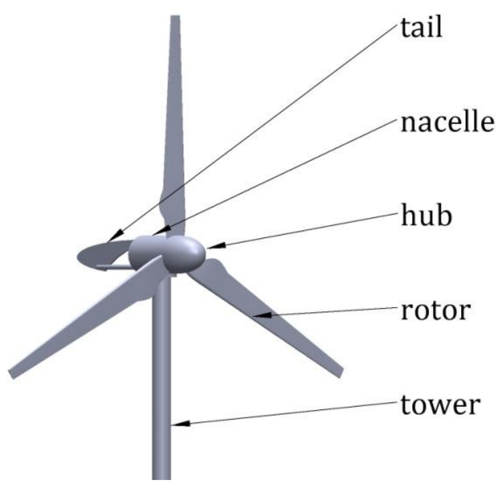

Figure 1-1: Wind turbine highlighting major components

Among renewable energy technologies, wind power is experiencing the most rapid growth worldwide (Global Wind Energy Council 2010). This being said, in modern society electricity generation is still a substantial source of greenhouse gas (GHG) emissions, with renewable energy still only accounting for 20% of world electricity generation (Sawin & Martinot 2010). Continuing industrial development and population growth in developed and undeveloped nations has increased global electricity demands beyond those ever seen in history. The majority of electricity is generated using fossil fuels, therefore meaning GHG emissions will continue to increase in the future unless alternatives that are less emissions intensive are used to satisfy electricity demand and replace older generation technologies. As renewable energy sources such as wind energy have inherent environmental advantages as well as economic competitiveness in recent years, they are gaining more attraction as an alternative to fossil fuels (Martinez et al. 2009; Krohn et al. 2009).

With the exception of the global economic slowdown of 2010, newly installed global wind generating capacity increased with each year in the last decade and is expected to grow even faster in future (Global Wind Energy Council 2010). Wind energy has grown almost ten-fold in the last six years in Canada to an installed generating capacity of 4611 MW as governments and individuals looked to meet energy needs, stimulate rural and industrial economic development, and reduce the environmental impact of electricity generation (CanWEA 2011). In 2010, Canada joined the top 10 nations globally in new installed capacity and overall cumulative installed capacity. Alberta ranks second in Canada in 2010 for installed wind generation capacity with 803 MW of installed wind generation facilities, behind Ontario with 1656MW of wind facilities. A large number of proposed wind projects in South and Central Alberta are waiting for approval, with over 4000 MW waiting in the Alberta Electric Systems Operator (AESO) grid connection queue (Alberta Electric System Operator 2010).

A large majority of the recent wind energy growth discussed so far is due to utility-scale wind farms. These wind farms are comprised of turbines rated from 100kW to several megawatts which are built together and connected to the transmission system of the power grid. These turbines are owned and operated by electric utility companies, but can often be owned by members of a community cooperative. Community wind cooperatives, comprised of homeowners, farmers, and small businesses, originated in Northern Europe and is how wind energy developed and expanded in Europe in the 1980's (Gipe 2004). This type of wind development differs from the massive utility-scale wind farms which originated in North America and in comparison is more of a distributed approach to wind energy. Distributed generation refers to the concept where generation is located throughout the electricity grid. This type of generation has the advantages of developing cleaner sources of energy, increasing power security in terms of electric grid decentralization, and improving of weaker electric grids (Wood 2010). Distributed applications of wind energy include smaller clusters of utility scale wind turbines, smaller community or privately owned wind turbines connected to the distribution system of the electric grid, or small off-the-grid or remote wind turbines. Distributed wind is a method for homes, farms, businesses, and public facilities such as schools to off-set all or part of on-site energy consumption.

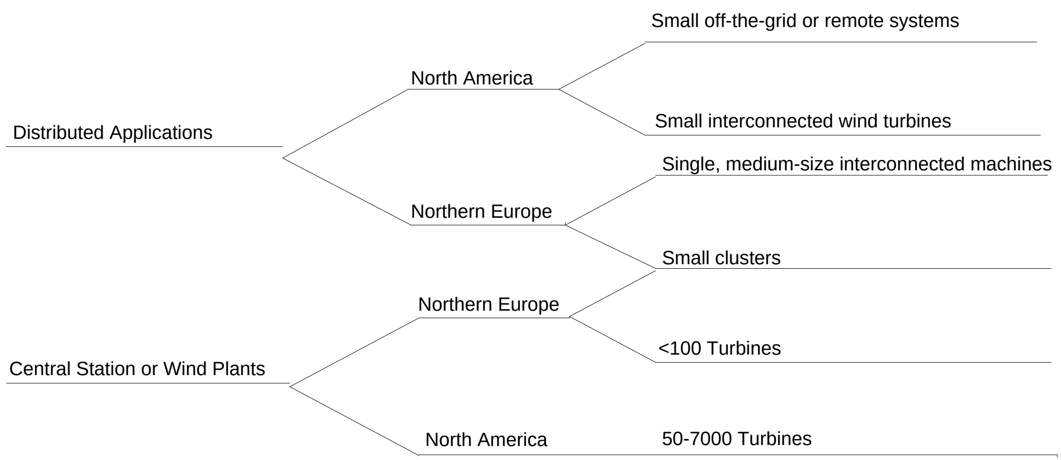

Figure 1-2: Models of wind development - adapted from (Gipe 2004)

When discussing the numbers of wind turbine installations, smaller distributed wind turbines are the most numerous and have experienced rapid growth similar to utility-scale wind turbines on a national and global scale in the past decade. According to a market survey conducted on behalf of the Canadian Wind Energy Association (CanWEA), Canada's domestic sales of small wind turbines (defined as 300kW and less) grew 77% in 2008 and 32% in 2009 (CanWEA 2010). National sales grew from $10 million to $14 million USD. Similarly, the global small wind turbine market grew 110% in 2008 and 40% in 2009 and sales grew from $188 million to $244 million USD. Although growth slowed during the economic slowdown of 2010, the market continued to expand and the number of small wind turbine installations nationwide grew to almost 11,000, with a cumulative installed capacity of 12.6MW. Putting the number of turbines in perspective, Canada's number of utility scale wind turbines stands at 2570 wind turbines operating on 131 wind farms with a cumulative installed capacity of 4285 MW (CanWEA 2011).

The small wind industry has a great opportunity to make positive change in assisting the global population in satisfying its growing energy demands in a more sustainable fashion. Unfortunately, even with this potential and the substantial growth of the small wind market in recent years, the performance of many turbines on the market has not been tested in a clear, concise, and organized manner. In fact, underperformance of turbines compared to predicted values has been well documented (The Cadmus Group 2008). Individuals interested in purchasing small wind turbines have many options but often lack detailed turbine information such as the environmental benefits or a well outlined predicted power output, necessary to select a quality turbine. Only by properly testing and certifying wind turbines with a certain well-defined standard will consumer confidence increase and develop the industry to be more 'mainstream' (Small Wind Certification Working Group 2007).

This thesis is part of an effort toward small wind turbine research in the Mechanical Engineering Department at the University of Alberta. Although south-western Alberta is better known for its strong winds and large wind farm developments, areas of central and eastern Alberta are also attractive wind regions with consistent winds, low population density, and limited geographic features which make small wind power a very appealing investment. Almost all acreages and agricultural operations located in these areas have an existing grid connection which is the first step to producing energy to offset their energy use. Obvious differences between rural and urban settings translate to higher energy use in rural homes. These differences include a lack of rural public infrastructure such as water supply and sewage management, as well as increased exposure to weather. In addition, agricultural operations are energy intensive, especially in cold climates such as the Canadian Prairies where large amounts of energy are used to heat both additional buildings and water for livestock. According to data from the Energy Resources Conservation Board (Government of Alberta 2010), there are 81247 customers identified as 'farms' in Alberta, consuming 1708GWh of energy, which is almost 3 times more consumption per capita than the average Alberta residence. Large areas of Alberta are flat, sunny, and windy with a large number of grid-connected agricultural operations located in good wind generation areas. This represents an excellent opportunity to allow the residents of these homes and operations to develop a renewable resource to offset the necessary energy to inhabit these areas.

To properly assess the environmental benefits of small wind energy for interested individuals, the energy use and expected production of small wind turbines must be properly analyzed. The most widely accepted manner to perform an environmental feasibility report is the method of life cycle assessment (ISO 2006a). An excellent way of educating the public and displaying the benefits of small wind energy is to monitor the performance of a turbine in-situ. The current accepted method to perform a turbine performance analysis will be discussed and utilized. Evaluating the feasibility of these techniques and adapting this method to analyze turbine performance in-situ will be presented here.

1.1 Background and Literature Review

The following section will introduce literature applicable to the scope of the project. This discussion will serve as the foundation that will guide the experimental principles contained within this thesis, as well as assist in creating conclusions from the resulting analysis.

1.1.1 Life cycle assessment of several small wind turbines

As populations look to progress forward in an increasingly carbon-constrained world, technologies with smaller environmental impact will continue to expand. Small wind turbines are one technology that will be employed in the future to replace current greenhouse gas intensive technologies. Evaluation of the cradle-to-grave environmental, energy and economic impacts of these generation technologies is necessary in order to justify adoption and long term reliance on them for clean energy (Martinez et al. 2009).

The environmental benefits of utility-scale wind turbines, both individually and in wind farm configuration, are widely available (Schleisner 2000; White 2007; Ardente et al. 2008). Cradle-to-grave environmental and energy impacts of these components are typically performed using some variation of the life cycle assessment approach. Life cycle assessment is a methodology which quantifies the environmental net effect of a physical system. The procedures of process-analysis-based life cycle assessment (LCA) are part of the ISO 14000 environmental management standards and are contained within two documents (ISO 2006a; ISO 2006b). ISO 14040 presents the framework on which life cycle assessment is conducted, and ISO 14044 discusses the requirements of a thorough LCA.

The standard ISO 14044 discusses in detail the four segments to an LCA study. This includes the goal and scope definition phase, the inventory analysis phase, the impact assessment phase, and the interpretation phase. The scope details the system boundary and level of detail of the study, which is typically directed by the study goal. The life cycle inventory analysis phase (LCI phase) is the step in which all input and output data are compiled with regard to the system being investigated. The life cycle impact assessment phase (LCIA phase) is the stage where the data from the product system is analyzed for environmental significance. The life cycle interpretation phase is the final step where the results of the LCI and LCIA phases are summarized and a series of conclusions are created for recommendations regarding the goal and scope definition.

The scope of the study should clearly define the function of the system. This assists in determining the functional unit, which is the method in which the input and output data are mathematically normalized. The functional unit allows systems within the study to be compared on a fair basis. Keeping in mind various assumptions, the functional unit also creates a method of measurement that can be compared between various studies. Each study must be defined with a process flow diagram, which visually describes the relationship between the functional unit and the system. In this method, the system is comprised of various unit processes, which have a beginning defined by raw material or an intermediate product input, some type of transformation or process, and an ending defined by the output of the products to the next unit process.

Cut-off criteria are used in LCA studies to define what should be included in the assessment. In many cases, mass contribution compared to other inputs in terms of an overall percentage is a deciding factor on omission from the study. Other criteria include energy and environmental significance. After mass contribution, energy inputs are used to determine if an input is included in a system. Special attention is paid to the environmental significance of an input, as some material with smaller mass and energy significance may be more emission intensive.

In LCA studies, input data is typically raw materials and output data is typically environmental emissions. Parameters include emissions to land, air or water, but in special cases data representing land use, odor, noise, vibration, and waste heat can be important factors to analyze. In all cases, quality of data is analyzed on a number of requirements. A variety of requirements are stated in ISO 14044; certain ones to highlight include obtaining data from the same time frame, geographical area, and level of technology. Data characteristics are addressed in terms of typical requirements such as precision, completeness, consistency, and uncertainty.

In the case of a wind turbine, the scope of the system can include but is not limited to: manufacturing, transportation, installation, operation, maintenance, and end of life disposal. When comparing the environmental impact of different wind turbine systems, it is important to utilize a common scope, as noted in previous reports (Lenzen 2002). According to this report, main factors causing the most variation between assessment studies include wind turbine size, operation lifetimes, embedded energy calculations, and treatment of systems at the end of their lifespan. The importance of consistent treatment of operation lifetime as well as end-of-life recycling and disposal of wind turbine systems is apparent from the results of this study. An economy of scale relationship between wind turbine size and environmental impact makes sense from other studies (Tremeac & Meunier 2009), but the magnitude of this relationship between different small wind energy systems is one of interest.

A study focused on the global market of small wind turbines was performed in 2009 by the American Wind Energy Association (AWEA 2009a). Within this market study, the growth of different small wind turbine applications within the global market was discussed. A recent trend in the market presented was a shift to larger, grid-tied systems. The market for off-grid turbines used for battery-charging and non-grid connected functions has recently leveled off, and more growth occurring in the residential and commercial/light industrial market segments. Life cycle assessments which compare the impacts of off-grid small wind energy battery charging applications to diesel generation are available (B. Fleck & Huot 2009) and serve as an excellent guide for further analyses. This being said, the AWEA market study shows the increasing importance of comparative studies for grid-connected small wind turbines as this market continues to develop and grow into the future.

Economic studies of utility scale wind energy facilities are also available (M. I. Blanco 2009), with some studies being applied in the context of provincial generation technology scenarios extrapolated into the future (Bell & Weis 2009). No matter what size of wind generation facility, economic feasibility is a very important aspect to justifying their introduction. Economic feasibility studies are key in determining the amount of incentives, financing, and other economic means necessary to create a competitive marketplace and encourage adoption of the technology by consumers. Studies into these different economic means of financing distributed generation are available (Walker 2001). It is often difficult to describe the economic feasibility of a developing technology such as small wind energy because the feasibility is constantly changing depending on factors such as current electricity price, government incentives, turbine material and transportation costs (B. Fleck & Huot 2009). In this sense, the assumptions contained within an economic assessment have to be carefully studied to ensure that they are applicable to current market conditions.

Although life cycle assessment is the global standard for conducting environmental impact assessments, several shortcomings to the technique can impact the results of any LCA study. The process-based approach utilizes very specific analyses, such that it is possible for the data to be very large, making the LCA time-consuming (Committee on Environmental Impacts of Wind Energy Projects & NRC 2007). In addition, the boundary and scope of the analysis is often complicated, making comparison between studies complex. Uncertainties in available data and methods have a large impact on the results of the study. Therefore it is highly important to assess the source quality of data when including it in any LCA and classify each input using quality indicators, which are then used to determine an uncertainty in the results (M. a J. Huijbregts et al. 2001). An additional concern is that process-based life cycle assessments do not commonly consider other real impacts such as land usage or animal impact. In order to conduct a thorough LCA, these concerns have to be addressed in order to draw well thought out conclusions.

1.1.2 Wind resource assessment

The energy in the wind changes as the cube of the wind velocity, meaning the first step to using the wind for generation of electricity in an economical and efficient manner is to know if there is enough wind (Burton et al. 2001). The relationship between power output of a wind turbine and the wind velocity is given as follows in Equation (1.1):

$$P = \tfrac{1}{2} C_p \rho A_d U_\infty^{\ 3} \tag{1.1}$$

where P is electric power (W), ρ is the air density (kg/m^3), C_p is the turbine power coefficient (unitless), A_d is the swept area of the rotor (m^2), and U_∞ is the free stream wind velocity at turbine hub height (m/s).

Other relationships that should be kept in mind from this equation are that wind power is directly proportional to the density of air and proportional to the square of the diameter of the rotor. Turbine power coefficient, C_p, will be discussed in detail in Section 1.1.4 as well as a developed discussion on the relationship between turbine power output and wind velocity.

As can be seen from Equation (1.1), knowledge of the wind resource is very important for turbine performance – for example, a 10% increase in wind equates to an increase of 33.1% in available power. Wind resource assessment is, by definition, a systematic quantification of the available wind resource based on field measurements. A wind resource assessment typically contains three main stages: preliminary area identification, area wind resource evaluation, and micrositing (B. Bailey et al. 1997). Preliminary wind resource assessment is used to screen possible areas of interest for wind development using local airport data, basic topography, and environmental indicators such as flagged trees. Area wind resource evaluation is the next step in wind resource assessment and characterizes the wind resource in a defined area. This data can be used to verify wind resources from preliminary assessments, justify pursuing micrositing, screen turbine installation sites, and compare areas for development potential. Micrositing is the most advanced stage of wind resource assessment and is used to characterize the small-scale variability of the wind resource over a particular terrain. This step can be used to maximize the output of one or more wind turbines at a particular location.

The American Wind Energy Association (AWEA) identified the need for more small wind resource assessments as one of the key opportunities in increasing the global market potential of small wind energy (AWEA 2009a). Developing small wind resource assessments includes building tools accessible to customers and educating individuals interested in utilizing small wind energy. Easily accessible and thorough small wind resource assessments will reduce project investment risk and increase confidence in the small wind industry by having well sited turbines performing at efficiencies consistent with manufacturer expectations or claims.

Small wind turbine site selection using this method is complicated by three factors: vertical wind shear, turbulence, and acceleration (E. H. Lysen 1983). For these reasons, it is important to carefully identify and study an area's wind resource so that the highest wind velocity in the area is selected.

1.1.2.1 Vertical Wind Shear

Vertical wind shear is the variation of wind velocity with respect to elevation (J. F. Manwell et al. 2010). Close to the earth's surface, variation of wind velocity depends on surface roughness and terrain. A rough surface such as trees and buildings will have more drag than a smooth surface such as a lake, causing reduced wind velocity near the surface. Under neutral stability conditions, wind velocity varies with height following a power or logarithmic law. The power law is defined as:

$$\frac{U}{U_{ref}} = \left(\frac{z}{z_{ref}} \right)^{\alpha} \qquad (1.2)$$

where U is the calculated wind velocity at height z, U_{ref} is the measured wind velocity at reference height z_{ref} and α is the power law exponent relating height and wind velocity. The power law exponent is a highly variable quantity and varies with elevation, time of day, season, nature of the terrain, wind velocity, temperature, and various thermal and mechanical mixing parameters (J. F. Manwell et al. 2010). If the wind is being measured at a single height, the power law exponent can be estimated using tables that relate α to the characteristic roughness length of the surrounding terrain (Elkinton et al. 2006). If no terrain value is available, the power law exponent is sometimes assumed to be 1/7, according to the '1/7th power law' (Gipe 2004; Farrugia 2003). The power law exponent can be derived by experimentally fitting a power law profile to measurements at multiple elevations (Lubitz 2009). This is done by solving for the power law exponent in Equation (1.2), resulting in:

$$\alpha = \frac{\ln(\frac{U}{U_{ref}})}{\ln(\frac{z}{z_{ref}})} \tag{1.3}$$

The logarithmic law is an analytically derived relationship between wind velocity and elevation and is described in Equation (1.4):

$$U = \frac{U_*}{\kappa} \ln\left(\frac{z}{z_o}\right) \tag{1.4}$$

where U_* is the friction velocity, a variable related to the shear stress close to the ground, κ is von Karman's constant, and z_o is the surface roughness of the surrounding terrain. Like the power law exponent, values of friction velocity and surface roughness are found in literature for different types of terrain. Also similar to the power law exponent, these values are highly variable, but assumptions can be avoided by fitting the profile using measurements at multiple heights. Further discussion on this topic will occur in Section 1.1.4.

1.1.2.2 Turbulence

The wind is highly variable in velocity and direction. This complex variability is described in the phenomenon of turbulence. Characterization of turbulence at a site is important as high levels of turbulence decrease harnessable power and cause unequal loading on wind turbines which can weaken and damage it. Wind turbulence is the dissolution of the wind's kinetic energy into thermal energy by the production and destruction of gradually smaller eddies or gusts (J. F. Manwell et al. 2010). It is useful to describe turbulence in the wind using statistics.

Movement of air is comprised of longitudinal, lateral, and vertical components. The instantaneous velocity of the longitudinal component U can be expressed as:

$$U = \overline{U} + u \tag{1.5}$$

where $\overline{U}$ is the short-term mean of this component and u is the fluctuating component. Instantaneous lateral and vertical components of the flow are characterized in similar manner. As part of their definition, all fluctuating components have a zero mean over each averaging period, although within this period these fluctuating components can have important effects on the flow. From this it is seen that there is more energy in the wind then indicated by the average.

A basic measure used to characterize turbulence in the wind is turbulence intensity (abbreviated TI, variable I). TI is defined as the ratio of mean of the prevailing wind direction over the standard deviation on a time scale in excess of turbulent fluctuations but shorter than other variations such as weather patterns. The sampling period for small wind turbines mandated by International Electrotechnical Commission (IEC) is a period of 1 minute and the industry standard for wind resource assessments is a period of 10 minutes. TI is expressed as:

$$I = \frac{\sigma}{U} \tag{1.6}$$

where U is the mean wind velocity of the sampling period and σ is the standard deviation of wind velocity of the same period, calculated by:

$$\sigma = \sqrt{\frac{1}{n-1}\sum_{i=1}^{n}(\overline{U_i} - U)^2} \tag{1.7}$$

Turbulence intensity is typically in the range of 0.1 (10%) for smooth terrain up to 0.2 (20%) or more for terrain with higher surface roughness. Highest values of TI occur at low wind velocities. A plot of typical wind data sampled at 1Hz over 10 minutes is depicted in Figure 1-3, with a mean of 9.48m/s and standard deviation of 1.28. Therefore the turbulence intensity over this period is 0.136. Discussion of the turbulence with respect to the effect on small wind turbine output is continued in Section 1.1.4.

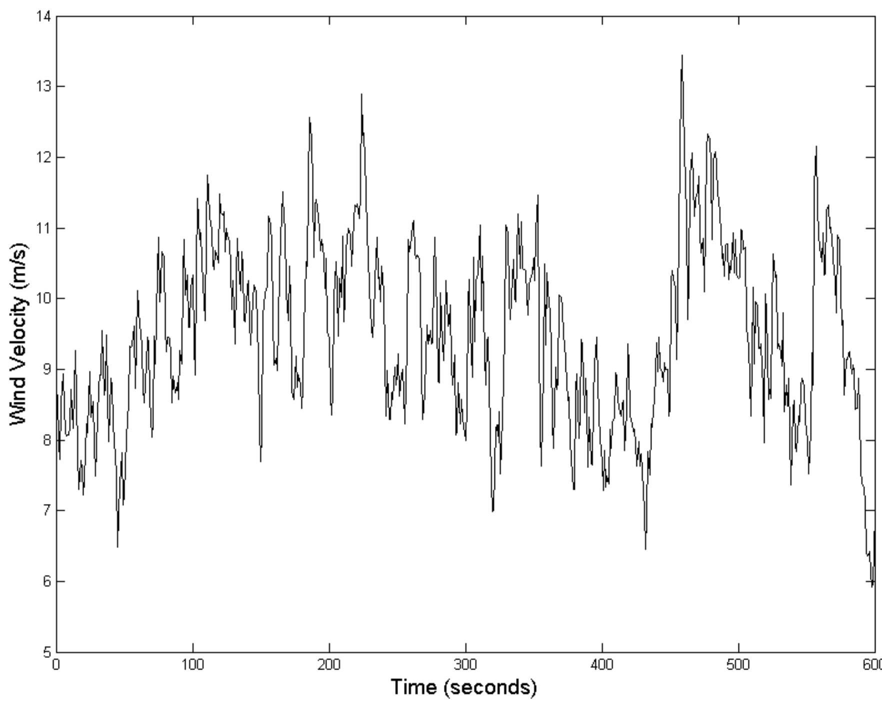

Figure 1-3: Typical wind data measured at 1Hz at Halkirk, Alberta

1.1.2.3 Acceleration

Topographical features such as ridges can greatly affect the wind flow over it. This is not particularly applicable at the turbine site studied in this thesis, but these features are common across the Canadian prairies. Therefore a brief summary of the effects is a good addition to wind resource assessment discussion. Ridges have three advantages: they act as a large tower by being raised into a region of higher winds due to the affects of wind shear, they avoid the unwanted effects of night cooling created near the ground at lower elevations, and they act as a concentrator by accelerating airflow, increasing available energy within the wind (Wegley et al. 1978). Orientation of the ridge is important to improved energy availability, and preference is to being oriented perpendicular to the prevailing direction of the wind. Excessively sloped or poorly oriented ridges can create unwanted turbulence levels in the area which can increase turbine losses. Topographic maps can allow individuals to screen these locations and identify features where increased wind velocities can occur compared to general surroundings (B. Bailey et al. 1997). Topography is an important aspect in classifying a turbine testing site and contributes greatly to initial testing procedure steps such as site calibration. Continued discussion of standards in classifying topographic terrain of a wind turbine site will occur in Section 3.1.1.

1.1.3 Methods of data analysis

Summarization of wind velocity information for a given site is useful in determining the suitability of the site for wind energy. Two manipulations of wind data in characterizing the wind are most important: temporal and frequency distribution (E. H. Lysen 1983). Temporal distribution characterization can give insight into various seasonal and diurnal patterns compared to annual averages. Temporal distributions can also provide information on frequencies of low wind velocities at a site, which is useful in calculating necessary backup power or energy storage necessary. Frequency or probability distribution, describes the probability of a wind velocity domain being at a certain level. This probability is described as a probability density function *p(U)* or cumulative probability *C(U)*, and they are related by the following:

$$\frac{dC}{dU} = p \tag{1.8}$$

The Weibull continuous probability model is the most commonly utilized model for the assessment of wind velocity variation and is shown in Equation (1.9):

$$p(v) = \left(\frac{k}{c}\right)\left(\frac{v}{c}\right)^{k-1} \exp\left[-\left(\frac{v}{c}\right)^{k}\right] \tag{1.9}$$

where p is the probability of the wind achieving velocity v and described by the shape and scale factors, k and c, respectively. Probability distributions are calculated from collected wind data and with this distribution estimates of wind energy production can be made. The Rayleigh distribution is the simplest velocity probability distribution as it assumes a shape factor of 2 and only uses one customized parameter, scale factor. Continued discussion of statistical analysis will occur as topics are introduced in Section 3.

1.1.4 In-situ wind turbine performance testing

Performance characterization of small wind turbine power curves is conducted using one of three methods: open or closed wind tunnel tests (Antonio et al. 2010; Comyn et al. 2011), tow tests (Larwood et al. 2001), and field tests (R. Jacobson et al. 2003). Individuals interested in analyzing the performance of a small wind turbine have to balance the needs of locating the turbine where it will be eventually employed and testing it in a consistent flow field (Ozgener 2006). Performance analysis is completed in order to field certify a turbine design which further promotes high performance as well as to field test the claims of turbine manufacturer, thereby increasing consumer confidence (AWEA 2009b).

Until recently, third-party small wind turbine certifications were limited to those conducted by organizations located in Europe and various certifications subsidized by the United States Department of Energy (DOE) conducted at the National Wind Technology Center (NWTC). In 2009, a joint effort between the United States DOE, the National Renewable Energy Lab (NREL), and several US states resulted in the formation of the Small Wind Certification Council (SWCC) as the North American certification body. The goal of the SWCC is to act as an independent certification body, which will certify small wind turbines to a common standard of performance, safety, reliability, and sound performance. The certifications will be conducted according to the requirements of the AWEA Small Wind Turbine Performance and Safety Standard (AWEA 2009b), one of several standards which have been developed over the last several years. The AWEA standard is derived largely from existing international wind turbine standards developed by the IEC (IEC 2005a), specifically IEC 61400-12-1, ed.1 (Performance); IEC 61400-11, ed.2 (Acoustic Noise); and IEC 61400-2, ed.2 (Design Requirements). IEC 61400-12-1 Annex H is an adaptation specifically for small wind turbines of performance testing standards for utility size wind turbines contained within IEC 61400-12-1. 61400-12-1 Annex H is specific to small wind turbines as it applies to wind turbines with a swept area of $200m^2$ or less. This equates to a rotor diameter of roughly 16m for a horizontal axis turbine.

The SWCC does not conduct the tests, but verifies and certifies the results submitted by regional test centers located across North America and issues turbines with labels for annual energy output, rated power, and rated sound level. In some states, certification will make turbines eligible for certain incentive funds. Since May 2010, 27 turbines have entered into agreement with the SWCC in order to get certified. The next steps in the process include the turbine test being conducted, the reports being submitted to the SWCC and reviewed, and the certification being granted. Unfortunately, the process of certification can take upwards of a year to be completed, and there are a limited number of test sites being competed for by a large number of applicants. The certification procedure is a step towards consistent and standardized performance specifications, but a need still remains for techniques for in-situ performance analysis of small wind turbines. A brief explanation of wind energy performance curves will preface a discussion of current small wind turbine testing practices and their application to in-situ turbine performance analysis.

As discussed previously in Equation (1.1), the power available in the wind is proportional to the cube of wind velocity. The relationship between wind velocity and the actual power harvested is described by the turbine power curve. Important aspects of this power curve include the cut-in wind velocity, the rated wind velocity, and the cut-out wind velocity. The cut-in wind velocity is the velocity at which the turbine will begin generating electricity. The rated wind velocity is the velocity at which the turbine produces the advertised power output. Cut-in and rated wind velocities are labelled in an example power curve in Figure 1-4.

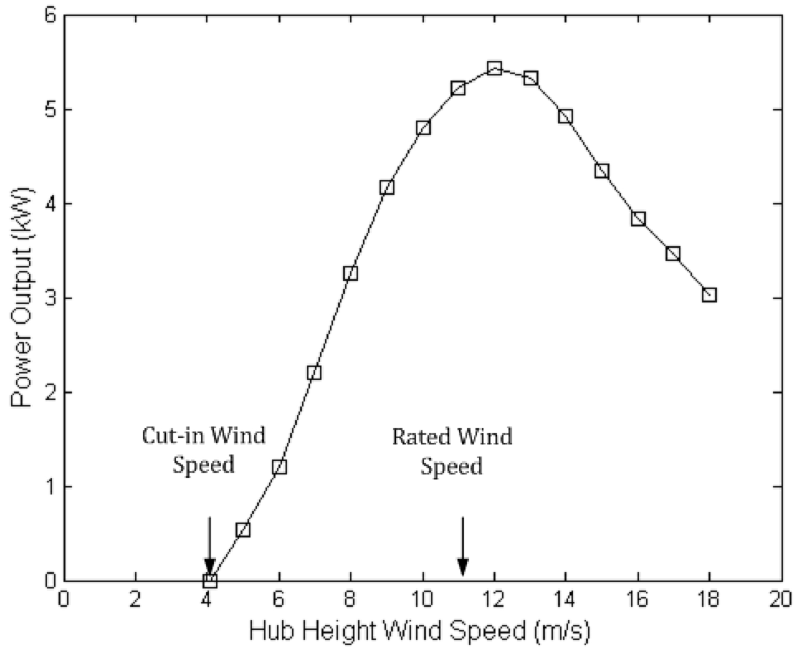

Figure 1-4: A typical SWT power curve, highlighting important features (cut-out velocity not shown – located at 25m/s)

It is necessary for small wind turbines (SWTs) to have a mechanical or electronic control system to reduce power output at a cut-out wind velocity in order to protect the machine from structural damage. SWTs typically use one or a combination of these high wind velocity control methods: a furling mechanism where the rotor turns out of the wind causing it to slow down, braking mechanism where an electrical or mechanical brake physically slows the rotor, or passive stall where the rotor blade has been aerodynamically designed so that at high wind velocities, lifting force is reduced and stall is gradually created (J. F. Manwell et al. 2010). Utility-size wind turbines use variable pitch blades which mechanically change the blades angle of attack, but this method complicates the hub and is not common in small wind turbines. High wind velocity protection is dependent on the type of electrical generator used in the turbine design – constant rotor velocity machines with induction generators typically utilize passive stall and braking, whereas variable rotor velocity machines which use synchronous generators and operate at faster rotor velocities typically use furling.

Accurate power curve development is highly dependent on properly characterizing the local wind resource at the height of the turbine. As discussed earlier in this section, the current standard for characterizing the performance of small wind turbines is IEC 61400-12-1 Annex H. This standard presents a systematic procedure for characterizing the site of a turbine, determining measuring power curves, calculating annual energy production (AEP) estimates, and considering the combined effects of all sources of uncertainty. The standard is applicable to singular wind turbines of all types and sizes that are connected to the electrical grid. Special provisions for power performance testing of SWTs are outlined in Annex H and will be the focus of further discussion here.

A crucial aspect of small wind turbine power performance is measurement of wind velocity at hub height. 61400-12-1 utilizes the practice of assuming the flow field of a wind turbine to be the free stream velocity at hub height. This assumption is sufficient for SWTs but is questionable when applied to megawatt size wind turbines and utility size wind farms, as their large rotor diameters create an uncertainty in the hub height wind which translates to a power curve uncertainty (S. Frandsen et al. 2000; Sinclair & Raker 2006; Ioannis Antoniou et al. 2009). Another issue is power curve biasing, caused by the relationship between wind velocity probability and power output. Studies have shown that the relationship between power and wind can have a systematic bias about the mean wind velocity created by the nature of wind (Christensen et al. 1986). For example, at short wind gusts lower than the mean, there is a higher probability that the wind velocity at the tower is lower, and therefore the power associated is lower. The opposite effect is seen at higher wind velocities, where the probability of the wind being lower at the anemometer compared to the wind seen by the wind turbine. This is explained graphically by Figure 1-5.

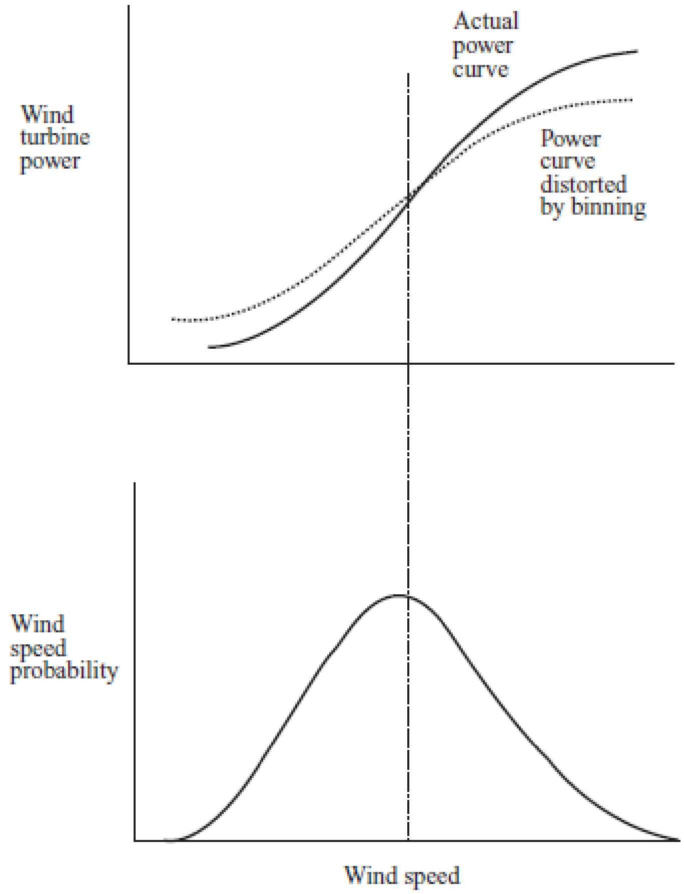

Figure 1-5: Power curve biasing (Burton et al. 2001)

61400-12-1 suggests that a meteorological mast be installed in the region of the wind turbine in order to establish the wind velocity that drives the wind turbine. Hub-height wind velocity is correlated to concurrent measurements of turbine power which is used to create a power curve. This power curve is adjusted to standard air density in order to create comparable datasets between testing sites. The power curve is also applied to a reference wind velocity frequency distribution in order to calculate an AEP. The standard identifies the test site as having the potential to significantly influence measured power performance of the wind turbine in terms of the uncertainty created by the flow distortion between meteorological mast and turbine. The test site should be analyzed for sources of wind flow distortion in order to properly position the meteorological mast, identify a measurement sector free of disturbances, and estimate the uncertainty created by wind flow distortion. The disturbances to be identified include topographical variations and local obstacles such as buildings, trees, or other turbines.

Placement of the reference mast is to be carefully considered. The mast is to be positioned between 2 and 4 times the rotor diameter (D_{rotor}) of the turbine, with a distance of 2.5 rotor diameters as the recommended offset. Locating the meteorological mast farther away increases the error in hub height wind velocity measurement. The standard presents a procedure to calculate disturbed measurement sectors created by local obstacles on the flow field of the mast.

The standard provides a number of test site requirements which the topography of the test site must meet. Otherwise a site calibration must be completed which assesses the differences in wind velocity between the met mast and the turbine and creates flow correction factors as a function of direction. The topographical variations focused on are maximum slope of the sectoral terrain and maximum terrain variation from the plain. If the test site passes the terrain requirements, the uncertainty in the wind velocity value contributed by flow distortion is assumed to be 2% or 3% depending on how close to the turbine location the met mast is situated (2% is assumed if the met mast is 2-3D_{rotor} away and 3% if the met mast is 3-4D_{rotor} away). If the test site fails the terrain requirements, a test site calibration must be conducted which will result in an uncertainty value for each wind direction bin. This value is derived from the uncertainty in the ratio of wind velocity at the wind turbine and anemometer at the met mast.

The standard discusses the requirements of the test equipment in detail. As discussed earlier, wind velocity measurement is of utmost importance in characterizing turbine performance. The wind velocity measured is defined as the average magnitude of the 2-D wind velocity, meaning only the lateral and longitudinal components. Cup anemometers of certain quality are accepted as the industry standard for this type of measurement. Cup anemometers of Class 1.7A are to be used, meaning their measured mean wind velocity must be within 7% for any mean wind velocity from 4m/s to 16m/s. This accuracy is applicable to a range of temperatures, air densities, turbulence intensities and inclination angles.

Test equipment used to measure the power output of the turbine shall be a power transducer or equivalent device, located between the wind turbine and electrical connection so as to only measure the net power of the turbine and not the consumption of associated test equipment. The class of the instruments used must be equivalent to at least Class 0.5, meaning the accuracy of the resulting power must be within 0.5% of full scale across the entire measuring range. The power measurement device should be capable of measuring both positive and negative power generated or consumed by the turbine and should be set to -50% to 200% of the wind turbine rated power. Annex H discusses requirements related to the power instruments used in testing of battery-charging wind turbines, while not relevant here, are good to note.

Other relevant parameters to be measured as part of the turbine test include air density (to be calculated using simultaneous readings of temperature and pressure) as well as wind direction (using a wind vane mounted on the reference mast). Relative humidity is an important factor on air density at high temperatures and should be measured if these conditions are encountered. If necessary, blade conditions such as icing, precipitation, bug build up, or dust are to be reported. Other measurement considerations include rotational velocity for variable velocity machines, which can be related to power output. The logging of control system status can also make data rejection easier.

The measurement procedure should be clearly documented so that the data can be of a certain level of quantity and quality in order to accurately document wind turbine performance. The procedure is done to a certain level so that steps and conditions can be reviewed and if necessary, repeated. A digital data acquisition system should be used and wind velocity, direction, and power output should be sampled at a rate of at least 1Hz. Measurements of parameters such as temperature and pressure are to be taken once per minute or more. Data set statistics for the appropriate averaging period such as mean value, standard deviation, minimum, and maximum value. Data from averaging periods will be rejected when conditions prevent turbine operation such as icing or control system status or the wind is from directions outside undisturbed measurement sectors.

Datasets will be sorted using the method of bins, where bins are centered on 0.5 m/s increments and spanning 0.5 m/s. The data sets should cover a wind velocity range from 1 m/s below turbine cut-in to 1.5 times the wind velocity at 85% of the rated power of the wind turbine. The dataset is considered complete when there are at least 60 hours of wind turbine operation and each wind velocity bin from 1 m/s below turbine cut-in to 14 m/s contains at least 10 minutes of sampled data. The power curve is created by averaging the power output contained in each wind velocity bin. The power curve is then normalized to two air densities: sea level density (1.225 kg/m^3) and average site air density during the measuring campaign. Wind turbine efficiency is also calculated for each wind velocity bin.

AEP is estimated by applying the measured power curve to reference wind velocity frequency distributions. 61400-12-1 outlines the use of the Rayleigh frequency distribution – discussed earlier in Section 1.1.3. As a refresher, the Rayleigh distribution is simply a Weibull distribution with a constant shape factor of 2 and a scale factor according to the average wind velocity. The distribution describes an estimate of the frequency of the wind at a site occurring within each wind velocity bin, and by applying the power value associated with that bin, an estimate for annual energy production can be estimated.

A test report is created detailing a synopsis of the testing procedure and results. From the testing procedure it includes a description of the turbine configuration, the turbine site, and the test equipment. From the results, the testing report includes a summary of findings including measured power curve, calculated power coefficient, AEP estimates, and relevant site conditions such as turbulence intensity. A summary of the uncertainty analysis is presented as well as any deviations from the testing standard.

As discussed earlier, 61400-12-1 is a testing standard for all types and sizes of grid connected wind turbines. Certain provisions have to be made for testing of small wind turbines and these are detailed in Annex H. Of certain interest is Annex H subsection 'g' where it is proposed that, if more convenient for testing purposes than a separate meteorological mast, an anemometer can be mounted on a long boom attached to the turbine tower. In order to reduce the potential affect of the anemometer, the wind vane, and mounting hardware on the turbine, these components must be situated at least 3 m from any part of the turbine rotor. In addition, any part of mounting should be arranged so that their influence is minimal within 1.5m of hub height. Other provisions detailed in Annex H include the previously discussed 1 minute data averaging requirement for SWT and some additional points on reporting and AEP calculations.

There are several issues in the utilization of 61400-12-1 for the performance analysis of small wind turbines. As the tower of a wind generator system is a large part of the initial cost, the purchase and erection of a separate tower for the testing of a small wind turbine is often not economically viable. As well, space can be a large constraint in considering installing a met tower within 2 to 4 rotor diameters upwind as some SWTs often have diameters of less than a couple meters. These close quarters may reduce the quality of the wind that the wind turbine is subjected to. The guy wires and lay down area may be too close and not allow the towers to be safely laid down for maintenance. The comment in Annex H regarding tower mounting a boom and cup anemometer for testing seems to be an afterthought, with little procedure detailed.

Improvements to the met tower method of studying turbine performance have been widely studied in utility-sized wind turbines. These studies include the cutting edge use of SODAR (Sound Detection And Ranging) and LIDAR (Light Detection And Ranging), which used ground based remote sensing devices to improve wind shear models created with cup anemometers on wind resource assessment met towers (M. a Lackner et al. 2010) and wind farm met towers (Wharton & Lundquist 2010; Ioannis Antoniou et al. 2009). Ground based remote sensing devices are relatively new technology, and are far too expensive to justify using in small wind turbine applications. Other improvements that have been attempted with very good success in the utility scale wind industry include nacelle cup anemometry (Hunter et al. 2001). This procedure includes using an upwind met tower in conjunction with a cup anemometer mounted behind the blades on the nacelle to create a machine-specific transfer function, which is then used to adjust wind velocities from cup anemometers on other turbines of the same model in the wind farm. This method is to be detailed in a future IEC publication, IEC 61400-12-2 - Power performance of electricity producing wind turbines based on nacelle anemometry.

The application of different aspects of 61400-12-1 on small wind turbine performance analysis has been previously studied, including alternative hub height wind measurement methods (Lubitz 2010; Ziter 2010). This study looked to improve on field verification methods of various studies. Previous field methods include two anemometers and power law extrapolation in a study on 6 SWTs by

Summerville (but no guidelines on mounting height or accuracy study) and one anemometer 6m below hub height and arbitrary power law exponents in a study of 4 SWTs by NREL (Summerville 2005; Sinclair 2005). In Ziter's study, a reference mast with a hub height cup anemometer was installed upwind of a SWT on a 15m tower. The turbine had a nacelle mounted anemometer and the tower had cup anemometer installed at 5m and 10m. The study found good performance of the nacelle anemometers at low to medium wind velocities, but at wind velocities close to furling, the erratic tendencies of the turbine led to poor predictions by the corrected nacelle wind velocity. Also, the need for a separate met tower in order to create a model for the turbine negated the benefits of only having a nacelle anemometer for performance analysis. The accuracy of tower mounted anemometers for hub height wind estimation was found to be the most promising in terms of IEC 61400-12-1 small wind turbine performance testing, with several recommendations being put forward. It was advised that multiple anemometers be used in order to create a model and extrapolate to hub height from the top anemometer. Location of the topmost anemometer was recommended to be one rotor diameter from hub height, with the location of the lower anemometer being less important but avoiding the extremes of being too close to the ground or topmost anemometer. This recommendation agrees with conclusions made from previous studies pertaining to utility scale met tower extrapolation (M. Taylor et al. 2004). Further discussion on vertical extrapolation, as well as the application of Ziter's recommendations, will be continued in Section 3.4.

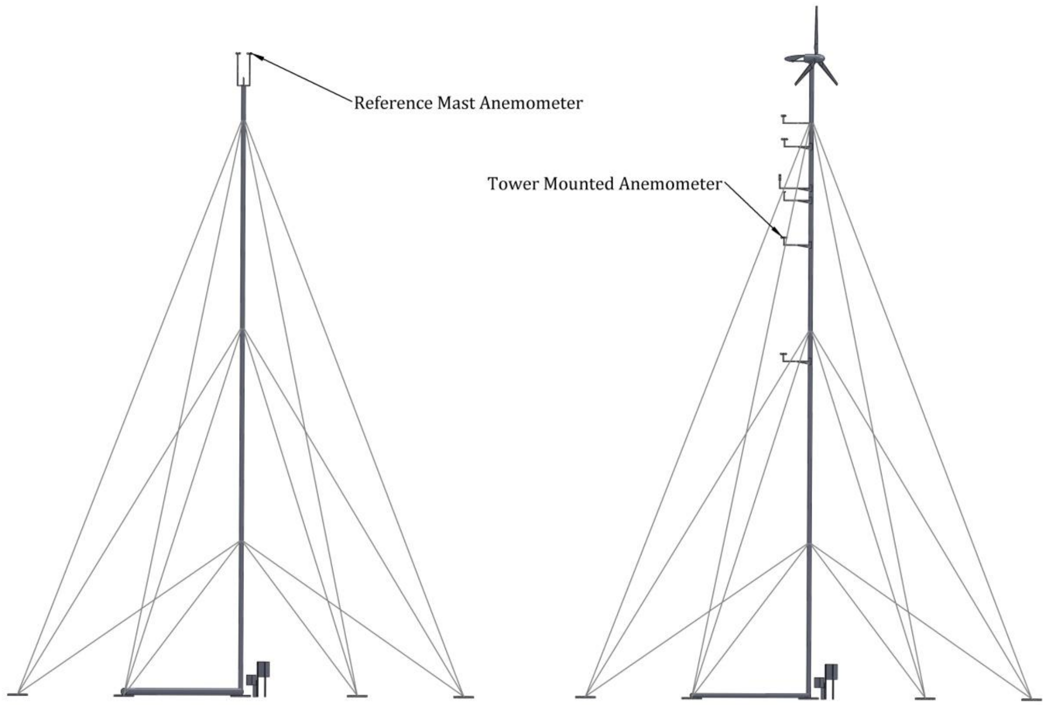

Figure 1-6: Methods for estimating hub height wind velocity for small wind turbines

Another aspect of the application of 61400-12-1 that has been previously studied is that of averaging on SWT performance (de Paz et al. 2004; Klemen 1998; Makkawi et al. 2009). Because of differences between turbulence between sites, it is possible that different averaging schemes will affect power curve estimates, which translates to error in annual energy production estimates.

An additional topic relevant to users of wind energy on the Prairies to be discussed is low temperature performance. Recently, it has been put forward that efforts must be undertaken to better understand the effect of temperature on turbine performance (Lacroix & J.F. Manwell 2000), although few studies with public data are available and most studies focus on icing (Bose 1992; Walsh 2010) or alpine environments (Barber et al. 2011). Wind turbines in alpine environments are subjected to more turbulent wind due to turbulence generated by terrain, but experience similar temperatures as the Prairies. Because there is less convective mixing when there are lower solar heat fluxes and surface absorptivity at colder times, cold temperatures correlate strongly with lower turbulence intensities. The relationships between these variables and power performance will be studied and discussed in Section 3.3.2.7.

1.2 Objectives

The objective of this research project was to study the environmental and power performance of a grid connected small wind turbine. In order to reach this objective, the following elements were examined:

- Evaluate and compare the benefits of different sizes of grid connected small wind turbines on the basis of environmental, economic, and energy sited in a specific location that is a good representation of a typical rural area of East Central Alberta using applicable standards
- Examine factors affecting the performance of small wind turbines using data collected from the site of a grid connected small wind turbine over 17 months in the form of a wind resource assessment and power performance analysis
- Investigate and discuss the use of tower mounted anemometers for in-situ turbine performance analysis

1.3 Format

This thesis is presented in the form of two papers with a third that discusses and relates the conclusions of each of the individual papers. The first paper, Chapter 2, is published in the Elsevier journal *Renewable Energy* (Kabir et al. 2012). This paper discusses the theoretical life cycle assessment comparison of three small wind turbines for the production of 100kW of nameplate power in East Central Alberta. The three options outlined for the production of 100kW of nameplate power include twenty turbines rated at 5kW, five turbines rated at 20kW, and one turbine rated at 100kW and each option is compared on an emission, energy, and economic basis. The author of this thesis, Braden Rooke, cooperated extensively with the co-authors, Md. Ruhul Kabir and Malinga Dassanayake, during data collection, first draft composition, and proof reading phases. The second section, Chapter 3, has been submitted as two papers for publishing in the Multi-Science journal *Wind Engineering* (Rooke, B. A. Fleck & Tyree 2011b; Rooke, B. A. Fleck & Tyree 2011a). Chapter 3 presents a wind resource assessment and performance analysis of a small wind turbine installed in a rural location near Halkirk, Alberta based on field data collected at the turbine site over the span of 17 months. Each paper is structured with three key elements in mind. First of all, standards are introduced which govern the standardization of turbine performance and wind resource assessment.

Secondly, performance data is presented clearly and concisely. Last of all, conclusions are drawn from discussion of the results and improvements to the governing standards are presented.

1.4 References

AWEA, 2009a. *AWEA Small Wind Turbine Global Market Study*, Available at: http://e360.yale.edu/images/digest/2010_AWEA_Small_Wind_Turbine_Global_Market_Study-1.pdf. [Accessed April 2011].

AWEA, 2009b. *AWEA Small Wind Turbine Performance and Safety Standard*, Available at: http://www.awea.org/learnabout/smallwind/upload/AWEA_Small_Turbine_Standard_Adopted_Dec09.pdf. [Accessed April 2011].

AWEA, 2009c. *Policies to Promote Small Wind Turbines*, Available at: http://www.awea.org/learnabout/smallwind/upload/Policies_to_Promote_Small_Wind_Turbines.pdf. [Accessed June 2011].

Alberta Electric System Operator, 2010. Grid Connection Queue. Available at: http://www.aeso.ca/21647.html [Accessed April 2011].

Antonio, J., Alé, V., Simioni, S., Gilberto, J. & Chagas, A., 2010. Procedures Labaratory for Small Wind Turbines Testing. In *EWEC Proceedings*. Available at: http://ewec2010proceedings.info/allfiles2/180_EWEC2010presentation.pdf. [Accessed May 5, 2011].

Antoniou, Ioannis, Pedersen, S.M. & Enevoldsen, P.B., 2009. Wind Shear and Uncertainties in Power Curve Measurement and Wind Resources. *Wind Engineering*, 33(5), pp.449-468.

Ardente, F., Beccali, M., Cellura, M. & Lobrano, V., 2008. Energy performances and life cycle assessment of an Italian wind farm. *Renewable and Sustainable Energy Reviews*, 12(1), pp.200-217.

Bailey, B., McDonald, S., Bernadett, D., Markus, MJ & Elsholz, K., 1997. *Wind resource assessment handbook: Fundamentals for conducting a successful monitoring program*, SAGE Publications. Available at: http://www.osti.gov/energycitations/product.biblio.jsp?osti_id=486127 [Accessed February 16, 2011].

Barber, S., Chokani, N. & Abhari, R.S., 2011. Assessment of Wind Turbine Performance in Alpine Environments. *Wind Engineering*, 35(3), pp.313–328.

Bell, J. & Weis, T., 2009. *Greening the Grid: Powering Alberta's Future with Renewable Energy*, Pembina Institute. Available at: http://www.pembina.org/pub/1763 [Accessed June 25, 2011].

Blanco, M.I., 2009. The economics of wind energy. *Renewable and Sustainable Energy Reviews*, 13(6-7), pp.1372-1382.

Bose, N., 1992. Icing on a small horizontal-axis wind turbine--Part 1: Glaze ice profiles. *Journal of Wind Engineering and Industrial*, 45, pp.87-96.

Burton, T., Sharpe, D., Jenkins, N. & Bossanyi, E., 2001. *Wind energy handbook*, John Wiley and Sons.

CanWEA, 2011. Growth in global wind energy continues. Available at: http://www.canwea.ca/media/release/release_e.php?newsId=115 [Accessed April 2011].

CanWEA, 2010. Small Wind Market Survey. Available at: http://www.canwea.ca/pdf/SmallWind/canwea-smallwindmarketsurvey-e-web.pdf. [Accessed October 2010]

Christensen, C.J. et al., 1986. *Accuracy of Power Curve Measurements*, Available at: http://130.226.56.153/rispubl/reports/ris-m-2632.pdf. [Accessed February 7,2011]

Committee on Environmental Impacts of Wind Energy Projects & NRC, 2007. *Environmental impacts of wind-energy projects*, National Academies Press. Available at: http://scholar.google.com/scholar?hl=en&btnG=Search&q=intitle:Environmental+Impacts+of+Wind-Energy+Projects#0 [Accessed June 25, 2011].

Comyn, G.I., Nobes, D.S. & Fleck, B.A., 2011. Performance Evaluation and Wake Study of a Micro Wind Turbine. In *Canadian Society for Mechanical Engineering*. pp. 101-117.

Elkinton, M.R., Rogers, a L. & McGowan, J. G., 2006. An Investigation of Wind-shear Models and Experimental Data Trends for Different Terrains. *Wind Engineering*, 30(4), pp.341-350.

Farrugia, R., 2003. The wind shear exponent in a Mediterranean island climate. *Renewable Energy*, 28(4), pp.647-653.

Fleck, B. & Huot, M., 2009. Comparative life-cycle assessment of a small wind turbine for residential off-grid use. *Renewable Energy*, 34(12), pp.2688-2696.

Frandsen, S. et al., 2000. Redefinition power curve for more accurate performance assessment of wind farms. *Wind Energy*, 3(2), pp.81-111.

Gipe, P., 2004. *Wind power: renewable energy for home, farm, and business* 2nd ed., Chelsea Green Publishing.

Global Wind Energy Council, 2010. *Global Wind Energy Outlook 2010*, Available at: http://www.gwec.net/fileadmin/documents/Publications/GWEO 2010 final.pdf. [Accessed June 25, 2011].

Government of Alberta, 2010. *Electricity Statistics*, Available at: http://www.energy.alberta.ca/Electricity/682.asp#est.[Accessed April 25, 2011].

Huijbregts, M. a J., Norris, G., Bretz, R., Ciroth, A., Maurice, B., Bahr, B., Weidema, B. & Beaufort, A.S.H., 2001. Framework for modelling data uncertainty in life cycle inventories. *The International Journal of Life Cycle Assessment*, 6(3), pp.127-132.

Hunter, R., Albers, T.F.P., Dunbabin, Penny, Antoniou, Ioannis, Frandsen, Sten, Klug, H., Albers, A. & Lee, W.K., 2001. *European Wind Turbine Testing Procedure Developments Task 1: Measurement Method to Verify Wind Turbine Performance Characteristics*, Available at: http://130.226.56.153/rispubl/VEA/veapdf/ris-r-1209.pdf. [Accessed June 25, 2011].

IEC, 2005. 61400-12-1: Power performance measurements of electricity producing wind turbines.

ISO, 2006a. ISO 14040:2006 - Environmental management -- Life cycle assessment -- Principles and framework.

ISO, 2006b. ISO 14044:2006 - Environmental management -- Life cycle assessment -- Requirements and guidelines.

Jacobson, R., Meadors, M., Jacobson, E. & Link, H., 2003. *Power Performance Test Report AOC 15 / 50 Wind Turbine , Test B Revision 3*, Available at: http://www.nrel.gov/wind/pdfs/34305.pdf.

Kabir, M.R., Rooke, B., Dassanayake, M. & Fleck, B.A., 2012. Comparative life cycle energy, emission, and economic analysis of 100 kW nameplate wind power generation. *Renewable Energy*, 37(1), pp.133-141.

Klemen, M., 1998. Wind Speed Data and its Application to Wind Generated Power. *Home Power*, (January), pp.34-38.

Krohn, S., Morthorst, P.-E. & Awerbuch, S., 2009. *The Economics of Wind Energy*, Available at: http://www.ewea.org/fileadmin/ewea_documents/documents/publications/reports/Economics_of_Wind_Main_Report_FINAL-lr.pdf [Accessed March 4, 2011].

Lackner, M. a, Rogers, A.L., Manwell, James F. & McGowan, Jon G., 2010. A new method for improved hub height mean wind speed estimates using short-term hub height data. *Renewable Energy*, 35(10), pp.2340-2347.

Lacroix, A. & Manwell, J.F., 2000. *Wind energy: cold weather issues*, Available at: http://www.ecs.umass.edu/mie/labs/rerl/research/Cold_Weather_White_Paper.pdf [Accessed September 19, 2011].

Larwood, S.M., Sencenbaugh, J. & Acker, B., 2001. Controlled Velocity Testing of an 8-kW Wind Turbine. In *AWEA Windpower*. Available at: http://citeseerx.ist.psu.edu/viewdoc/download?doi=10.1.1.134.213&rep=rep1&type=pdf [Accessed March 18, 2011].

Lenzen, M., 2002. Energy and CO2 life-cycle analyses of wind turbines—review and applications. *Renewable Energy*, 26(3), pp.339-362.

Lubitz, W.D., 2009. Power Law Extrapolation of Wind Measurements for Predicting Wind Energy Production. *Wind Engineering*, 33(3), pp.259-271.

Lubitz, W.D., 2010. Predicting Hub-Height Wind Speed for Small Wind Turbine Performance Evaluation Using Tower-Mounted Cup Anemometers. *Wind Engineering*, 1, pp.673-699.

Lysen, E.H., 1983. *Introduction to Wind Energy* 2nd ed., CWD - Consultancy Services Wind Energy Developing Countries. Available at: http://books.google.com/books/about/Introduction_to_wind_energy.html?id=c9FoHQAACAAJ [Accessed June 27, 2011].

Makkawi, a, Celik, a & Muneer, T., 2009. Evaluation of micro-wind turbine aerodynamics, wind speed sampling interval and its spatial variation. *Building Services Engineering Research and Technology*, 30(1), pp.7-14.

Manwell, J. F., McGowan, Jon G. & Rogers, A.L., 2010. *Wind Energy Explained: Theory, Design, and Application*

Martinez, E., Sanz, F., Pellegrini, S., Jimenez, E. & Blanco, J., 2009. Life cycle assessment of a multi-megawatt wind turbine. *Renewable Energy*, 34(3), pp.667-673.

Ozgener, O., 2006. A small wind turbine system (SWTS) application and its performance analysis. *Energy Conversion and Management*, 47(11-12), pp.1326-1337.

de Paz, L.A., Avia, F., Cano, L., Cruz, I. & Soria, E., 2004. Power Performance Testing of Small Wind Turbines: Experiences and findings obtained testing the Bornay 1500 Inclin Neo Wind Turbine. In *2004ewec.info*. Available at: http://www.2004ewec.info/files/23_1400_felixavia_01.pdf [Accessed February 16, 2011].

Rooke, B., Fleck, B.A. & Tyree, M., 2011a. Power Performance Results from a Grid-Connected Endurance S-343 Small Wind Turbine Installed in Rural East-Central Alberta. *Wind Engineering*. [Submitted 2011]

Rooke, B., Fleck, B.A. & Tyree, M., 2011b. Wind Resource Assessment and Annual Power Performance of a Grid Connected Small Wind Turbine in East Central Alberta. *Wind Engineering*. [Submitted 2011]

Sawin, J.L. & Martinot, E., 2010. *Renewables 2011 Global Status Report*, Available at: http://www.ren21.net/Portals/97/documents/GSR/GSR2011_Master18.pdf [Accessed August 5, 2011].

Schleisner, L., 2000. Life cycle assessment of a wind farm and related externalities. *Renewable Energy*, 20(3), pp.279-288.

Sinclair, K., 2005. Regional Field Verification--Case Study of Small Wind Turbines in the Pacific Northwest: Preprint. In *American Wind Energy Association WindPower 2005*. Available at: http://www.osti.gov/energycitations/product.biblio.jsp?osti_id=882795 [Accessed February 16, 2011].

Sinclair, K. & Raker, J., 2006. Regional Field Verification—Operational Results from Four Small Wind Turbines in the Pacific Northwest. In *National Renewable Energy Laboratory, Conference Paper\# NREL/CP-500-38110*. Available at: http://www.nrel.gov/wind/smallwind/pdfs/sinclair_rfv_operational_results.pdf [Accessed February 16, 2011].

Small Wind Certification Working Group, 2007. *North American Certification for Small Wind Turbines: The Case for Funding Consumer-Friendly Performance Ratings for Homes, Farms & Businesses*, Available at: http://www.weican.ca/documents/070827-swcc-case-statement.pdf. [Accessed February 16, 2011].

Summerville, B., 2005. *Small Wind Turbine Performance in Western North Carolina*. Available at: http://www.at.appstate.edu/documents/researcharticlesmallwindperformanceBJS.pdf [Accessed March 17, 2011].

Taylor, M., Brower, M.C., Markus, Michael, Meteorologist, S. & Truewind, A.W.S., 2004. An Analysis of Wind Resource Uncertainty in Energy Production Estimates. In *European Wind Energy Conference*. pp. 1-11. Available at: http://www.2004ewec.info/files/23_1400_marktaylor_01.pdf. [Accessed February 16, 2011].

The Cadmus Group, 2008. *Status Report on Small Wind Energy Projects Supported by the Massachusetts Renewable Energy Trust*, Available at: http://www.cadmusgroup.com/pdfs/MRET.pdf. [Accessed March 16, 2011].

Tremeac, B. & Meunier, F., 2009. Life cycle analysis of 4.5MW and 250W wind turbines. *Renewable and Sustainable Energy Reviews*, 13(8), pp.2104-2110.

Walker, A., 2001. *Financing Distributed Generation Preprint*, Available at: http://www.nrel.gov/docs/fy01osti/30554.pdf. [Accessed March 10, 2011]

Walsh, M., 2010. *Accretion and Removal of Wind Turbine Icing in Polar Conditions*. Aalto University School of Science and Technology Master's Thesis. Available at: http://www.tuulivoimayhdistys.fi/tuulivoimayhd-files/Wind_Turbine_Ice_Removal.pdf.pdf [Accessed September 19, 2011].

Wegley, H.L., Orgill, M.M. & Drake, R.L., 1978. *A Siting Handbook for Small Wind Energy Conversion Systems*, United States Department of Energy. Available at: http://www.fastonline.org/CD3WD_40/JF/427/21-489.pdf. [Accessed June 19, 2011].

Wharton, S. & Lundquist, J.K., 2010. *Atmospheric Stability Impacts on Power Curves of Tall Wind Turbines - An Analysis of a West Coast North American Wind Farm*, Available at: http://atoc.colorado.edu/~jlundqui/wharton_lundquist2010LLNLTR424425.pdf. [Accessed June 19, 2011].

White, S.W., 2007. Net Energy Payback and CO2 Emissions from Three Midwestern Wind Farms: An Update. *Natural Resources Research*, 15(4), pp.271-281.

Wood, D., 2010. Small Wind Turbines for Remote Power and Distributed Generation. *Wind Engineering*, (2006), pp.241-254.

Wood, D., 2011. *Small Wind Turbines: Analysis, Design, and Application*, Springer.

Ziter, B., 2010. *Alternative Methods of Estimating Hub-height Wind Speed for Small Wind Turbine Performance Evaluation*. Master's Thesis, University of Guelph. http://www.soe.uoguelph.ca/webfiles/wlubitz/Thesis_Ziter_2010.pdf [Accessed February 7, 2011].

2 Life Cycle Assessment

2.1 Introduction

Electricity generation is a substantial source of green house gas (GHG) emissions. As most of the primary energy sources used for electricity production are fossil fuels, GHG emission is likely to increase globally for the foreseeable future and this eventually puts our environment and society in a vulnerable position. Simultaneously protecting the climate and satisfying the growth in electricity demand has become one of the greatest dilemmas and challenges of the 21st century. As renewable energy sources have inherent environmental benefit, they are gaining more attraction as an alternative to fossil fuels. Among the renewables, wind power is experiencing a rapid growth worldwide in the last two decades and is expected to grow even faster in future (Martinez et al. 2009; Krohn et al. 2009).

Roughly, 82% of the total electricity production in Alberta is generated from coal combustion, which results in the highest grid emission factor in Canada (Environment Canada 2007). Alberta is planning to mitigate 37 Million tonne (Mt) carbon dioxide equivalent ($CO2_{eq}$) by 2050 by "greening" its energy sector with renewable sources (Government of Alberta 2008). Installation of small wind turbines (300W-300kW) is becoming popular and there are more than 11,000 of them are in now operation in Canada (CanWEA 2010). Small wind power facilities are growing for a number of reasons. Small wind turbines can operate both on and off-grid, providing remote communities, educational institutions, agricultural producers, and businesses with a source of clean and economic energy. Areas of central and eastern Alberta are attractive wind regions with consistent winds, low population density, and limited geographic features. This study is based on establishing 100kilowatt electric (kW) nameplate wind power facility in the Halkirk region of east central Alberta, Canada. Three turbine manufacturers have been analyzed using Life Cycle Assessment (LCA) methodology. Each manufacturer produces wind turbines of different capacity. Options under study are: installing 20 Endurance (EN) 5kW, or 5 Jacobs (JA) 20kW, or 1 Northern Power (NP) 100kW turbines for the proposed 100kWe nameplate wind facility.

LCA is the standard methodology to quantify the environmental impacts from any physical system (ISO 2006a). LCA evaluates the environment impact of a product throughout its life cycle. Typically, life cycle of any product starts with raw material acquisition, followed by production, use, maintenance, and finally recycling and disposal of the product (ISO 2006a). Although there are available LCA studies on large-scale wind power generation (Martinez et al. 2009; Martínez et al. 2008; Crawford 2009) studies are rare for small scale machines (B. Fleck & Huot 2009). Studies performing comparative LCA on different capacity wind turbines in order to generate the same power were unavailable. This study focuses on addressing these gaps in LCA studies of small wind power.

Studies are available which discuss the economic feasibility of wind power (Krohn et al. 2009; M. I. Blanco 2009). Economical analysis helps in determining the amount of subsidy or incentive required to make wind power competitive to other alternatives. In order to make this study more informative to the potential investors, an economic assessment of the three alternatives has been included. Energy payback period is another important parameter that needs to be considered for renewable energy options (Schleisner 2000). In order to evaluate that, this study tracks all the primary non-renewable energy input for the wind turbine configurations over their life cycles.

The overall objective of this study is to compare three configurations of wind turbines with different capacity all producing the same nameplate power, by quantifying their relative energy, environmental, and economic benefit.

2.2 Methodology

Capacity factor is defined as the ratio of actual power to the theoretical power (nameplate power) output during a specified span of time in a certain wind regime. It is good practice to calculate a capacity factor rather than assuming one, as each wind turbine has a unique power curve which it produces power in accordance to wind velocity. Unlike other LCA studies mentioned earlier, this study determines the capacity factor for each wind turbine which is specific to the Halkirk wind regime. The power curve method has been used to determine the capacity factor using the methodology stated by (Gipe 2004). Power output from different wind turbines at different wind velocities were provided by the manufacturer in the form of a power curve (JA) and set of tables (EN and NP). The average wind velocity for Halkirk at a height of 30m was provided by the Canadian Wind Energy Atlas (Environment Canada 2011a) was converted to obtain the velocity at hub heights of respective turbines using the 1/7th power law as found from Equation (2.1) (Gipe 2004; Farrugia 2003).

$$U_{hub} = U_o \left(\frac{h_{hub}}{h_o} \right)^{\alpha} \tag{2.1}$$

where α is the wind shear factor (unitless), h_{hub} is the height above ground level (m), H_o is the reference height (m), U_{hub} is the wind velocity at height of h meters above ground level (m/s), and U_o is wind velocity at reference height (m/s).

Assuming typical ground cover for the Halkirk area as short grass, α was assumed to be 0.14 (Gipe 2004). Wind velocity at hub height found from the equation was used to create a Weibull distribution using the shape factor and scale factor of 2 and 6.24 respectively, provided by the Canadian Wind Energy Atlas (Environment Canada 2011a). From this wind distribution, net annual power output from each turbine from different manufacturer has been calculated using the power curve method. In this way, the capacity factor was calculated for each configuration.

The life cycle of the turbine has been broken into five unit processes for the ease of analysis. These are: turbine production, transportation and installation, power generation, turbine maintenance, and decommissioning, recycling and disposal. Detailed description of the unit processes is given under section 2.4. All non-renewable primary energy input has been tracked for every unit process. To ensure accurate quantification, raw material and fuel embodied energy and emission factors have been considered from a life cycle perspective which is kept consistent throughout the study. The net energy input to a unit process was calculated based on Equation (2.2).

$$E_{net} = \sum E_{in} - \sum E_{out} \tag{2.2}$$

where $\sum E_{in}$ is the total non-renewable primary energy input to a unit process, $\sum E_{out}$ is the total energy output from a unit process, and $\sum E_{net}$ is the net energy input to a unit process. A negative sign of $\sum E_{net}$ indicates energy savings and vice versa.

The total power available during the service life from each turbine configuration based on the determined capacity factor was used to normalize the life cycle energy, emissions and economic input corresponding to the functional unit (FU).

Some information necessary for a fully all-inclusive inventory data set was not available. Therefore, uncertainties in the obtained LCA results were inevitable. To investigate the imperfections of data, a systematic aggregate uncertainty analysis is recommended before drawing a conclusion based on the LCA result (M. Raynolds, M.D. Checkel 1999). The standard method of analysis is a Monte Carlo calculation. The methodology for the uncertainty analysis has been detailed under section 2.5.

2.3 Goal definition

This study has been carried out to find out the most suitable configuration of wind turbines to establish a 100kW wind based electricity generation facility at Halkirk, Alberta, Canada. For a theoretical 100kW wind facility the total number of required turbines are twenty EN, five JA, and one NP respectively. Each configuration has been compared from energy, environment, and economic aspect.

2.4 System boundary

As mentioned earlier, this LCA study has been done for Halkirk, Alberta, Canada. However, NP, EN, and JA turbines are produced in USA at Barre (Vermont), Ferndale (Washington), and Minneapolis (Minnesota) respectively. There was no clear picture available for the materials supply chain for the turbine manufacturers. This being said, material processing technologies for turbine production and their accompanying emission factors vary depending on country. To resolve the issue, energy and environmental impact of raw materials production for turbines manufacturing have been estimated based on the United States (US) standards. In cases where US data were not available, European data were used (Crawford 2009; B. Fleck & Huot 2009; Schleisner 2000).

Environmental impacts of diesel transportation fuel were estimated based on Alberta standard. This data were in an aggregated format which includes fuel extraction, refining, and transportation to service stations.

Concrete and steel rebar used in the turbine foundation is most likely to be procured from local facilities in Alberta. Therefore, environmental impacts from the raw construction materials estimated is based on Alberta specific data. Due to lack of data availability, evaluation of impacts from decommissioning, recycling and disposal were mostly based on European data (Martinez et al. 2009; GHK 2006; Giurco et al. 2006; Rieradevall et al. 1997).

A consolidated system boundary under this study has been shown in Figure 2-1. The scope of the unit processes are further detailed in the following subsections.

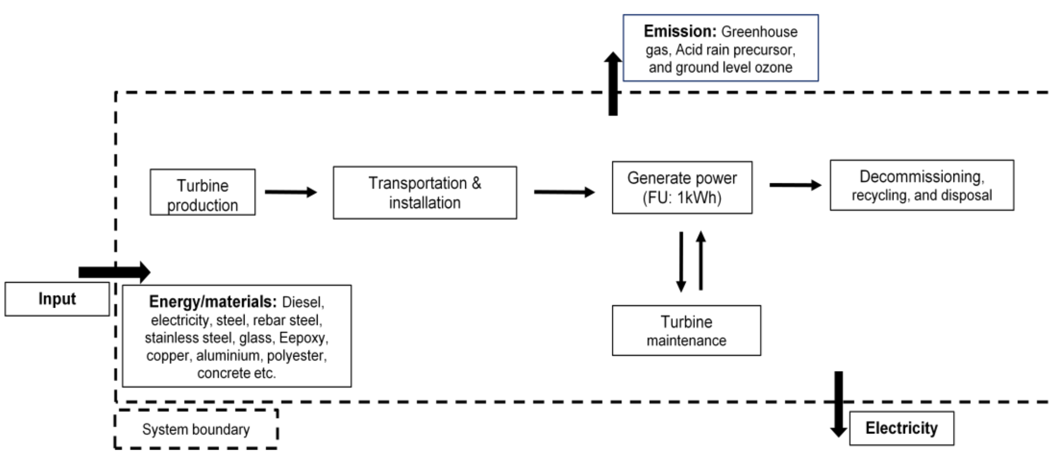

Figure 2-1: System boundary of the study

2.4.1 Turbine production

Energy and emission impact from production of all required raw materials to manufacture the turbine parts have been considered under this unit process. All inventory data are based on the material life cycle. Impacts during turbine manufacturing and assembling have been ignored as they were estimated to be negligible during analysis. The impacts of painting turbine parts were ignored in this study for two reasons. Firstly, previous studies have demonstrated limited impacts from painting compared to other processes. Secondly, there was a lack of applicable data for the wind turbines in this study. A detailed material description is presented in Table 2-1.

2.4.2 Transportation and installation

Transportation of all turbine parts is considered from each manufacturer to the wind site. Transportation of raw material to the turbine manufacturer has been ignored for two reasons: first, it is almost impossible to trace the complete raw material supply chain and second, their contribution in overall energy demand and environment was found to be insignificant with arbitrarily assigned values of transportation distance. This unit process also incorporates the production and transportation of foundation material to the site. All transportation distance (rail and truck) have been determined based on the information provided by the Canadian National railway (CN) (Coleman & Lessard 2011). The foundation material description is presented in Table 2-1.

Table 2-1: Inventory data for 100kWe nameplate wind power production facility

Components	Sub-components	EN		JA		NP	
		Weight	**Materials**	**Weight**	**Materials**	**Weight**	**Materials**
	Blade	0.5 t	Glass 0.3 t	0.34 t	Glass 0.20 t	1.8 t	Glass 1.08 t
Rotor			Epoxy 0.2 t		Epoxy 0.14 t		Polyester 0.72 t
	Hub	-	-	-	-	0.29 t	Steel 0.29 t
Nacelle	Generator	1.84 t	Steel 1.47 t	1.4 t	Steel 1.1 t	2.85 t	Steel 2.28 t
			Copper 0.37 t		Copper 0.3 t		Copper 0.57 t
	Frame, machinery and shell	1.84 t	Steel 1.36 t	1.4 t	Steel 1.03 t	2.85 t	Steel 2.11 t
			Copper 0.22 t		Copper 0.17 t		Copper 0.34 t
			Aluminum 0.17 t		Aluminum 0.13 t		Aluminum 0.26 t
			Glass 0.06 t		Glass 0.04 t		Glass 0.08 t
			Polyester 0.04 t		Polyester 0.03 t		Polyester 0.06 t
	Gearbox and hub	1.84 t	Steel 1.84 t	1.4 t	Steel 1.4 t	-	-
Tower	Main tower	41.2 t	Stainless steel 32.64 t	17.24 t	Steel 17.24 t	13.1 t	Steel 13.1 t
	Gin pole		Stainless steel 6.33 t	-	-	-	-
	Guy wire		Galvanized steel 2.20 t	-	-	-	-
Foundation	-	351.5 t	Concrete 350 t	352.5 t	Concrete 346.8 t	201.5 t	Concrete 192.4 t
			Steel rebar 1.5 t		Steel rebar 5.7 t		Steel rebar 9.1 t
Tower height	-	36.6 m		36.7 m		37 m	
Rotor diameter	-	5.5 m		9.45 m		21 m	

2.4.3 Generate power

This unit process represents the power production and does not associate any emissions. As all systems are grid connected, the establishment of a back-up power facility has been ignored due to irrelevance to the overall goal of the study. The power transmission and distribution has been kept out of the scope since it was assumed that this process is similar for all turbine configurations and therefore would not contribute sufficiently to differentiate them.

2.4.4 Turbine maintenance

This unit process considers the impacts from transportation of maintenance vehicle to the turbine site. It has been assumed that each turbine requires maintenance once in a year. In case of multiple turbine configurations (EN and JA), the maintenance requirement has been calculated by simply multiplying by the number of turbines under each configuration. Impacts associated with the lubrication (oil and grease) of wind turbine parts have been assumed to be negligible from a life cycle perspective.

2.4.5 Decommissioning, recycling and disposal

This unit process incorporates the impacts from dismantling, recycling and disposal of the turbine materials after the useful life of turbines. The steel, copper and aluminum recycling rates and associated emission coefficients are adopted from the best practices used in European wind turbine decommissioning (Martinez et al. 2009; B. Fleck & Huot 2009; GHK 2006; Giurco et al. 2006). It is assumed that recycled materials would be utilized to replace the virgin raw materials for future turbine manufacturing. Thus recycling contributes significantly in energy saving and avoiding emissions. After dismantling, impacts from non recyclable waste transport to the landfill and heavy equipment operations during landfilling are included (Rieradevall et al. 1997). Assumptions involved in this unit process and data references are presented in Table 2-2.

Table 2-2: Recycling and Waste Disposal (Martinez et al. 2009)

Material	Type of Dismantling
Steel	90 % recycled and 10% landfilled
Copper	95 % recycled and 5% landfilled
Glass fiber	100% landfilled
Aluminum	95 % recycled and 5% landfilled
Concrete	100% landfilled
Epoxy	100% landfilled

2.4.6 Environmental stressors

The environmental stressors that have been considered for the turbine systems are presented in Table 2-3. Despite having available data, environmental stressors like eco-toxicity, organic respiration, and inorganic respiration were not calculated in order to maintain the focus of the study. Other stressors such as land use, noise pollution, and impact on birds were not studied as they were assumed to be trivial for properly sited small wind turbine installations (Martinez et al. 2009; Martínez et al. 2008; Crawford 2009; B. Fleck & Huot 2009; Schleisner 2000).

Table 2-3: Environmental Stressors and weighting factors (Intergovernmental Panel on Climate Change 2007; Stranddorf & Hoffmann 2003)

Stressors	Units	Gases	Weighting factors
Greenhouse gases	gCO_{2eq}	CO_2	1
		CO	3
		CH_4	21
		N_2O	310
		HC	1
Acid rain precursor	gSO_{2eq}	SO_2	1
		NO_x	0.7
Ground level ozone	$g(NO_x+VOC)$	NO_x	1
		VOC	1

2.4.7 Functional unit

In order to compare turbine configurations, their performance characteristics i.e. required energy input, impacts on the environment and cost must be quantified under a fixed reference unit. This unit is known as functional unit (FU). This is necessary to ensure comparability of life cycle assessment results (ISO 2006a). The production of 1kWh of nameplate electricity has been used as the FU in this study.

2.5 Inventory assessment

2.5.1 Material inventory data

Raw material inventory data for different turbines are presented in Table 2-1. This information has been mainly adopted from previous studies (Endurance Wind Power 2009; Endurance Wind Power 2010a; Endurance Wind Power 2010b; Wind Turbine Industries Corp. 2009; Palmer n.d.; Northern Power Systems 2010; Northern Power Systems 2009a; Northern Power Systems 2009b). Though almost all the information was publicly available, some inventory data had to be obtained by personal communication with representatives from respective manufacturers. It is important to mention that EN and JA inventory data are adjusted for 100kW nameplate facilities i.e. data correspond to twenty EN and five JA turbines. Also, the addition of material weights is not always equal to the weight of a sub-component when the numbers were rounded off.

2.5.2 Material embodied energy and emission

Embodied energy and emission factors have been considered for all the required raw materials' production, recycling and disposal. Each factor has been determined by summing up the respective impact in every stage of material's life cycle. Embodied energy and emission factors can be found in Table 2-4. Table 2-4 also shows the factors for material recycling and landfilling. Some emission factors for recycling operations were very difficult to find but these were for processes with extremely small contributions to the overall life cycle impact, and so their differential impacts (the difference in impact between each of the three systems) was deemed to be extremely small.

Table 2-4: Embodied energy and emission inventory data (Martinez et al. 2009; Schleisner 2000; GHK 2006; Rieradevall et al. 1997; ICF Consulting 2005; White 2007; Athena Institute 2006; Athena Institute 2002)

Material	GJ/t	kg CO_2/t	kg CO/t	kg CH_4/t	kg N_2O/t	kg SO_2/t	kg NO_x/t	kg VOC/t
Material Production								
Steel	34.00	2473.00	0.93	0.04	0.07	14.50	9.50	0.16
Stainless steel	53.00	3275.00	0.93	0.04	0.07	14.50	9.50	0.16
Rebar steel	34.26	2163.83	26.53	0.10	0.07	6.62	2.88	3.74
Glass	8.70	566.00	0.65	0.04	0.01	1.23	2.45	0.15
Epoxy	45.70	3941.00	1.10	0.08	0.12	22.91	14.71	0.20
Polyester	45.70	3941.00	1.10	0.08	0.12	22.91	14.71	0.20
Copper	78.20	6536.00	1.57	0.16	0.19	35.61	23.19	0.25
Aluminum	39.15	3433.50	0.75	0.07	0.11	21.00	13.00	0.15
Concrete	0.81	119.02	-	0.03	8.7E-5	0.13	0.70	-
Material Recycling		**kg CO_{2e}/t**						
Steel	9.70	1819.00	-	-	-	-	-	-
Aluminum	16.80	738.00	-	-	-	-	-	-
Copper	6.40	3431.00	-	-	-	-	-	-
Landfilling								
Operations	0.04	0.90	0.01	0.04	-	0.002	0.01	0.01

2.5.3 Transportation data

Some unit processes in this study involve the transportation of products and materials. Transportation modes included light duty vehicle (LDV), high duty vehicle (HDV), and rail. Table 2-5 describes the turbine transportation scenario from each manufacturer to the wind site as provided by CN. Turbines will be transported using 53ft containers of International Organization for Standardization (ISO) standard. It is assumed that the LDV would be used during regular maintenance of turbines. Table 2-6 describes the emission factors involved in different transportation modes. When a vehicle is operating under no additional load e.g. during maintenance, while HDV would be released from Vancouver to collect turbines from Ferndale etc. emission factors were determined based on the distance travelled. In these cases, the vehicle fuel efficiencies (L/km) were evaluated based on 55% city and 45% highway driving (Transport Canada n.d.). Later, diesel emission factors were used to determine the overall emission. Under loaded conditions, emission factors were determined based on tonne-kilometre (tkm) travel. In all cases, diesel with the respective vehicle standard was considered to be the transportation fuel.

Table 2-5: Turbine transportation inventory data (Coleman & Lessard 2011)

Media	EN	km	JA	km	NP	km
HDV	Ferndale-Vancouver	325km	Peoria-Chicago	550km	Montreal-Barre	640km
Rail	Vancouver-Edmonton	870km	Chicago-Edmonton	1900km	Montreal-Edmonton	2930km
HDV	Edmonton-Halkirk	530km	Edmonton-Halkirk	530km	Edmonton-Halkirk	530km

Table 2-6: Transportation embodied energy and emission inventory data (Transport Canada n.d.; The Railway Association of Canada 2002; H. Mahmudi, P.C. Flynn 2005)

Mode	MJ	kg CO_2	kg CO	kg CH_4	kg N_2O	kg SO_2	kg NO_x	kg VOC	kg HC
HDV (tkm^{-1})	3.41	7.6E-02	7.5E-04	4.5E-05	2.9E-05	2.7E-05	1.6E-03	3.3E-04	1.1E-04
LDV (tkm^{-1})	5.08	3.5E-01	6.4E-04	8.9E-06	2.8E-05	4.0E-05	8.2E-04	3.5E-04	1.2E-03
Rail (tkm^{-1})	0.25	2.2E-02	6.3E-05	7.6E-06	5.5E-05	1.5E-05	3.3E-04	1.2E-04	1.7E-05

2.5.4 Assumptions and limitations

This life cycle study has been performed under some inevitable limitations and considerable assumptions. The assumptions not mentioned in previous sections are outlined below.

- Turbine lifetime has been assumed to be 25 years.
- Though this study accounts for regular turbine maintenance, component replacement is not considered for any of the configurations.
- For EN and JA, the relative weights of nacelle parts were not available. Therefore, it has been assumed that the subcomponents of nacelle (i.e. generator, frame, m/c & shell, and gearbox & hub) share the total nacelle weight equally. The raw material breakdown of these subcomponents has been adopted based on a previous study (Ancona & Mcveigh 2001).
- Taking into account the location of the turbine site to relevant facilities, the round trip transportation distance for foundation material delivery to the wind turbine site is assumed to be 200 km. Considering the location of turbine site to major cities where personnel would likely travel from, round trip distance for maintenance vehicle has been assumed as 400 km.
- The distance for landfilling and recycling is assumed to be 100 km from wind site for all configurations under decommissioning, recycling and disposal.
- The lower heating value of diesel has been assumed to be 39 MJ/L.

- The quality of data is inherently inconsistent. Since not all metrics were obtained from the same geographical and/or technological standards, uncertainty is inherent in these input data. It is assumed that uncertainty analysis performed in this study to assess an upper bound of the effects of this variability.
- This study does not include the impact analysis from water and solid pollutants.
- The energy and environmental impact from the transportation sector under all unit processes have been evaluated based on Canadian fuel and vehicle standard.

2.6 Energy and Environmental impact analysis

2.6.1 Energy impact

The calculated capacity factors for EN, JA and NP were found to be 0.23, 0.22 and 0.24 respectively. Based on the determined capacity factor configurations are capable of producing 5.1, 4.9, and 5.3 GWh, respectively, in their lifetime of 25 years. The primary energy required from fossil fuel sources for the configurations are 424.3, 221.5, and 133.3 kJ/kWh respectively. Figure 2 portrays the energy impact from each unit process for all configurations. In each configuration, 'Turbine production' has the highest energy share. This is reflected in the higher energy savings during recycling. EN has an exceptionally higher energy requirement for 'Turbine maintenance'. This is due to the assumption that the higher number of turbines in a configuration will require more maintenance since this calculation has assumed that maintenance trips will not be combined. The energy intensity factors for 100kW wind facility were found in the range of 118-1642 kJ/kWh based on 8 studies (Lenzen 2002). It is very difficult to compare this study with those, as they were performed in different locations and under different assumptions. This being said, the factors determined in this study fit within the mentioned range. Based on the conventional power plant efficiency of 40%, energy payback time for the turbine configurations is 1.4, 0.8, and 0.6 years respectively for EN, JA and NP, which compare well with previous studies which found the energy payback period between 0.39 to 2.29 years (Martinez et al. 2009; Schleisner 2000; Tremeac & Meunier 2009).

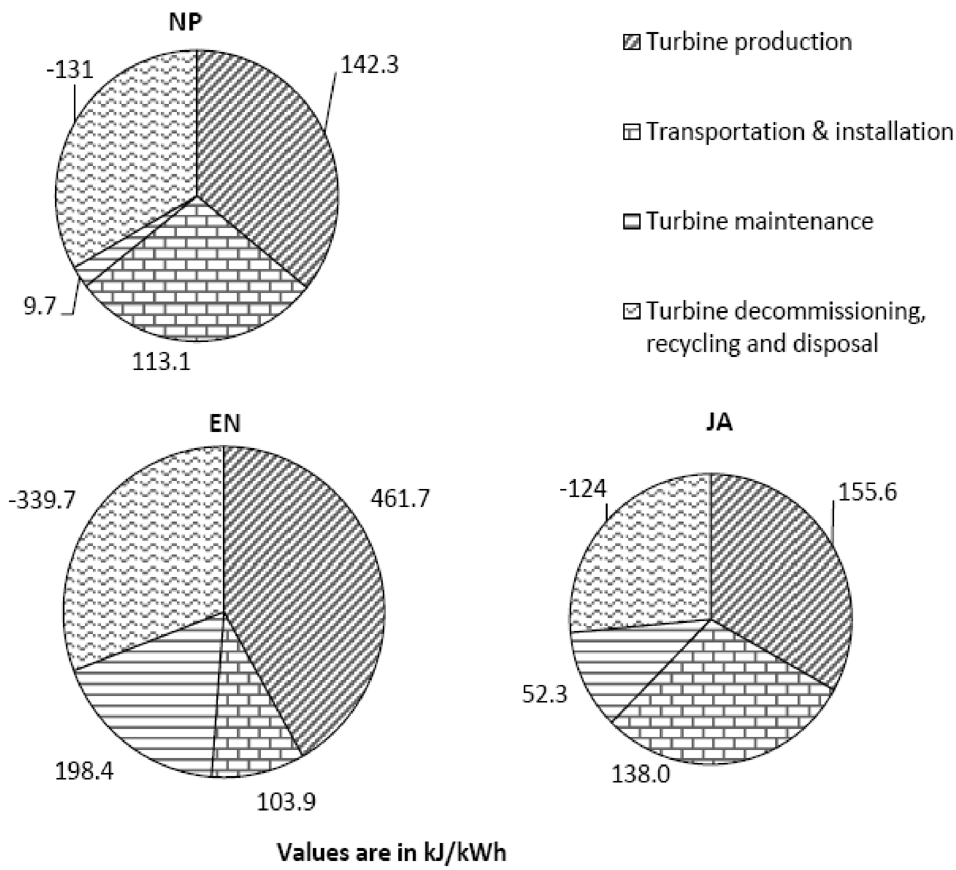

Figure 2-2: Breakdown of energy use by unit process for different configurations

2.6.2 Environmental impact

As mentioned earlier, this study investigated the environmental impact from wind systems taking three stressors into account; global warming, acidification, and ozone depletion. Figure 3 describes the environmental performance of EN, JA and NP. If a vertical line is drawn from the locator point (on primary horizontal axis) of each configuration, the intersecting points on the curves and secondary horizontal axis would provide the ozone depletion, acidification and global warming impacts for the respective configuration. For NP the ozone depletion, acidification and global warming impacts are 6.2×10^{-2} g($VOC+NO_x$)/kWh, 4.2×10^{-2} gSO_{2eq}/kWh and 17.8 gCO_{2eq}/kWh respectively. For JA and EN, impacts are 10.5×10^{-2} and 13.9×10^{-2} g($VOC+NO_x$)/kWh, 8.8×10^{-2} and 11.2×10^{-2} gSO_{2eq}/kWh, 25.1 and 42.7 gCO_{2eq}/kWh respectively. Similar results were found from other studies as well (Martinez et al. 2009; Schleisner 2000; Lenzen 2002; Tremeac & Meunier 2009; Mcculloch et al.

2000). As Figure 2-3 suggests, the bigger the size of a single turbine in a configuration, the more environmental advantage can be achieved; this finding is similar to size advantage known as "economies of scale" (Decarolis & Keith 2006). Figure 2-4 describes how different unit processes in each configuration contribute to the overall environmental impact. The current grid emission factor for Alberta can be estimated as 820g CO_{2eq}/kWh, 0.570g SO_{2eq}/kWh, 0.585g NO_x/kWh (Environment Canada 2007; Cuddihy et al. 2005). Based on this, the GHG emission payback periods were found 1.4, 0.8 and 0.5 years respectively for EN, JA, and NP. Acid rain and ozone depletion payback periods were found less than a week for all the configurations.

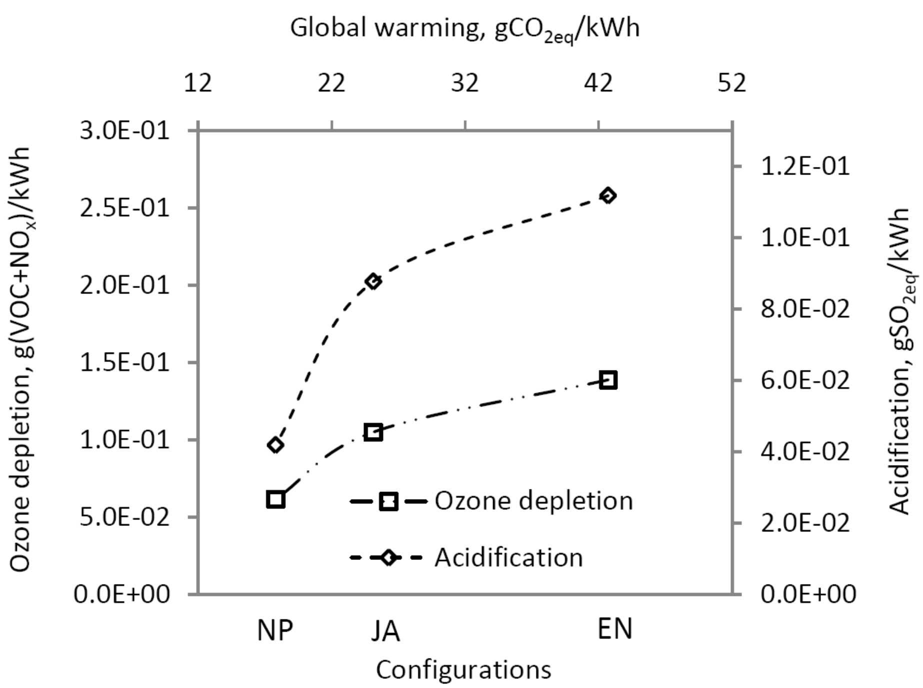

Figure 2-3: Environmental impact from three configurations

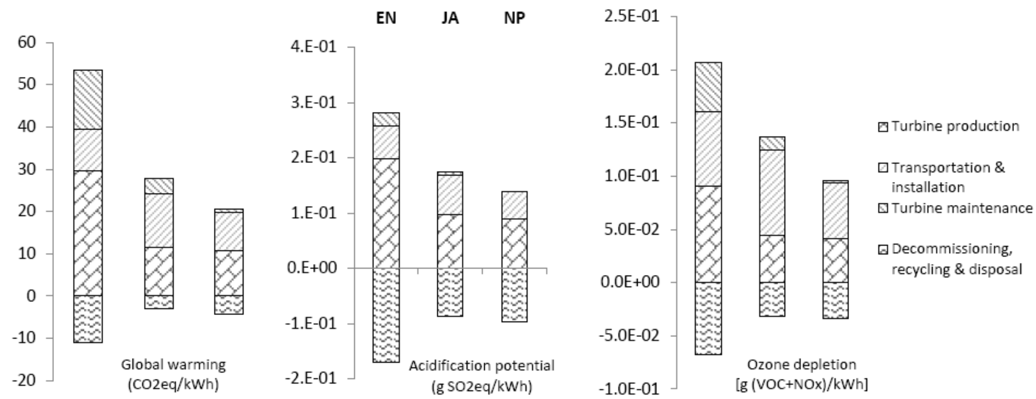

Figure 2-4: Relative environmental impacts by unit process

2.7 Uncertainty analysis

It is important to remember that 'inventory data' are important factors that critically determine the success of any LCA study. Since almost no data, irrespective of the source, are absolutely perfect, uncertainty analysis is a well accepted and recognized approach to improve the reliability of LCA results and estimate a bound of how inaccurate these estimates could be. In order to address the problems associated with 'inventory data', different data quality indicators have been proposed by a previous study (B. P. Weidema & Wesnæs 1996) which introduced five data quality indicators: reliability, completeness, temporal correlation, geographical correlation, and technological correlation. Data sources used in this study are reliable and complete within the defined system boundary of this study. Hence it is assumed that reliability and completeness criteria of inventory data are properly met in this study. In order to take care of other three quality indicators, methodologies described by previous studies were reviewed (M. a J. Huijbregts et al. 2001; B. P. Weidema 1998; van den Berg et al. 1999). Based on the review, a data quality matrix was developed as found from Table 2-7 and was applied to all inventory data to quantify the associated uncertainty. Overall uncertainty for an input datum was determined by taking the square root of the sum of squares of the three uncertainty factors, thus assuming uncorrelated errors, as determined from the matrix. From these values, uncertainty for a unit process has been determined using the weighted average method. Based on the developed data quality matrix, uncertainties found for different unit processes are presented in Table 2-8.

Table 2-7: Uncertainty determination matrix of inventory data

Assumed Uncertainty	5%	10%	20%	30%	50%
Temporal correlation	Less than 3 years of difference to year of study	Less than 6 years difference	Less than 10 years difference	Less than 15 years difference	Age of data unknown or more than 15 years of difference
Geographical correlation	Data from area under study (e.g. Alberta)	Data from larger area but including area under study (e.g. Canada)	Data from outside the specified location but with similar condition (e.g. USA/Denmark)	Data from outside the area but with slightly similar condition (e.g. Outside of North America and Europe)	Data from unknown area
Technological correlation	Data for similar process and materials from same producer and technology under study	Data for similar process or materials under study but from different producer	Data for similar processes or materials but from different technology	Data for related processes or materials but from same technology	Data for related processes or materials but from different technology

Table 2-8: Uncertainties for unit processes of all turbine configurations

Unit process	EN	JA	NP
Turbine production	32.2%	32.4%	33.1%
Transportation & installation	21.5%	21.5%	21.7%
Turbine maintenance	17.3%	17.3%	17.3%
Decommissioning, recycling and disposal	32.2%	32.4%	33.1%

It is important to note that assumed uncertainties for unit processes might be somewhat overestimated in few circumstances. However, they are helpful in detailing the LCA results by providing inputs from a probable range of values corresponding to different unit processes to Monte Carlo (MC) simulation. The MC simulation tool takes random values from a specified range (in this case +/- uncertainty range) for different unit processes, runs repeated iterations and provides an overall uncertainty in the final LCA results (Giurco et al. 2006; M. A. J. Huijbregts 1998) assuming a large enough sample size of test runs. Thus, it helps in conveying more information to the decision maker rather providing a fixed value, which could be of limited use. Figure 2-5 portrays the findings from MC analysis. It is apparent that for acidification, the impact of the configuration is comparable. However, if global warming and ground level ozone is the concern, the NP configuration is the best choice among the alternatives.

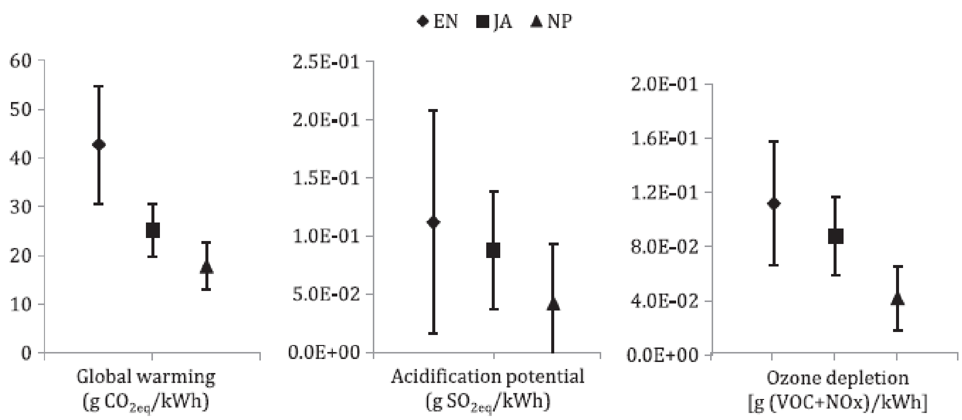

Figure 2-5: Comparison of impacts from configurations' under 95% confidence range uncertainties

2.8 Economic analysis

Economic analysis has been included in this LCA study to provide a comparative idea about the most likely power cost from the three options. Obviously this economic analysis is not a rigorous one but it covers all the fundamental and major aspects of wind energy economics. Unless otherwise mentioned, currency used in this analysis is 2010 Canadian dollar ($). Table 2-9 describes the assumptions associated with the economic analysis. Findings from the economic analysis are summarized in Table 2-10. It is apparent from Table 2-10 that, under the current electricity price, none of these configurations are close to economic viability; this reinforces the accepted belief that small wind power is not as economically attractive, and is usually only considered when electricity cost is not incentive for considering installation. Nevertheless, keeping the environmental advantages in mind, as well as considering the economic advantages that may occur with emission incentives these configurations can be quite effective.

Table 2-9: Input data and assumptions for economic analysis

Parameter	**Comments/Remarks**
Capital cost	It includes turbine purchasing, turbine transportation (delivery) and foundation cost. Purchasing cost of each 5kW turbine of EN is $49,830, each 20kW turbine of JA is $74,815 and 100kW of NP is $283,000. Turbine transportation cost was determined based on the quotation provided by CN plus the fuel surcharge cost for November 2010 (Coleman & Lessard 2011; Canadian National Railway 2011). Delivery costs of EN, JA, and NP configurations' are $3580, $3270, and $4500 respectively. Foundation cost was determined based on the quotation of steel and concrete price. Foundation costs were found $21,175 $25,650, $20,700 for EN, JA, and NP respectively.
O&M cost	Assumed as 2.5% of turbine cost. It includes the administration, regular maintenance, repair and insurance cost (Krohn et al. 2009).
Recycling and landfilling cost	It includes recycling cost, waste transportation and landfilling cost. Total costs were estimated $71,870, $70,350 and $39,900 for EN, JA and NP configuration respectively (Friesen et al. 2008).
Availability of turbine	Assumes as 97% due to probable shut down during maintenance.
Inflation rate	Assumed as 2% based on last 8 years average inflation rate of Canada (Statistics Canada 2010).
Internal rate of return	Scenarios have been developed for 10% and 15% Internal rate of return (IRR)
Interest	It has been assumed that the investment is 100% equity. So the project will be interest free.
Others	Road access to the proposed wind site already exists. So, Road construction cost has been ignored. Cost of grid connection is not included. It is assumed that the land required in the wind facility is owned by the investor. This discards the land rental cost as well from the analysis.

Table 2-10: Findings from economic analysis

	IRR	EN	JA	NP
Price of electricity ($/kWh)	10%	0.61	0.25	0.21
	15%	0.82	0.34	0.27
Simple payback period (years)	10%	9.68	9.53	7.82
	15%	6.89	6.85	5.92
Simple payback period under current electricity price in Alberta ($0.08/kWh)	-	Never	Never	Never

2.9 Conclusion

It was observed that 'Turbine production' and 'Transportation and installation' are the unit processes that mostly affect the life cycle energy and emission of small wind power. To reduce the impact of these unit processes, a solution would be to make raw material production more energy efficient and therefore less emission intensive. For example, as the majority of the raw material is steel, an improvement in energy efficiency of steel industries can make a significant improvement in the overall performance of all the configurations. The financial performance of the configurations is not attractive from an investor's standpoint. Government subsidy and incentives in support small wind would indeed need to be great to make such energy systems attractive from a purely revenue based perspective.

Three configurations of wind turbines' EN, JA, and NP were compared in this analysis from life cycle energy, emission and economic aspects. NP was found to be the superior configuration from all aspects. The differences between the relative performances of configurations are significant enough to pick NP as the suitable alternative for the intended nameplate wind power of 100kW.

A current issue in Alberta that this study addresses is the need to install small wind turbines using the local grid as the constraining variable, not the energy use of the installing individual or business. From an energy, emission, and economic standpoint, installing many smaller capacity wind turbines in order to reduce the effect of more emission intensive generation in Alberta is not the best solution. Although from an availability standpoint, more smaller capacity wind turbines may make more sense if maintenance issues or poor wind seasons in parts of the province arise. This all being said, this study does not consider any back up power facility for the configurations. Addressing the issue of availability of wind, natural gas and diesel can be considered as a complementary fuel to wind. Configurations under study can be integrated with any of these. Under such circumstances, how this life cycle study changes would be interesting to analyze and is strongly recommended for future studies.

2.10 References

Ancona, D. & Mcveigh, J., 2001. *Wind Turbine - Materials and Manufacturing Fact Sheet*, Available at: http://www.perihq.com/documents/WindTurbine-MaterialsandManufacturing_FactSheet.pdf. [Accessed June 22, 2011].

Athena Institute, 2006. *A life cycle perspective on concrete and asphalt roadways: embodied primary energy and global warming potential*, Available at: http://www.athenasmi.ca/publications/docs/Athena_Update_Report_LCA_PCCP_vs_HMA_Final_Document_Sept_2006.pdf. [Accessed June 22, 2011].

Athena Institute, 2002. *Cradle to Gate Life Cycle Inventory: Canadian and US Steel Production by Mill Type*, Available at: http://www.athenasmi.ca/tools/impactEstimator/companionReports/Steel_Production.pdf. [Accessed June 22, 2011].

van den Berg, N.W., Huppes, G., Lindeijer, E.W., van der Ven, B.L. & Wrisberg, M.N., 1999. *Quality assessment for LCA*, Available at: http://www.leidenuniv.nl/interfac/cml/ssp/publications/quality.pdf [Accessed June 22, 2011].

Blanco, M.I., 2009. The economics of wind energy. *Renewable and Sustainable Energy Reviews*, 13(6-7), pp.1372-1382.

CanWEA, 2010. Small Wind Market Survey. Available at: http://www.canwea.ca/pdf/SmallWind/canwea-smallwindmarketsurvey-e-web.pdf. [Accessed October 2010].

Canadian National Railway, 2011. Fuel Surcharge. Available at: http://www.cn.ca/en/shipping-prices-tariffs-fuel-surcharge.htm [Accessed October 2010].

Coleman, D. & Lessard, M., 2011. Personal Communication.

Crawford, R.H., 2009. Life cycle energy and greenhouse emissions analysis of wind turbines and the effect of size on energy yield. *Renewable and Sustainable Energy Reviews*, 13(9), pp.2653-2660.

Cuddihy, J., Kennedy, C. & Byer, P., 2005. Energy use in Canada : environmental impacts and systems. *Canadian Journal of Civil Engineering*, 32, pp.1-15.

Decarolis, J. & Keith, D., 2006. The economics of large-scale wind power in a carbon constrained world. *Energy Policy*, 34(4), pp.395-410.

Endurance Wind Power, 2011. S-343 Specifications. Available at: http://www.endurancewindpower.com [Accessed February 7, 2011].

Endurance Wind Power, 2010a. S-Series Guyed Tower Installation Manual. Available at: http://www.ctcleanenergy.com/Portals/0/Endurance_Tilt-Up_Tower_Installation_Manual_(58-221208) (3).pdf.

Endurance Wind Power, 2010b. S-Series Installation Manual. Available at: http://www.endurancewindpower.com/pdf/Endurance_S-250_Installation_Manual_69-030509.pdf.

Environment Canada, 2011. Canadian Wind Energy Atlas. Available at: http://www.windatlas.ca/en/nav.php?no=44&field=E1&height=50&season=ANU [Accessed March 2011].

Environment Canada, 2007. *National Inventory Report 1990-2007: Greenhouse Gas Sources and Sinks in Canada*, Available at: http://www.ec.gc.ca/Publications/B77E6264-D0E3-45B5-BE56-5A395C0B7653/NationalInventoryReport19902007GreenhouseGasSourcesAndSinksInCanada.pdf. [Accessed March 2011].

Farrugia, R., 2003. The wind shear exponent in a Mediterranean island climate. *Renewable Energy*, 28(4), pp.647-653.

Fleck, B. & Huot, M., 2009. Comparative life-cycle assessment of a small wind turbine for residential off-grid use. *Renewable Energy*, 34(12), pp.2688-2696.

Friesen, B., Morawski, C. & Morris, J., 2008. *True Costs of Composting Municipal Organic Waste*, Recycling Council of Alberta. Available at: http://www.recycle.ab.ca/2008Proceedings/BarryFriesen.pdf. [Accessed August 7, 2010].

GHK, 2006. *A study to examine the benefits of the End of Life Vehicles Directive and the costs and benefits of a revision of the 2015 targets for recycling, re-use and recovery under the ELV Directive*, Available at: http://ec.europa.eu/environment/waste/pdf/study/final_report.pdf.

Gipe, P., 2004. *Wind power: renewable energy for home, farm, and business* 2nd ed., Chelsea Green Publishing.

Giurco, D., Stewart, M., Suljada, T. & Petrie, J., 2006. Copper Recycling Alternatives: An Environmental Analysis.*Environmental Engineering Research Event*. Available at: http://www.isf.uts.edu.au/publications/Giurcoetal2006copperrecycling.pdf [Accessed August 7, 2010].

Government of Alberta, 2008. *Alberta's 2008 Climate Change Strategy*, Available at: http://environment.gov.ab.ca/info/library/7894.pdf. [Accessed August 7, 2010].

H. Mahmudi, P.C. Flynn, M.D.C., 2005. Life cycle analysis of biomass transportation: trains vs. trucks. In *SAE World Congress & Exhibition*. pp. 2005-01-1551.

Huijbregts, M. a J., Norris, G., Bretz, R., Ciroth, A., Maurice, B., Bahr, B., Weidema, B. & Beaufort, A.S.H., 2001. Framework for modelling data uncertainty in life cycle inventories. *The International Journal of Life Cycle Assessment*, 6(3), pp.127-132.

Huijbregts, M.A.J., 1998. Application of Uncertainty and Variability in LCA. *The International Journal of Life Cycle Assessment*, 3(5), pp.273 - 280.

ICF Consulting, 2005. *Determination of the Impact of Waste Management Activities on Greenhouse Gas Emissions: 2005 Update*, Available at: http://rcbc.bc.ca/files/u3/ICF-final-report.pdf. [Accessed June 7, 2010].

ISO, 2006. ISO 14040:2006 - Environmental management -- Life cycle assessment -- Principles and framework.

Intergovernmental Panel on Climate Change, 2007. *Climate Change 2007: The Physical Science Basis* H. L. M. Solomon, S., D. Qin, M. Manning, Z. Chen, M. Marquis, K.B. Averyt, M. Tignor, ed., Cambridge University Press.

Krohn, S., Morthorst, P.-E. & Awerbuch, S., 2009. *The Economics of Wind Energy*, Available at: http://www.ewea.org/fileadmin/ewea_documents/documents/publications/reports/Economics_of_Wind_Main_Report_FINAL-lr.pdf [Accessed March 4, 2011].

Lenzen, M., 2002. Energy and CO2 life-cycle analyses of wind turbines—review and applications. *Renewable Energy*, 26(3), pp.339-362.

M. Raynolds, M.D. Checkel, R.A.F., 1999. Application of Monte Carlo analysis to life cycle assessment. *SAE Technical Paper*. Available at: http://papers.sae.org/1999-01-0011. [Accessed June 7, 2010].

Martinez, E., Sanz, F, Pellegrini, S, Jimenez, E. & Blanco, J, 2009. Life cycle assessment of a multi-megawatt wind turbine. *Renewable Energy*, 34(3), pp.667-673.

Martínez, E., Sanz, Félix, Pellegrini, Stefano, Jiménez, E. & Blanco, Julio, 2008. Life-cycle assessment of a 2-MW rated power wind turbine: CML method. *The International Journal of Life Cycle Assessment*, 14(1), pp.52-63.

Mcculloch, M., Raynolds, M. & Laurie, M., 2000. *Life-Cycle Value Assessment of a Wind Turbine*, Available at: http://pubs.pembina.org/reports/windlcva.pdf. [Accessed August 12, 2010].

Northern Power Systems, 2009a. Northwind 100 Logistics & Installation Guidelines. , (May). Available at: http://www.dcpowersystems.com/documents/Northwind100-InstallationGuidelines.pdf. [Accessed June 7, 2010].

Northern Power Systems, 2009b. Northwind 100 drawing. Available at: http://www.planning.eastlothian.gov.uk/WAM/doc/Drawing-777307.pdf;jsessionid=7A6465B5F7FF345353939963A2E19C91?extension=.pdf&wmTransparency=0&id=777307&wmLocation=0&location=VOLUME1&contentType=application%2Fpdf&wmName=&pageCount=1. [Accessed August 7, 2010].

Northern Power Systems, 2010. Northwind 100 specification sheet. , p.2. Available at: http://www.northernpower.com/pdf/specsheet-northwind100-us.pdf. [Accessed August 7, 2010].

Palmer, C., Personal Communication.

Rieradevall, J., Domènech, X. & Fullana, P., 1997. Application of life cycle assessment to landfilling. *The International Journal of Life Cycle Assessment*, 2(3), pp.141-144.

Schleisner, L., 2000. Life cycle assessment of a wind farm and related externalities. *Renewable Energy*, 20(3), pp.279-288.

Statistics Canada, 2010. *Latest release from the Consumer Price Index*.

Stranddorf, H. & Hoffmann, L., 2003. LCA Guideline: Update on impact categories, normalisation and weighting in LCA. Selected EDIP97-data. Available at: http://scholar.google.com/scholar?hl=en&btnG=Search&q=intitle:LCA+Guideline:+Update+on+impact+categories,+normalisation+and+weighting+in+LCA.+Selected+EDIP97-+data#8 [Accessed June 22, 2011].

The Railway Association of Canada, 2002. A response to the "Discussion paper on Canada"s contribution to addressing climate change'. , (July 2002). Available at: http://www.silvertipdesign.com/BR(Imperial)/%5B8%5D%20Railway%20Assoc%20of%20Canada.pdf 8 [Accessed March 16, 2011].

Transport Canada, Urban transportation emission calculator: GHG Emmission Factors. Available at: http://wwwapps.tc.gc.ca/Prog/2/UTEC-CETU/FuelEfficiency.aspx?lang=eng [Accessed October 2010].

Tremeac, B. & Meunier, F., 2009. Life cycle analysis of 4.5MW and 250W wind turbines. *Renewable and Sustainable Energy Reviews*, 13(8), pp.2104-2110.

Weidema, B.P., 1998. Multi-user test of the data quality matrix for product life cycle inventory data. *The International Journal of Life Cycle Assessment*, 3(5), pp.259-265.

Weidema, B.P. & Wesnæs, M.S., 1996. Data quality management for life cycle inventories–an example of using data quality indicators. *Journal of Cleaner Production*, 4(3-4), pp.167–174.

White, S.W., 2007. Net Energy Payback and CO2 Emissions from Three Midwestern Wind Farms: An Update. *Natural Resources Research*, 15(4), pp.271-281.

Wind Turbine Industries Corp., 2009. Jacobs Wind Systems Model 31-20 20kW specification sheet. Available at: http://www.windturbine.net/documents/WTIC Brochure 2010.pdf. [Accessed June 7, 2010].

3 Wind Conditions Assessment and Turbine Performance Evaluation

3.1 Introduction

Small wind turbine performance analysis is conducted by testing centers to certify the power curve of a wind turbine and to verify the performance of an installed and operating machine by interested owners. While it may be economically or logistically feasible for testing organizations to follow the 61400-12-1 testing standard and outfit a separate met tower for performance analysis, this is often not sensible for existing owners. To a certain degree, uncertainty from reference masts propagates in the horizontal plane of the flow region, whereas the uncertainty from a tower mounted anemometer is from vertical variation due to wind shear. The application of multiple cup anemometers in the performance assessment of a small wind turbine reduces the uncertainty in the vertical plane. Field-tested methods and performance data from well structured studies are highly beneficial in growing the small wind energy industry, which is the key goal in this study.

3.1.1 Research Approach

3.1.1.1 Research Questions

Considering the field testing of a small wind turbine, it is important to select specific queries to study:

- Can the wind resource of Halkirk, AB be properly characterized using instruments mounted on the tower of an operating wind turbine?
- Can the performance of a small wind turbine be properly characterized in-situ using tower mounted instruments?
- Can the horizontal wind velocity be accurately predicted at different locations below hub height using tower mounted instruments?

The purpose of this portion of this thesis was to develop a monitoring system capable of measuring the wind resource in which the turbine was installed. As well, characterizing the performance of the turbine using a combination of industry standards and practical methods was important. Lessons learned will lead to a specific set of methods for in-situ performance assessment.

3.1.1.2 Experimental Set up

The small wind turbine at the focus of this section of the study was installed in the fall of 2008 by Derek Brown and Steve McKnight. Derek Brown is an experienced wind energy professional, previously involved in a number of small wind turbine installations in Minnesota and met tower installs and maintenance throughout Southern Alberta. The turbine was tested and commissioned under supervision of a qualified and experienced electrician and began producing energy on February 4th, 2009. The turbine situated on the McKnight's property was the first wind turbine installed under the Alberta Microgeneration Regulation. The Alberta Microgeneration Regulation was brought into effect in January 1st, 2009 and greatly simplifies the process of grid connecting micro-generators to the distribution system in Alberta (Weis et al. 2010). In summary, the turbine was sized using the consumption of the farm and transformer connecting the yard to the distribution system as guides. The McKnights have a bi-directional energy meter which keeps track of their consumption as well as the turbine production. The electricity consumption of the McKnight's farm is offset and in addition, they are paid a negotiated rate from their energy retailer for any excess that the turbine produces.

The Endurance S-343 turbine was the result of work by Windward Engineering as part of a Department of Energy (DOE) contract from 2004 to 2006. The product of this work was then offered for sale through Endurance Wind Power in 2007. The turbine was designed specifically for the large number of homes that are grid connected, have suitable wind (Class 2 or higher), and sufficient space (1/2 acre or more) (Endurance Wind Power 2011). Performance monitoring of Endurance prototypes originally occurred both at the Spanish Forks facility and the National Wind Testing Center (NWTC) in Golden, Colorado as part of the DOE contract.

The performance monitoring of this turbine model was the first known to the author in Canada, be it monitored for commercial, educational, or personal purposes. The testing of an Endurance S-343 is currently being performed at the Windward Engineering testing facility in Spanish Fork, Utah, with public results as part of the certification process most likely available in the latter half of 2011. The testing commissioned by the Small Wind Certification Council (SWCC) in order to certify that it meets the requirements of the new American Wind Energy Association

(AWEA) Small Wind Turbine Performance and Safety Standard. The monitoring of an S-343 located at a high school in Coventry County, Connecticut was started in May 2011 through the Connecticut Clean Energy Fund's small wind turbine demonstration project. The installation of two S-343s is planned for construction in late 2011 at the WindTech Research and Development Facility, a joint venture led by Ryerson University which will include the a total of six SWTs of total power rating of 40.1kW.

The Endurance S-343 is an upwind, horizontal axis wind turbine with a manufacturer rated capacity of 5.2 kW at 11m/s. The turbine consists of a three blade, 6.37m diameter fixed-blade rotor directly coupled to a constant velocity synchronous induction generator via a gearbox. Rotor velocity necessary for AC energy production at grid frequency is achieved by drawing from the grid and motoring to up to the appropriate RPM. Passive stall and a compressed air braking system are utilized for rotor control at high wind velocities and emergency braking. The S-343 is mounted on a 38.7m tall, 8-inch tilt up tower in an open field to the North of the McKnight's yard. The turbine tower is tilted for maintenance to the turbine and instruments using a 3:1 pulley system ratio and a medium size farm tractor. Anemometers attached to tower mounted booms at multiple elevations on the turbine tower provide data for assessing turbine performance. A cross-section of the turbine nacelle is detailed in Figure 3-1. A representation of the turbine set-up and tower mounted instruments is shown in Figure 3-2 for reference. A summary of the turbine information is displayed in Table 3-1.

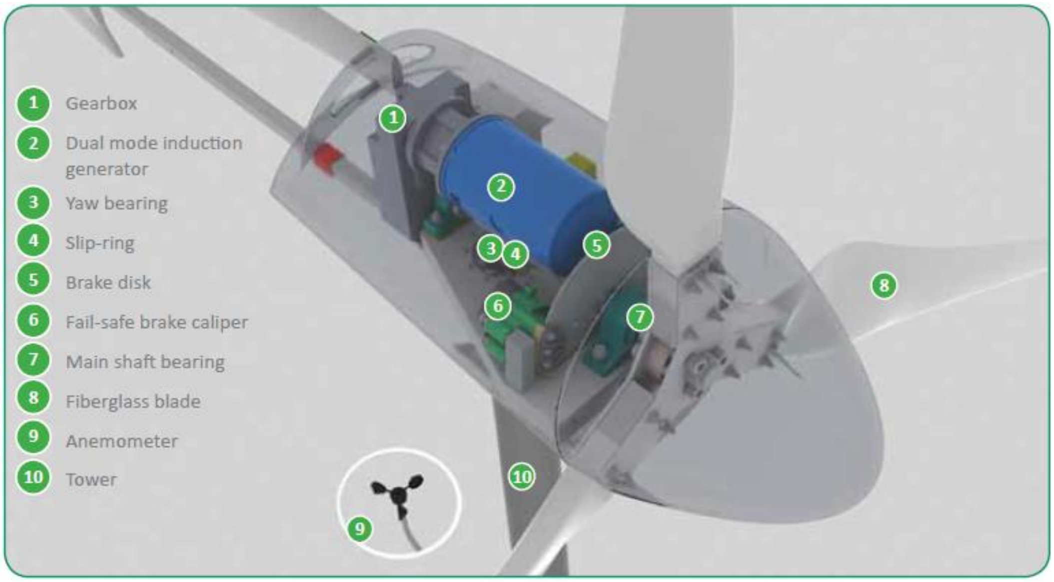

Figure 3-1: Endurance S-343 Cross-section (Endurance Wind Power 2011)

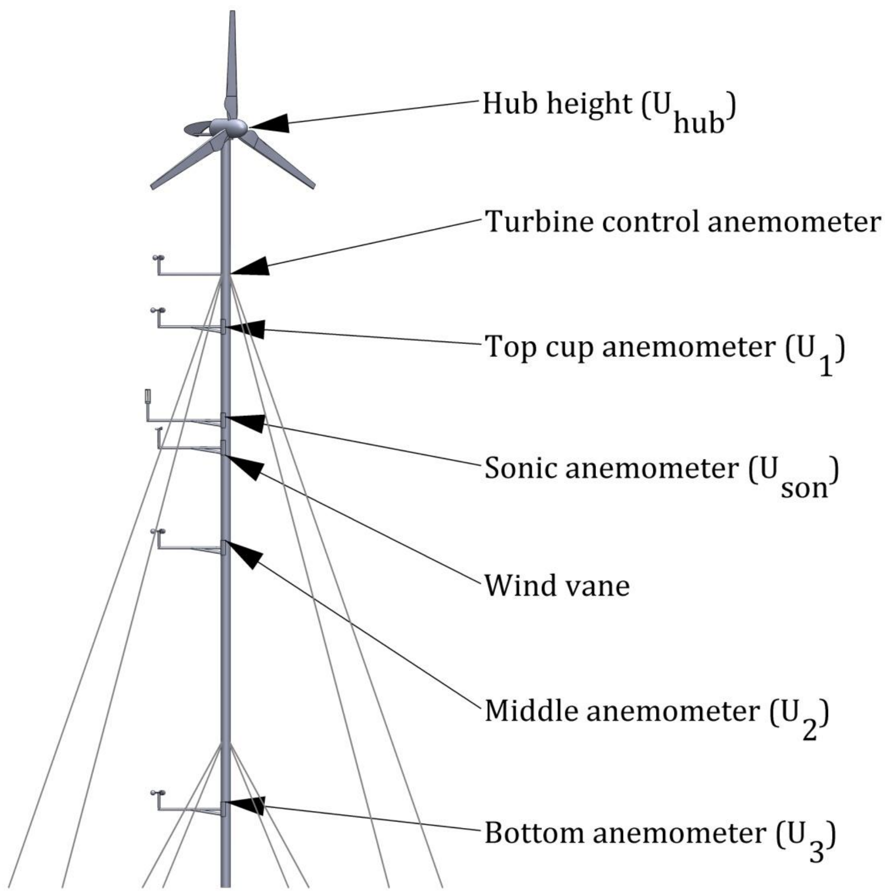

Figure 3-2: Instrument locations and accompanying variable definitions

Table 3-1: Turbine Configuration and Operational Data

General Configuration	
Turbine make, model, serial number, production year	Endurance, S-343, EWP-1G080049-25050, 2009
Rotation Axis (H,V)	Horizontal
Orientation (upwind/downwind)	Upwind
Number of Blades	3
Rotor hub type	Rigid
Rotor diameter (m)	6.37m
Hub height (m)	38.7m
Performance	
Rated electrical power (kW)	5.3
Rated wind velocity (m/s)	11
Cut-in Velocity (m/s)	4.1
Cut-out wind velocity (m/s)	24
Rotor/Blades	
Swept Area (m^2)	31.6
Direction of Rotation	Counterclockwise
Rotor situation	Upwind
Fixed or variable pitch	Fixed
Blade make, type, serial number	Endurance, fiberglass/epoxy,36-2
Rotor velocity wind range (rpm)	166
Emergency braking system	Rapid and redundant fail-safe mechanical brake on rotor shaft
Generator	
Type	Synchronous induction generator
Voltage	230V, single phase
Control system (device and software version)	Field-programmable embedded controller, software version 9.2.7, cup anemometer for cut-in and cut-out
Tower	
Tower type	Tubular guyed
Material	Galvanized steel
Height (m)	36.6
Yaw system	
Wind Direction Sensor	Tail Vane

Four anemometers were used in the data collection system: three NRG 40C cup anemometers and an R.M. Young 81000 three-dimensional sonic anemometer. The NRG 40C cup anemometer has three conical plastic cups and transfers the kinetic energy in the air into a low level AC signal, which is converted into a digital signal read by the data logger. The R.M. Young 81000 anemometer determines wind velocity from the change in the propagation of sound waves between a sound transmitter and a receiver due to the magnitude of the incoming wind flow and converts these readings onboard into digital or analog signals for logging. All tower mounted instruments were installed on the turbine tower at a boom offset of 67° to true north. This value was determined at install using a special inclinometer and corrected to true north using the deviation of Earth's geomagnetic field at the location. The three cup anemometers were installed on the turbine tower at heights of 33.8, 27.4, and 20.8 m from the ground. The sonic anemometer was installed with its sensing volume at a distance of 31.5 m from the ground. The distance from blade tip to the centre of the sonic anemometer's sensing volume is 4.0m, or 1.13 rotor diameters from hub height. These distances are described schematically in Figure 3-3. Additional drawings of the system are located in Appendix F.

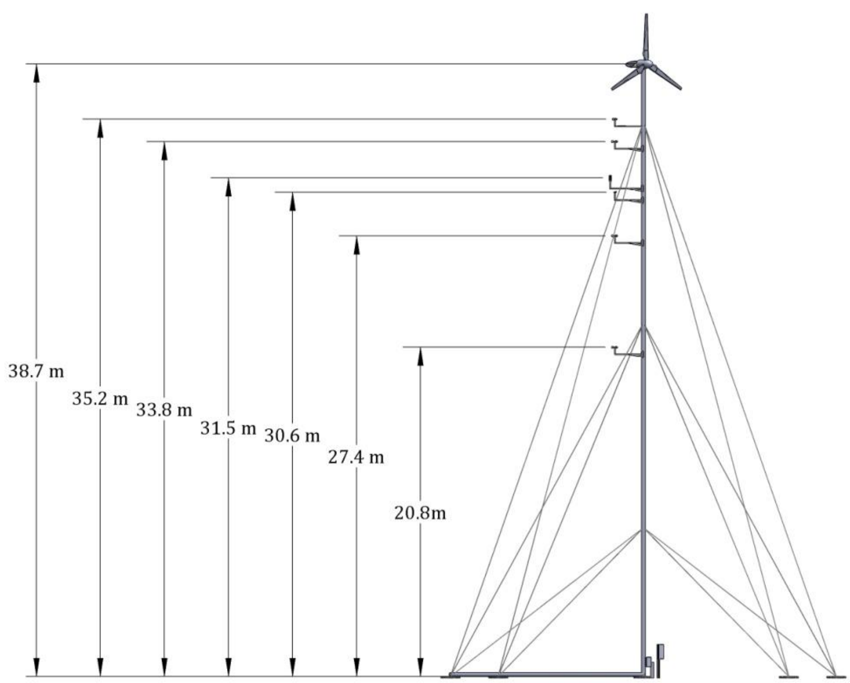

Figure 3-3: Experimental setup with instrument and turbine heights

The use of sonic anemometry in this study is by no means an endorsement of the technology. These instruments are very expensive, less robust, and more sensitive to icing and fogging incidents compared to traditional cup anemometers.

Wind direction was measured using an NRG 200S direction sensor installed at 30.6m. The wind vane is a 10K ohm potentiometer. The potentiometer is excited by a 5 volt power supply and a voltage drop is measured at the wiper which outputs a signal that varies linearly with wind direction. When available, azimuth was measured by the sonic anemometer along with 2-D horizontal and vertical components of wind velocity which were derived from the three-dimensional wind velocities and azimuth heading.

Power was measured using a bi-directional Ohio Semitronics Inc (OSI) PC5 series three-phase three-wire (two-element) watt transducer with external current transducer coil sensors. The watt transducer was installed on the turbine side of the grid connection that powered the data acquisition system so as to only measure power consumption and production from the turbine. The PC5 series watt transducers use Hall Effect multipliers that provide a 0-5V direct current (DC) output signal proportional to the electric power produced derived by continuously multiplying voltage and current readings (Ohio Semitronics Incorporated 1998). According to the instrument documentation, PC5 watt transducers are calibrated for voltage and current linearity, power factor, and initial set point using instrumentation traceable to the National Institute of Standards and Technology (NIST). Factory calibration is performed on a single phase power. Further details concerning post-calibration of the instrument are detailed in Appendix E.

3.1.1.3 Deviation from IEC Standard Procedures

Installation of a meteorological tower was not deemed logistically or financially feasible at this location for the collection of turbine hub height data. As discussed earlier, the recommended location of the met mast is between 2 and 4 rotor diameters upwind from the turbine. Installation of a met tower even at the maximum recommended distance of 4 rotor diameters (D_{rotor}) was not physically possible due to the location of turbine tower guy wires and guy wire foundation 15m upwind to the north, west, and south directions from the turbine base. The guy wires and guy wire foundations of a met tower of an equivalent height to the turbine tower height would impinge on the current guy wires and guy wire foundations of the turbine, making tilting of either mast for maintenance difficult and even dangerous. On top of these issues of turbine site logistics, erection of an additional 38.7m tower was not deemed financially feasible or essential in order to accomplish the project goal of in situ performance monitoring of a grid connected turbine installed in a rural location.

Practicality, financial resources, time constraints, and general scope of the project led to various compromises with respect to following IEC testing standard. Other differences are detailed below:

- The NRG 40C is a high quality instrument and the industry standard for wind resource assessment, but is not officially certified as Class 1.7A.
- The OSI transducer is a very robust piece of equipment used in the monitoring of many small wind turbines across North America, but is not certified to the requirements of Class 0.5 outlined in IEC 60186.
- The NRG pressure sensor was not mounted close to hub height as preferred, but was corrected to hub height according to ISO 2533 as per recommendations in 61400-12-1.

3.1.1.4 Data Collection and Processing

All onsite data was recorded using a Labjack UE9 data logger with a Campbell Scientific LLAC4 module for pulse channels and a netbook laptop computer for storage of data. Electric power to the system was drawn from the grid side of the power transducer, as opposed to the turbine side which would have caused error in the data due to self consumption. Data equipment was contained within an insulated custom enclosure mounted on a post at the base of the tower. Temperature control of the logging equipment enclosure was performed using a temperature sensor in combination with several relays, a 60W heating element, and two 3-inch computer fans. Hourly data log files were created using a data logger sampling rate of 10Hz, which was then decimated to 1Hz for storage. All channels were recorded at 1Hz except for pressure and temperature, which were logged every 10 seconds. An overview of the data acquisition system is presented in Figure 3-4. Wiring diagrams detailing connections is compiled in Appendix A.

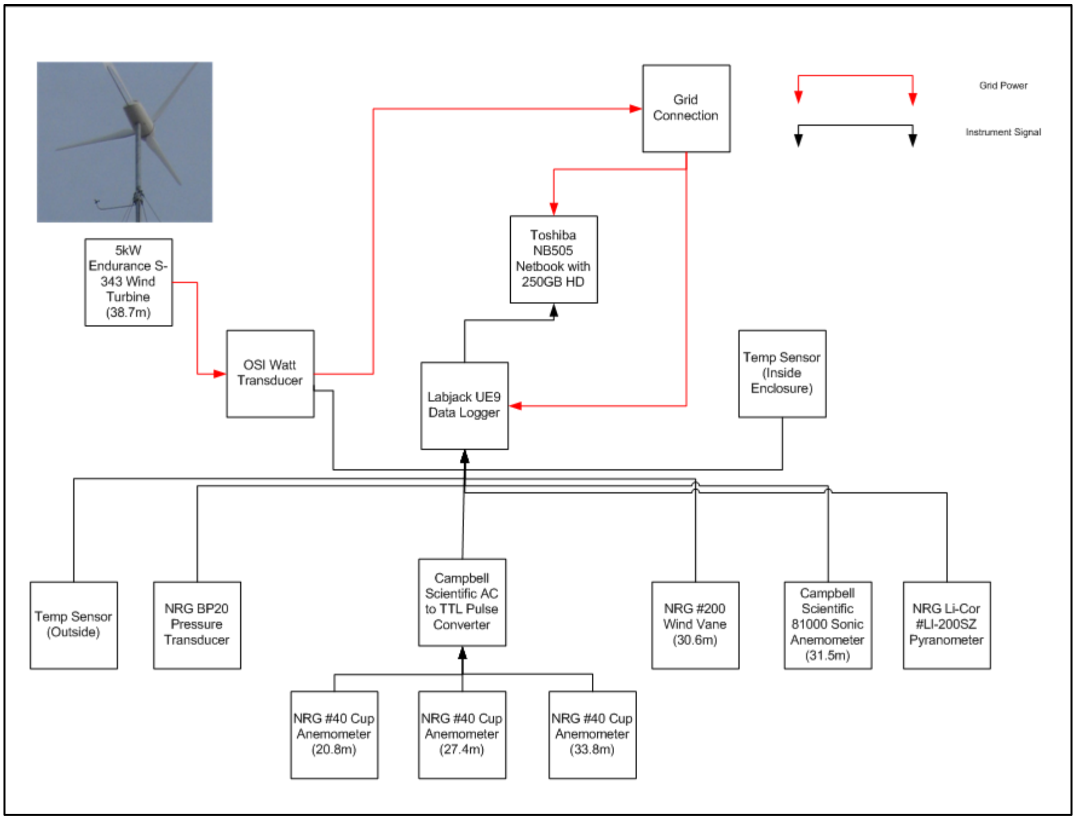

Figure 3-4: Overview of Data Acquisition System

Data collection occurred over a period of 482 days from March 5th, 2010 to July 1st, 2011. Datasets were retrieved from the site using remote desktop via Internet access. Measurements were not taken on some days due to turbine tower tilting for maintenance, power outages, icing events, and logging errors. Of the 482 days, the turbine was operational for 321 of these days, and wind data was available for 300 of these days. Sufficient data were collected in order to meet the requirements of IEC 61400-12-1 for power performance testing of a small wind turbine as well as a satisfactory amount of data to properly characterize the microsite of the turbine on an annual basis. Post processing of the data was completed using a combination of Microsoft Visual Basic, MATLAB 7.9.0, and Windographer wind data analysis software (Microsoft 2007; Mathworks 2009; Mistaya Engineering Inc. 2011). As per IEC 61400-12-1, part of post processing involved calculation of statistics of datasets including mean value, standard deviation, maximum, and minimum value for the selected time stamp.

During post-processing of the data, all wind direction sensor values from the NRG #200P after September 23rd, 2010 20:00 were called into question. Further investigation in January 2011 yielded the cause of failure to be electro-static discharge which left the instrument incapable of covering the entire instrument range, but still capable outputting reasonable enough values to not suspect issues. Because of this unfortunate event, it was decided that in-depth analysis of turbine power performance would focus on a period of 68 days between August 14th, 2010 and October 21st, 2010. The failure of an RPM sensor which prevented the turbine from operating after October 21st and the failure of the sonic anemometer on November 14th meant that simultaneously logged power and wind direction values were not available at the turbine site after October 21st, 2010. The period of 68 days from August 14th to October 21st will be referred to as the turbine performance measurement campaign during the rest of this thesis. Hourly statistics concerning directional instrument and turbine availability on a monthly basis over the measuring campaign are shown in Figure 3-5.

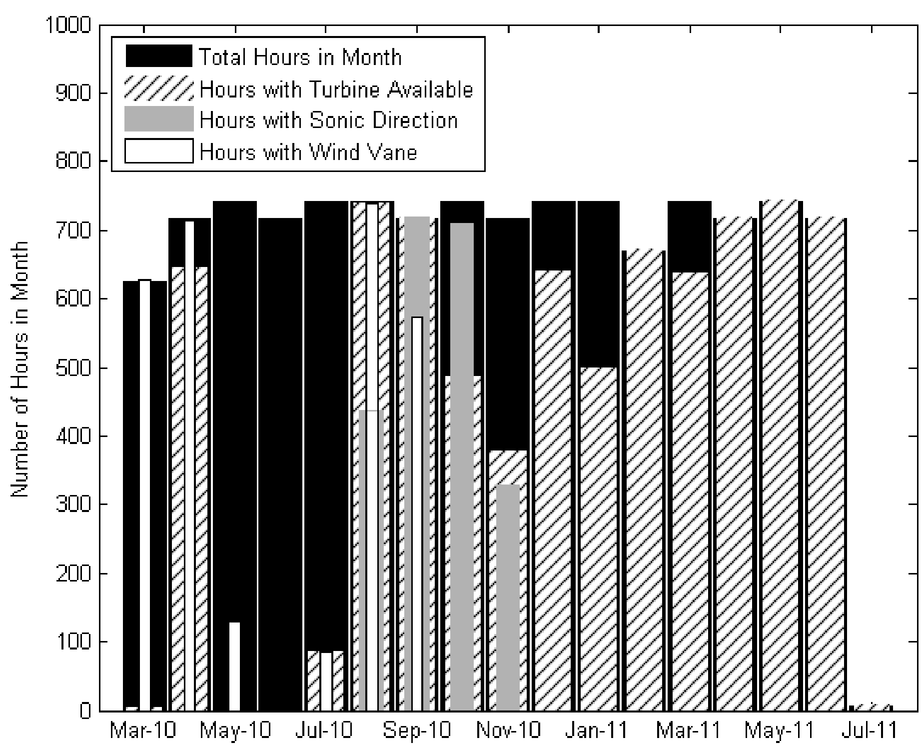

Figure 3-5: Turbine and wind direction instrument availability

In terms of the wind resource assessment performed, unless otherwise stated 60 minute averaged data were utilized from a dataset spanning the entire measuring campaign. The 60 minute averaging value is sufficient for wind resource assessment and allows wind direction values from the Environment Canada database of a local airport to be utilized. In both the turbine performance wind resource assessment, all channels except wind direction are averaged using the mean of all samples. Due to the non-linear measuring system of wind direction, the unit vector average value was calculated. The standard deviation for all channels except wind direction was determined as the true population standard deviation within each averaging interval. For wind direction, the Yamartino method was used to calculate the standard deviation due to its excellent results in most cases (Turner 1986) and recommendation by industry (D. T. Bailey 2000).

With regard to the turbine performance measurement campaign, 1 minute averaged data were utilized. The dataset includes averaged wind velocity values from 3.1m/s and higher, following the IEC standard that states that the cut-off for minimum wind velocities included in analysis should be 1 m/s lower than turbine cut-in wind velocity. The upper wind velocity requirement from this standard is a minimum of 10 minutes of data from a wind velocity of 1.5 times the wind velocity at 85% of the rated power of the turbine. The S-343 turbine is rated at 11m/s, resulting in an upper wind velocity requirement of 14.5m/s. During the period of time that the performance analysis measurement campaign occurred, the highest wind velocity bin filled using one minute averages was 16.5m/s, meaning sufficient amount of data to perform a full turbine performance analysis was acquired.

3.1.1.5 Site Description

The turbine monitored in this study is installed on a farm in east-central Alberta near the village of Halkirk at the exact location of 52°19'56.68"N, -112° 8'47.76"W and base elevation of 793m, approximately 200km southeast of the city of Edmonton. The location is shown in Figure 3-6. The turbine is installed north of the farm yard at which it connects to the electrical grid and is open to the north, west, and east directions. The prevailing wind for the turbine location is from the northwest. Instrument booms were installed to extend to the northwest in order for tower shadow to only affect measurements from the southeast direction. When analyzing a small wind turbine test site, according to IEC standards obstacles and terrain within $20D_{rotor}$ is the radius of interest. The most predominant obstacles within this radius to note include a dense row of mature coniferous trees 5-10m in height 30m to the south of the turbine location, separating the open pasture to the north from the farmyard. In addition, a stand of shorter less dense deciduous trees flank the turbine site 60m to the southwest. Other obstacles on site included a stack of railroad ties to the east of the turbine base which serve as a support for the turbine tower when it is tilted over for maintenance. The radius of interest at the turbine site is highlighted in Figure 3-7.

Figure 3-6: Turbine Location Overview with 50m Scale (Google Maps 2011)

The terrain of the turbine location is mostly flat, with slopes of the area of interest within 20 rotor diameters no greater that 2.5%. Surface roughness of the surrounding field varied with the seasons and contained non-grazed Prairie grass during the summer months and accumulations of snow during the winter months. Following the requirements outlined in Annex B of IEC 61400-12-1 for site assessment, it was concluded that the turbine site was not a complex terrain site. If the turbine site was considered a complex terrain site, site calibration would be necessary, which would mean the creation of correction factors depending on the horizontal variance of wind direction between the met mast and wind turbine. Because vertical extrapolation was used to determine hub height wind velocity during the testing of this turbine, flow correction factors were not possible, but the quality of the site in the undisturbed sector lent to the creation of a good wind shear model.

Determination of the undisturbed sector is crucial in finding a range of wind directions in which limited flow disturbances is present. A method for determining the disturbed sector caused by the wake of an obstacle on a turbine is estimated in IEC 61400-12-1 and is presented below in Equation (3.1):

$$\alpha_D = 1.3 \arctan\left(2.5\frac{D_e}{L_e} + 0.15\right) + 10 \tag{3.1}$$

where D_e is the equivalent rotor diameter (m) and L_e is the distance from the obstacle to the base of the turbine tower (m).

Figure 3-7: Overview with approximate distances to local obstacles and measurement sector (Google Maps 2011)

Equivalent rotor diameter is determined from the object's height and width (l_h and l_w, respectively) and is presented in Equation (3.2):

$$D_e = \frac{2l_h l_w}{l_h + l_w} \tag{3.2}$$

Calculation of disturbed sector caused by all nearby obstacles was calculated using equations (3.1) and (3.2). Measurements taken from these undisturbed sectors would then be the focus of the power performance analysis thesis for further statistical analysis. A summary of the disturbance calculation results is shown in Table 3-2.

Table 3-2: Disturbed sectors from nearby obstacles

Obstacle	Distance from Turbine, l_e (m)	Bearing to Center of Obstacle (°)	Height, l_h (m)	Width, l_w (m)	Equiv. Diameter, D_e (m)	Disturbed Sector, α_D (°)	Obstructed Sector	
							Start (°)	End (°)
SE Windrow	30	160	10	70	17.5	86	117	203
Railroad ties	32	90	2	2	2	32	74	106
SW Shrubs	60	240	7.5	60	13.3	56	212	268

Figure 3-8 shows the disturbed and undisturbed sectors determined from these calculations. The highlighted sectors to the south and east of the turbine were excluded from the analysis, as these regions contained objects which could potentially disrupt the flow field at the turbine tower. For the sake of simplicity, the undisturbed sector open to the north (268° to 74°) was included in the analysis of the turbine performance, and when used will be referred to as the test sector.

Figure 3-8: Site overview displaying disturbed and undisturbed direction sectors (Google Maps 2011)

According to IEC 61400-12-1 Annex B, the terrain at the turbine site must comply to the requirements shown below in Table 2-1. Topography requirements are specified for the test sector as well as for the non-test sector. The maximum slope of the best fit plane is calculated using the difference in elevation within the distance specific to the turbine from the base of the tower. Note that data pertaining to the specific site and turbine is also displayed, demonstrating that the topography both within the test sector and the non-test sector of the turbine site is very adequate for the siting and testing of a small wind turbine.

Table 3-3: IEC 61400-12-1 test site requirements - topographical variations

Criterion	Description	Distance (Guide)	Distance (m)	Sector (°)	Test Site condition	Pass/fail
1	Maximum slope of best fit plane <3%	< 5D	31.9	360	2.4%	Pass
2	Maximum variation from best fit plane <0.08 D (<0.5m)	< 5D	31.9	360	0.1	Pass
3	Maximum slope of best fit plane <5%	5-10D	31.9-63.7	Inside prel. meas. sector	1.6%	Pass
4	Maximum variation from best fit plane <0.15D (<0.95m)	5-10D	31.9-63.7	Inside prel. meas. sector	0.5m	Pass
5	Steepest slope of best fit plane <10%	5-10D	31.9-63.7	Outside prel. meas. sector	1.6%	Pass
6	Maximum slope of best fit plane <10%	10-20D	63.7-127.4	Inside prel. meas. sector	2.4%	Pass
7	Maximum variation from best fit plane <0.15 D (<1m)	10-20 D	63.7-127.4	Inside prel. meas. sector	0.5m	Pass
8	No neighboring and operating turbines	$<2D_n$	n/a	n/a	n/a	Pass
9	No obstacles	$<2D_e$	12.74	360	No	Pass
10	Preliminary measurement sector within available measurement sector	n/a	n/a	n/a	n/a	n/a

3.2 Wind Conditions Assessment

3.2.1 Introduction and Methodology

Data was collected over the course of 17 months at the Halkirk turbine site. It was decided that it would be insightful to study the daily, monthly, and yearly conditions measured over the course of these months. These different time frames will provide information on seasonal and daily variations that affect the performance of small wind energy conversion systems installed on the Prairies.

In addition, comparisons were made between the data collected at the turbine site to data available online over the same period from an Environment Canada (EC) 10m weather station located at the nearest airport in Stettler (50km due west of turbine site, elevation 819m), as well as to regional mesoscale statistics at 30m from the Canadian Wind Atlas (Environment Canada 2011a). The weather station datasets from the Environment Canada websites is public (Environment Canada 2011b) and likely where individuals would look who are interested in installing small wind turbines in these regions. Hourly data from the bottom two anemometer heights at Halkirk were used in conjunction with the power law method of Equations (1.2) and (1.3) in order to estimate the wind height at an equivalent height of 10m that the EC station data was collected. The same method was used to compare the regional mesoscale statistics from the Wind Atlas at an equivalent height of 30m.

Air density at the Halkirk turbine site was calculated from measured temperature and pressure readings as follows:

$$\rho_{avg} = \frac{1}{R} \cdot \frac{p_{avg}}{T_{avg}} \tag{3.3}$$

where ρ_{avg} is the air density averaged for the time step (kg/m^3), T_{avg} is the measured absolute air temperature averaged for the time step (K), p_{avg} is the measured air pressure averaged for the time step (Pa), R is the gas constant of dry air (287.05 J/kg K).

Mean wind energy, often referred to as wind power density (abbreviated WPD, variable P'), is the kinetic energy available in the wind at a particular location and height and has units of W/m². The kinetic energy available in the wind is a combination of air density and wind velocity and is expressed as follows:

$$P' = \frac{1}{2n}\sum_{i=1}^{n}\rho U_i^3 \tag{3.4}$$

where n is the number of records in the averaging interval, ρ is the air density (kg/m³), and U_i^3 is the cube of the i^{th} wind velocity value (m/s). WPD is a common method of comparing the amount of energy in the wind at different sites. Wind resource estimates are often expressed in terms of wind power density 'classes' varying from Class 1 'fair' to Class 7 'superb' at 10m, 30m, and 50m above ground level (B. Bailey et al. 1997).

3.2.2 Results and Discussion

3.2.2.1 Yearly Wind Behavior

The average air density over the 17 months of measurements was 1.194kg/m³, with a standard deviation of 0.056kg/m³. The average temperature at the turbine site over the 17 months was 3.45°C with a standard deviation of 12.33°C. These data are summarized in Figure 3-9 and Figure 3-10. These figures visually describe the wide ranging temperatures and resulting air densities that a typical small wind turbine installed on the Canadian Prairies would be subjected to.

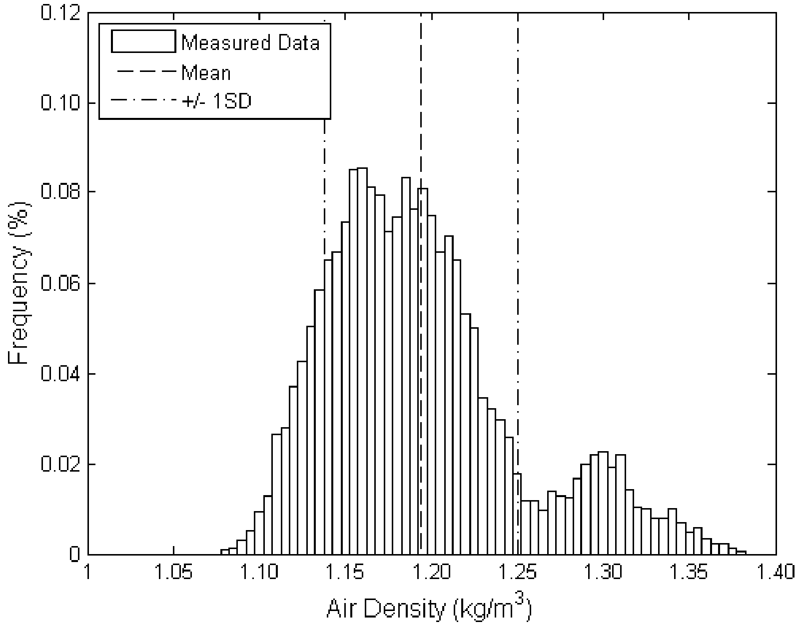

Figure 3-9: Yearly turbine site air density

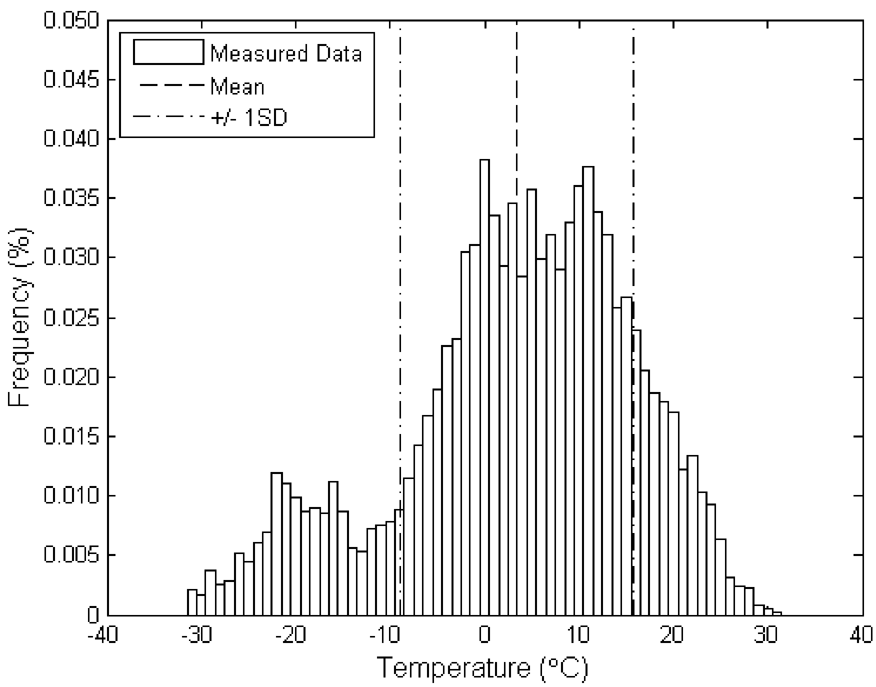

Figure 3-10: Year turbine site air temperature

Hourly wind data from the local Environment Canada 10m met station located at the Stettler Airport during the 16 months of data collection were processed and fit with Weibull distributions. The frequency distribution for the wind velocities at 10m at the Halkirk turbine site and Stettler are shown in Figure 3-11. Weibull and dataset statistics are shown below in Table 2-1. Frequency distributions derived from other wind velocity datasets collected at Halkirk are located in Appendix G.

(a)

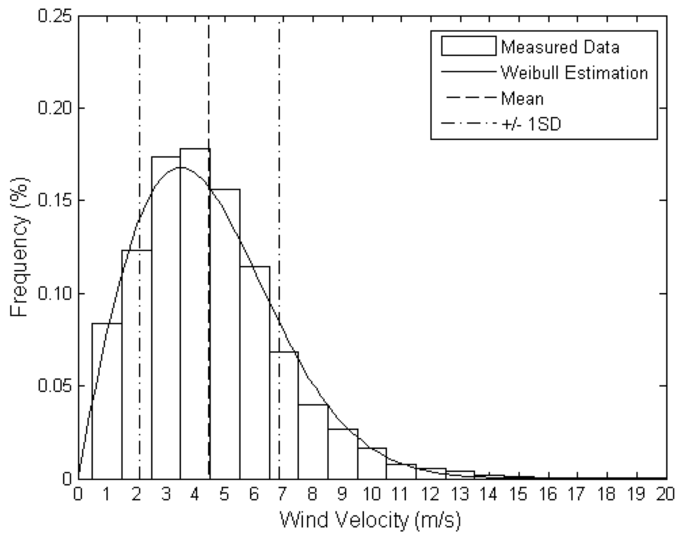

(b)

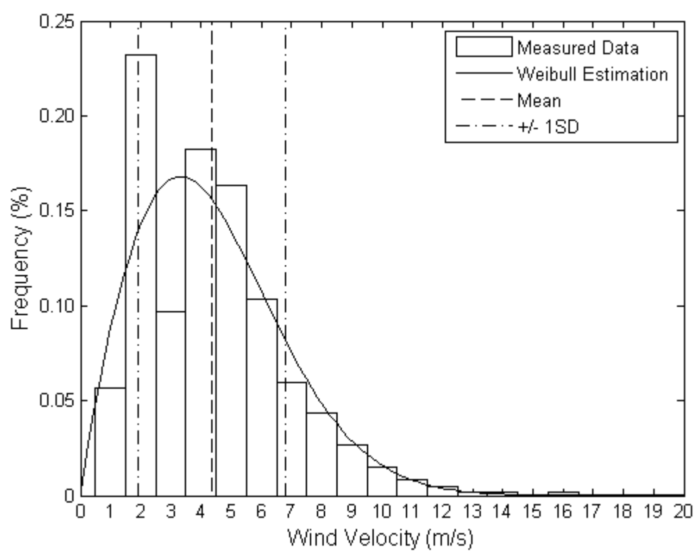

Figure 3-11: Synthesized Halkirk 10m (a) and Stettler Airport 10m (b) Frequency Distributions

Table 3-4: 10m Wind Dataset Statistics

Dataset Location	Weibull Scale Factor (c)	Weibull Shape Parameter (k)	Mean Wind Velocity (m/s)	Standard Deviation (m/s)
Stettler Airport 10m	4.930	1.895	4.363	2.435
Halkirk Synthesized 10m	5.036	1.958	4.463	2.383

As seen in Table 3-4, excellent agreement occurred between the two datasets. Both the Weibull and dataset statistics were very similar. Certain bins in the Stettler dataset at lower wind velocities contained slightly more data than predicted by the Weibull fit. The spread of the two datasets were also very similar, with maximum wind velocities in the range of 12-14m/s.

As discussed earlier, wind direction measurements at the Halkirk turbine site were not available for the entirety of the wind resource assessment study. For the period of 68 days that they were available, measurements were averaged on an hourly basis and compared to the Stettler EC site by plotting them in the form of a wind rose. As in all EC met stations, wind direction is recorded as one of 36 possible bins, which represents the 360 degrees possible for wind direction. The radial direction of the wind roses in Figure 3-12 represents the frequency, and the color gradient represents wind velocity. Good agreement between the wind rose of the two sites can be seen, with more dominant wind directions being from the Northwest, West, and South directions.

(a)

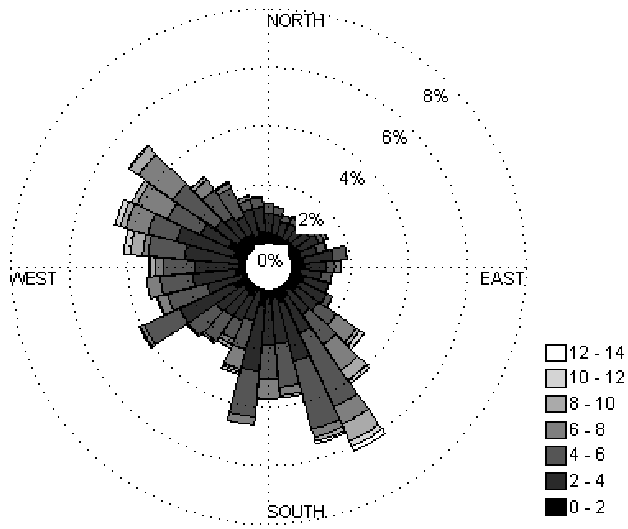

(b)

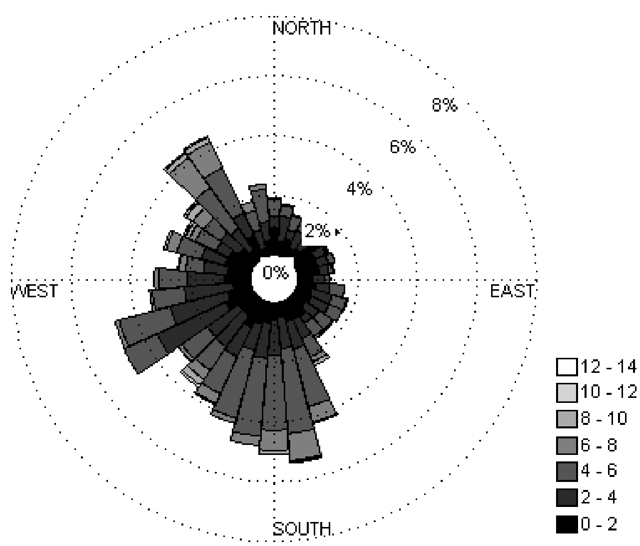

Figure 3-12: (a) Halkirk hourly averaged wind rose, synthesized 10 m wind velocity, (b) Stettler Airport hourly averaged wind rose, 10 m wind velocity

Regional mesoscale statistics are publically available for download from the Canadian Wind Energy Atlas website. These statistics are available at a number of heights and on an annual or seasonal basis. These data are created by Environment Canada by applying the statistical-dynamical downscaling method to each mesoscale domain in Canada. The mesoscale domains are 65 overlapping tiles which make up the representation of Canada's wind potential. The data making up each of these tiles are based on atmospheric data collected every 5 hours over 43 years, from 1958 to 2000. Therefore possible differences between the two estimates of the wind resource estimates were expected.

The values available for the Halkirk installation coordinates at 30m were compared to synthesized 30m ten-minute averaged wind values obtained over the 17 months of data collection at the Halkirk turbine site. The results are shown below in tabular form in Table 3-5. A comparison of the annual frequency distributions and Weibull statistics are shown in Figure 3-13. Figures comparing seasonal frequency distributions and Weibull statistics are found in Appendix G.

Table 3-5: Comparison of Mesoscale Statisitcs and Measured Data, Halkirk

		Canada Wind Atlas 30m Mesoscale, Latitude = 52.353, longitude = -112.143				Halkirk 30m Synthesized using Power Law in each time step			
Period		Mean Wind Velocity m/s	Mean Wind Energy W/m^2	Weibull shape parameter (k)	Weibull scale parameter (c)	Mean Wind Velocity m/s	Mean Wind Energy W/m^2	Weibull shape parameter (k)	Weibull scale parameter (c)
Annual		5.42	173.9	1.77	6.09	5.92	230.0	2.11	6.68
Winter	D/J/F	6.35	256.5	1.91	7.15	6.66	301.0	2.30	7.49
Spring	M/A/M	5.09	148.5	1.72	5.71	6.06	259.8	2.00	6.84
Summer	J/J/A	4.48	99.0	1.75	5.03	5.12	144.6	2.18	5.78
Fall	S/O/N	5.74	201.88	1.81	6.46	5.47	173.1	2.22	6.17

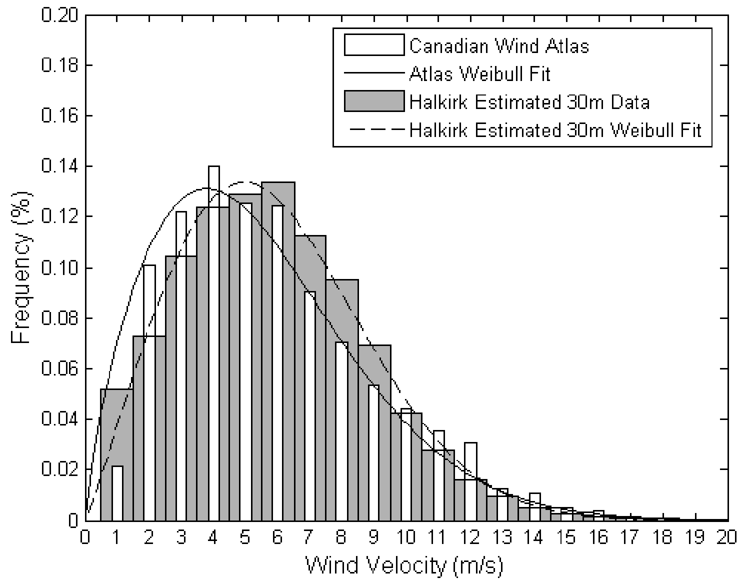

Figure 3-13: Comparison of frequency distributions and Weibull statistics, Canada Wind Energy Atlas and Halkirk ten-minute averaged data

It is observed from Table 3-5 and Figure 3-13 that the Canadian Wind Energy Atlas estimate of the wind resource available at the Halkirk site is low compared to the data collected on an annual basis and in all seasons except for the fall season. The annual Wind Energy Atlas WPD estimate of the wind resource at Halkirk is 32% lower than the WPD estimated from the data collected. Wind Atlas WPD seasonal estimates range from 75% low in the summer season to 15% high in the fall season. Resulting Halkirk WPD seasonal estimates classify the site as high Class 2 overall with as low as high Class 1 in the summer and as high as high Class 3 in the winter. Wind Atlas WPD seasonal estimates grade the site as low Class 2 overall with the low being Class 1 in the spring/summer and the high being low Class 3 in the winter. Wind Atlas estimates of seasonal wind velocity range from 19% low in the spring season to 5% high in the fall season. Weibull shape parameters available along with frequency distributions from the Wind Energy Atlas were also different. Interestingly, Halkirk 30m dataset had higher values in distribution bins from 5 to 9m/s compared to the Wind Atlas, and slightly lower values for bins from 10 to 16m/s, These bin differences contribute to the differences noted between the annual Weibull shape parameters between the two datasets.

3.2.2.2 Monthly Wind Behavior

The data collected at Halkirk and Stettler during the 17 months were averaged over each month and shown in Figure 3-14, where January is defined as Month 1. When available, overlapping months were added together in order to note the seasonal variation in the values. The mean monthly velocity at Halkirk varied from the yearly average by up to 33%, the mean temperature by as much as 6%, and the mean air density by as much as 6%. The monthly mean velocity at Halkirk was 10-30% higher than the yearly average in January to April, and 6-30% lower in June to October. No consistent directional variation was apparent between seasons.

Linear correlation coefficients (r) between monthly averaged values were calculated. On a monthly basis, the relationship between Halkirk 10m velocity mean and standard deviation showed a fair correlation (r=0.65), which could be reduced because of the significant obstacles affecting the dominant wind direction to the south of the site. The average velocity tends to increase with decreasing temperature (r=−0.75) and increase with air density (r=0.74). The majority of the higher than average winds with average standard deviation occurred during the coldest winter months of January and February.

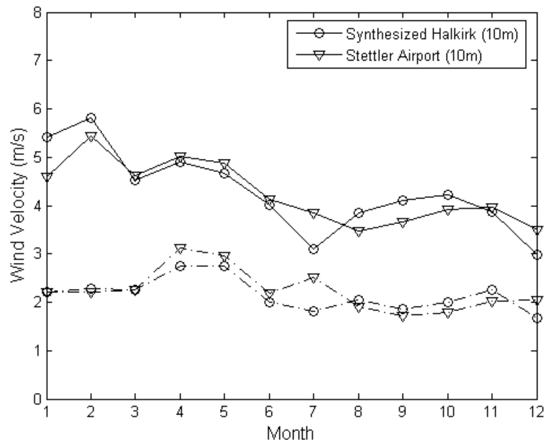

(a)

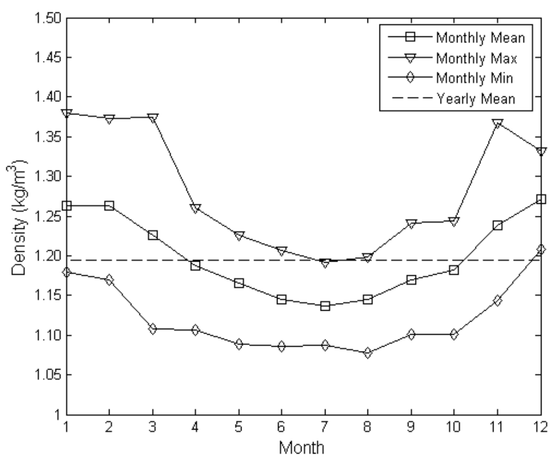

(b)

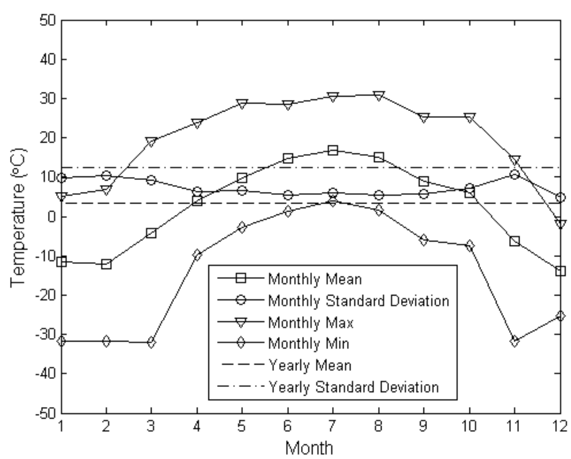

(c)

Figure 3-14: Halkirk turbine site (a) Monthly wind velocity at 10m; (b) Monthly air density; (c) Monthly air temperature

3.2.2.3 Daily Wind Behavior

The data collected at Halkirk and Stettler during the 17 months were averaged within each hour and shown in Figure 3-15, where 1:00 a.m. is defined as Hour 1 and 11:00pm is defined as Hour 23. Daily variations in the data as well as variations in wind velocity with height were studied. The mean hourly velocity at 10m at Halkirk varied from the yearly average of 4.463m/s by up to 15%, the mean temperature by as much as 140%, and the mean air density by as much as 2%. The mean hourly velocity at Halkirk estimated at 10m was 5-15% higher than the daily average from 11a.m. to 6pm 5-10% lower than the daily average from 8pm to 8 am. As expected from the simple topography of the surrounding area, no consistent daily directional variation was apparent.

Linear correlation coefficients (r) between daily averaged values were calculated. In terms of diurnal profile, the relationship between the Halkirk 10m velocity mean and standard deviation showed a good correlation (r=0.93). On a daily basis, the average velocity tends to increase with increasing temperature (r=0.86) and increase with decreasing air density (r=-0.86). The wind regime at Halkirk is a typical Prairie environment, with a diurnal profile that is characterized by strong vertical atmospheric mixing in the daytime caused by solar heating and a stable atmosphere with little mixing and reduced buoyancy at nighttime (Peterson & Parton 1983).

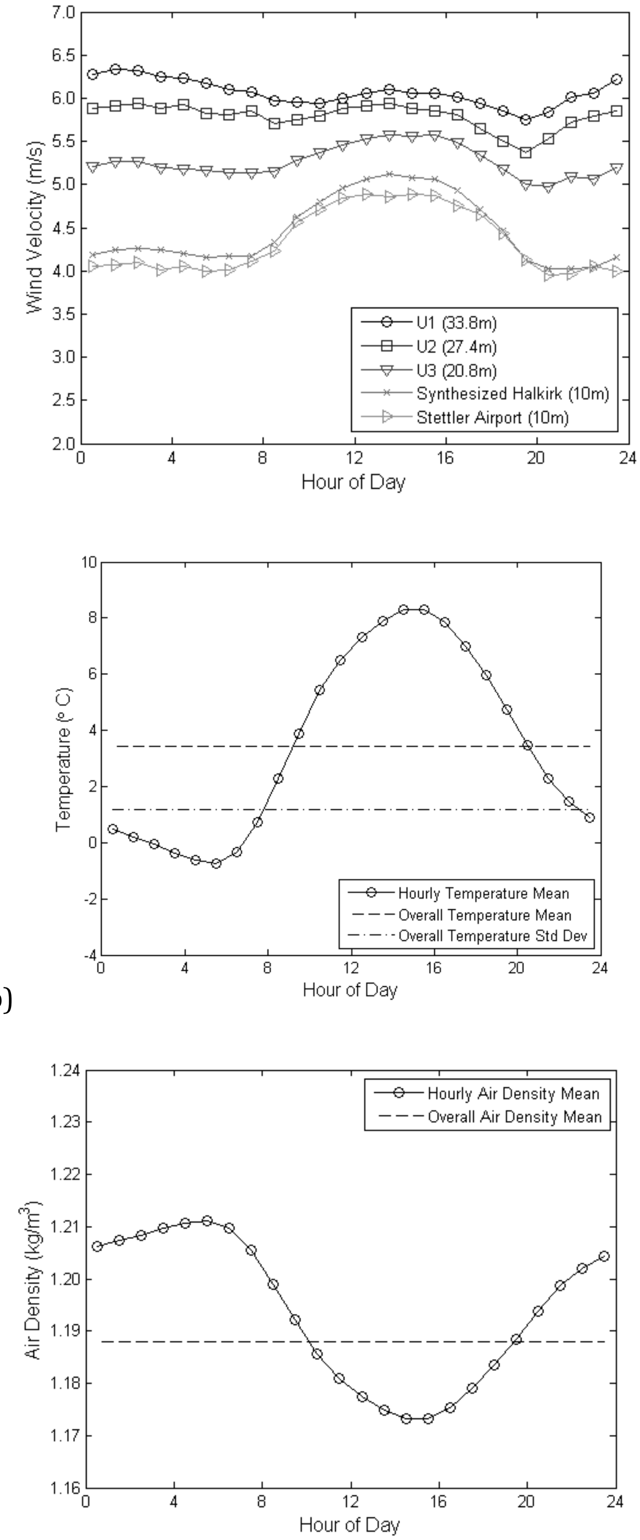

(a) (b) (c)

Figure 3-15: Halkirk turbine site (a) Hourly wind velocities at various heights; (b) Hourly air temperature; (c) Hourly air density

Turbulence intensity used in wind resource assessment studies is defined by the standard deviation of the wind velocity during the averaging period divided by the mean wind velocity during the averaging period. 10 minute averages are the industry standard when calculating TI. The TI for each season was calculated for U_1 and is shown in diurnal form in Figure 3-16(a). A stronger diurnal trend is apparent in the warmer seasons of spring and summer. In addition, wind shear values for U_1 to U_3 were calculated and shown in diurnal form in Figure 3-16(b). Similarly, a minor diurnal trend is apparent in the winter season compared to a strong diurnal trend in other seasons.

(a)

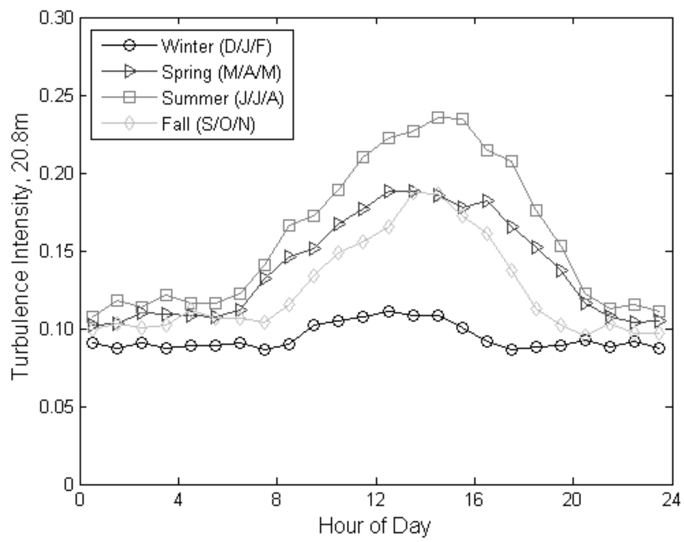

(b)

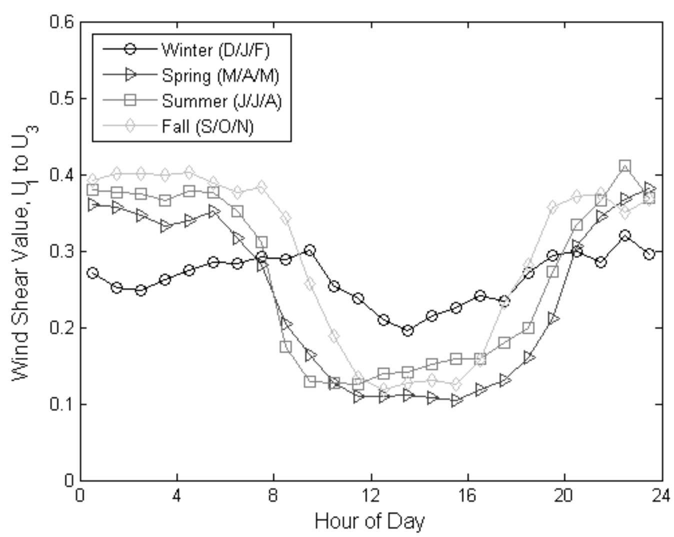

Figure 3-16: Seasonal diurnal variation in (a) turbulence intensity and (b) wind shear

A further study of the power law exponents details the effect of the diurnal relationship between temperature and wind. When available, the power law exponent (α) was calculated on an hourly basis between the three wind velocity heights. As expected, α varied substantially during the day. Patterns to be noted in Figure 3-17 include the variation in α with height as well as the variation from day to night. From 9am to 5pm, α from U_1 to U_2 was 22-62% lower than the daily average and from 7pm to 8am was 20-65% higher than the daily average. In the same way, α from U_2 to U_3 was 3-43% lower than the daily average from 9am to 5pm and was 18-42% higher than the daily average from 7pm to 8am. An interesting trend to note is the crossover time in the morning when the shear law exponent determined from the higher anemometers drops lower than the exponent determined from the higher anemometers. This is the result of daytime warming, which causes strong vertical mixing and a generally homogenous wind profile, characterized by high turbulence intensity and low wind shear values (Rareshide et al. 2009). The opposite relationship occurs in the evening. This relationship was noted to be more dominant in the warmer summer months at Halkirk than the winter months.

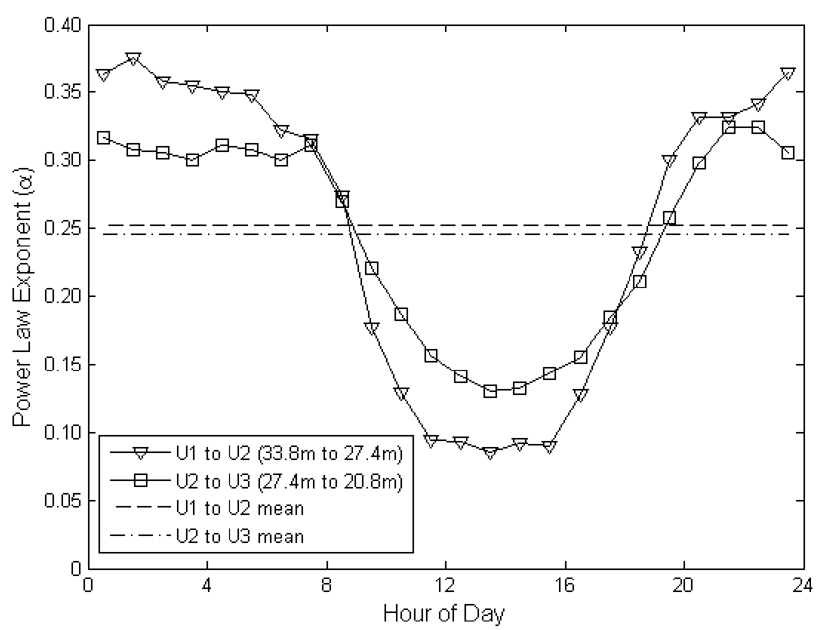

Figure 3-17: Hourly variation in shear factors between anemometer heights

A directional study of the power law exponents gave some insight into the relationship between the side disturbances in the vicinity and the wind velocities seen at the turbine tower. During the 68 days when directional information was available, power law exponent for U_2 to U_3 were determined for the 16 bins and additionally filtered on an hourly basis. The results are shown in Figure 3-18. In this figure, the rings represent increasing power law exponents, and the gradient represents the hourly bins. It is seen that the undisturbed sector to the north, west, and east of the turbine have significantly lower power law exponents for most of the day, denoting that less disturbed winds are present from these directions. The power law exponents from these undisturbed sectors were 11% to 40% lower than their overall daily average. This being said, the effect of nighttime cooling appears to affect all sectors, as power law exponents determined for these undisturbed sectors from 8pm to 8am were 7% higher compared to overall daily averages, although they were 34% lower compared to the disturbed sectors. Discussion on site disturbances and its affect on turbine performance will continue in Section 3.3.

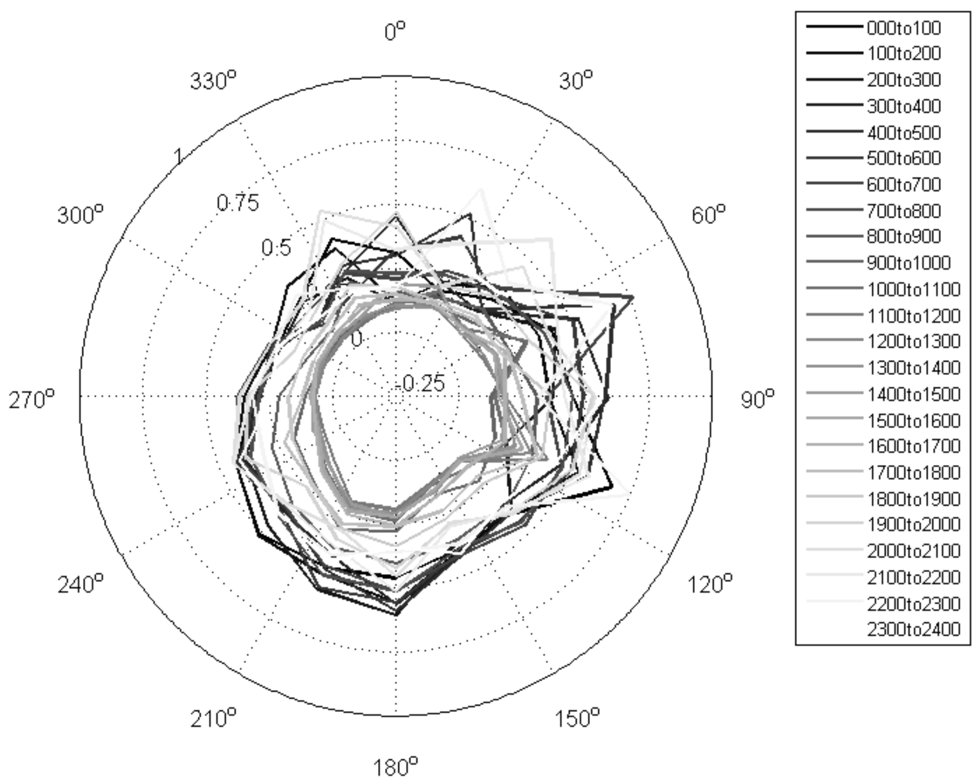

Figure 3-18: U_2 to U_3 shear factors, binned for direction and hour

3.2.3 Summary and Conclusions

The results of a wind resource assessment of the Halkirk turbine site derived from 17 months of data have been presented on a yearly, monthly, and diurnal basis. Consistent wind velocities were seen on a monthly basis, only varying from the yearly average by 33%. This compared to daily wind velocities, which varied on an hourly basis up to 15% from the daily average. This was in part influenced by the daily temperature, which varied on a diurnal basis by up to 2%. Wind shear and turbulence intensity both had strong diurnal trends which were more apparent in warmer months of the year.

In addition, statistical comparisons of the data collected to publically available sources of data were made. These comparisons included an evaluation of the agreement of the Halkirk data with data from the nearest Environment Canada weather station. Good agreement between the two sources of data on a yearly, monthly, and daily basis was found. Wind resource statistics available from the Canadian Wind Energy atlas were also evaluated in the context of the Halkirk data. A slight underestimate of the wind resource at the coordinates of the Halkirk turbine by the Wind Atlas were found. These differences could be due to a deficiency of the model in this area or because of a particularly windy year at the Halkirk turbine site. Both sources of publically available data were adequate for obtaining a general idea of the wind resource, but do not substitute the need to properly prospect the area wind resource of interest as well as properly site a turbine before installation.

3.3 Power Curve Development and Turbine Performance

3.3.1 Introduction and Methodology

The requirements for a standard small wind turbine test report outlined by IEC 61400-12-1 include a summary of the measured power curve, calculated power coefficient, AEP estimates, and relevant site conditions such as turbulence intensity at hub height. A summary of the methods used to produce these results will be outlined in this section. Time series data from 8pm August 12th 2010 to 7pm October 21th 2010 containing a wide range of temperatures and wind conditions were utilized in this section.

3.3.1.1 Data Normalizations

The manufacturer's standard power curve was provided by Endurance for the performance evaluation and comparison of power curves of the stall regulated turbine installed at Halkirk. The power curve is defined for steady conditions and sea level air density, referring to ISO standard atmosphere (1.225 kg/m^3 and 15°C).

Data normalization of the measured turbine performance data was completed to two air densities. The two air densities included the average of measured air density at the site during valid data collection, as well to sea level air density. The calculation for normalizing data for stall regulated wind turbines such as the S-343 is performed according to the following equation from IEC 61400:

$$P_n = P_{avg} \frac{\rho_o}{\rho_{avg}} \tag{3.5}$$

where P_n is the normalized power output (W), P_{avg} is the measured power averaged for the time step (W), and ρ_o is the reference air density (kg/m^3).

Site pressure was logged at enclosure height of 1m and was corrected to hub height as recommended by 61400 using Equation (3.6):

$$p_{hub} = p_b \left[1 + \tfrac{\beta}{T_b}\left(H - H_b\right)\right]^{-\left(\frac{g}{\beta R}\right)} \tag{3.6}$$

where p is the pressure at hub height (Pa), p_b is the measured pressure (Pa), β is the temperature gradient (lapse rate, -6.5E-3 K m^{-1}), T_b is the temperature at barometer height (K), H is the hub height (38.7m), H_b is the barometer height (1m), g is the acceleration due to gravity (9.807 m s^{-2}), and R is the ideal gas constant of dry air.

3.3.1.2 Power Curve

The 'method of bins' was used to create the normalized power curves for the test sector, as well as the sectors outside of the test sectors which were determined in Section 3.1.1.5 Bins of 0.5m/s width were used to calculate the mean values of the normalized wind velocity and corresponding normalized turbine power output for each wind velocity bin using Equations (3.7) and (3.8):

$$U_i = \tfrac{1}{N_i}\sum_{j=1}^{N_i} U_{\mathrm{n},i,j} \tag{3.7}$$

$$P_i = \tfrac{1}{N_i}\sum_{j=1}^{N_i} P_{\mathrm{n},i,j} \tag{3.8}$$

where $\underline{U_i}$ is the normalized and averaged wind velocity for bin i, $\underline{U}_{n,i,j}$ is the normalized wind velocity of data set j in bin i, P_i is the normalized and averaged power output in bin i, $P_{n,i,j}$ is the normalized power output of data set j in bin i, and N_i is the number of averaged data sets in bin i.

3.3.1.3 Productive Capacity

Annual energy production (AEP) is the amount of energy that can be expected to be produced by a particular wind turbine in a specific wind regime. The annual energy production is calculated by applying the binned power and wind velocity values to a Rayleigh cumulative probability density function (*F(U)*). This calculation is described in equation (3.9) and (3.10).

$$AEP = N_h\left[\sum_{i=1}^{n}(F(U_i) - F(U_{i-1}))\left(\frac{P_{i-1}+P_i}{2}\right)\right] \tag{3.9}$$

where N_h is the number of hours in a year, n is the number of wind velocity bins , U_i is the mean wind velocity for i^{th} bin, P_i is the normalized power output for the i^{th} bin.

$$F(U) = 1 - \exp\left(\frac{\pi}{2}\left(\frac{U}{U_{ave}}\right)^2\right) \tag{3.10}$$

where U is any wind velocity, U_{ave} is the annual averaged wind velocity at the location of interest (IEC 2005a). The last full wind velocity bin in the power curve was (16.5m/s) and is the upper cut-off point in the analysis performed. If binned power values are not available up to the cut-out wind velocity of the turbine (24 m/s in this case), the measured power value for the highest filled bin will be used in the calculation of an AEP estimate.

3.3.1.4 Power Coefficient Curves

It is useful to consider wind turbine performance results that are obtained via dimensional analysis. Three commonly calculated non-dimensional parameters include power, torque, and thrust coefficients (Wood 2011). Power coefficient is the most important parameter in field testing SWT and is the ratio of actual power produced to the total energy in the wind available to the turbine that passes through the blade's swept area. Coefficient of performance is defined as:

$$C_{p,i} = \frac{P_i}{\frac{1}{2}\rho_o A_d U_i^3} \tag{3.11}$$

where $C_{p,i}$ is the power coefficient in bin i (unitless), U_i is the normalized and averaged wind velocity in bin i (m/s), P_i is the normalized and averaged power output in bin i, A_d is the swept area of the wind turbine rotor (m^2), and ρ is the reference air density (kg/m^3).

Tip velocity ratio (TSR or λ) is an additional dimensionless value used in turbine performance analysis and is defined by:

$$\lambda = \frac{\left(\frac{RPM}{60}\right)2\pi R}{U_{hub}} \tag{3.12}$$

where R is the radius of the rotor (m), RPM is the revolutions per minute of the rotor, and U_{hub} is the hub height wind velocity (m/s).

The $C_p - \lambda$ curve, where λ represents the ratio of tip velocity to wind velocity as calculated in Equation (3.12), is a representation of how the turbine power would vary with rotational velocity as the wind velocity is held constant. For stall regulated turbines, a better method of representing turbine performance is suggested by Burton (Burton et al. 2001) and is defined by:

$$K_p = \frac{P_i}{\frac{1}{2}\rho(\Omega R_{tip})^3 A_d} \tag{3.13}$$

where Ω is the rotational velocity of the rotor (radians per second), ρ is the air density (kg/m^3), R_{tip} is the blade tip radius (m), and A_d is the swept area (m^2). As seen in Figure 3-19, the typical $C_p - \lambda$ curve is not very informative about the turbine performance at high tip velocities. K_p demonstrates the stall behaviour of the turbine at high tip velocities as the turbine's high wind velocity stall regulation behaviour is evident.

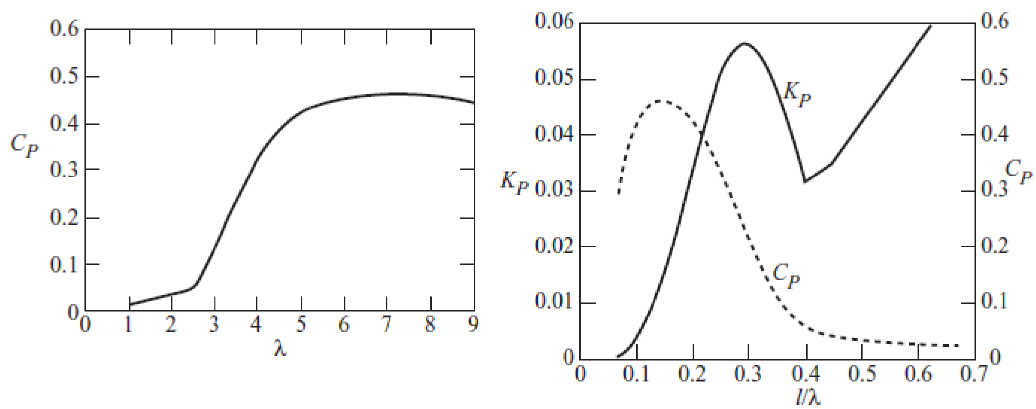

Figure 3-19: Non-dimensional power curves for constant velocity turbine operation - from (Burton et al. 2001)

3.3.1.5 Correlation Coefficient

In some areas, a correlation coefficient (*r)* was utilized to relate the outputs of two variables. A correlation coefficient is a dimensionless measure of the linear association between variables, lying in the interval between -1 and 1. Positive values describe a relationship between *x* and *y* variables where if the values of *x* increases, so does *y*. Negative values indicate an inverse relationship between *x* and *x* where if values for *x* increase, values for *y* decrease. The value of *r* is determined by the following process shown in Equations (3.14) to (3.20) (Montgomery & Runger 2007).

Assuming a linear relationship between independent variable *x* and dependent variable *y* in the form of:

$$y = \beta_0 + \beta_1 x \tag{3.14}$$

The slope (β_1) and the intercept (β_2) can be found by the following process:

$$\beta_0 = \overline{\overline{y}} - \beta_1 \overline{\overline{x}} \tag{3.15}$$

$$\beta_1 = \frac{S_{xy}}{S_{xx}} \tag{3.16}$$

$$S_{xx} = \sigma_x{}^2 (N - 1) \tag{3.17}$$

$$S_{yy} = \sigma_y{}^2 (N - 1) \tag{3.18}$$

$$S_{xy} = \sum_{j=1}^{N} \left(x_j - \overline{\overline{x}} \right) \left(y_j - \overline{\overline{y}} \right) \tag{3.19}$$

$$r = \frac{S_{xy}}{S_{xx} S_{yy}} \tag{3.20}$$

where $\overline{\overline{x}}$ and $\overline{\overline{y}}$ are the mean values of *x* and *y*, respectively, σ_x and σ_x are the sample sigma of *x* and *y*, respectively, S_{xx} and S_{yy} are the variances of the independent and dependent variables, respectively, S_{xy} is the covariance, and *N* is the total number of observations.

3.3.1.6 Uncertainty

IEC 61400-12-1 utilizes two types of uncertainty which contribute to the overall measurement uncertainty in the power curve and by association, annual energy production. Type A uncertainty is associated with the statistical distribution of measurements and in 61400-12-1 is treated as the standard error of the mean pertaining to the measurement in question. Type B uncertainty is associated with systematic errors and can be estimated using data provided in instrument calibrations and manufacturer specifications. The combined standard uncertainty is found by square rooting the sum of the squares of Type A and Type B uncertainties. The combined standard uncertainty gives a 68.27% level of confidence in the bin mean. Assuming a normal distribution of uncertainty, higher confidence levels can be found by applying a coverage factor. A summary of the uncertainty analysis along with detailed instrument data used in the calculation of power, power coefficient, and AEP estimate uncertainties is located in Appendix C.

3.3.2 Results and Discussion

3.3.2.1 Monthly Turbine Production

Turbine production at Halkirk was monitored over the course of 17 months. As discussed earlier, on some days data were not available from some instruments due to icing, logging issues, power outages, and turbine maintenance. The monthly number of hours that logging and turbine performance was available is shown in Figure 3-20. Over the 17 months, turbine production was measured by a bi-directional meter and the production value in kilowatt-hours tabulated by the turbine owners. This production number was compared to the values measured by the data collection system and shown in Figure 3-20.

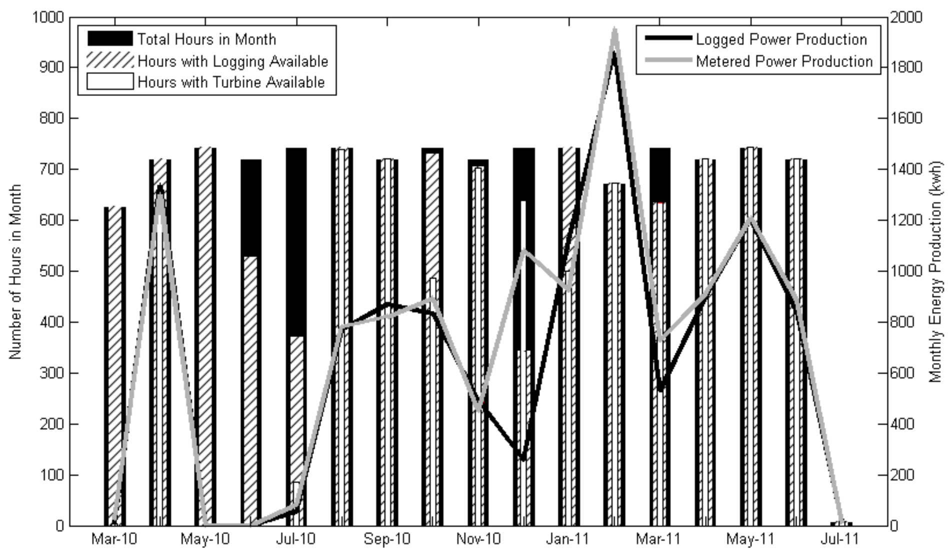

Figure 3-20: Monthly energy production and system availability at Halkirk over 17months

The monthly differences between the logged and metered production occurs for several reasons. From December 10th to 27th 2010 and March 27th to 31st 2011, the turbine produced when the logging system was not available to log data and therefore the metered value would be higher. In other months, metered values were not available on the first and last days of the month and values had to be estimated by interpolation. Considering the reasons for monthly differences, a good agreement between the two instrument values was found. The purpose of Figure 3-20 is to summarize the wide range of system availabilities over the 17 months and associated study challenges. Other major challenges include the time from May 5th to July 28th 2010 when the logging system was available but the turbine was laid over due to a generator issue, as well as the time from October 21st to November 14th 2010 when the turbine was offline due to a low speed shaft RPM sensor failure. Sonic anemometer values were only available from August 13th to November 14th 2010 due to instrument failure. Icing events from January 8th to 18th 2011 and March 19th to 23rd 2011 prevented turbine and cup anemometer operation during these periods. Cup anemometer connection issues in the lower anemometer prevented data collection from March 5th to April 16th 2010 and in the middle anemometer from April 30th to July 1st 2011. As discussed previously, wind vane failure reduced the amount of wind direction data available from the site. All of these issues were compounded by the fact that any logging issues or instrument maintenance performed required a 200km one-way drive to the turbine site. The resulting monthly power output means from combining the 17 months of data are shown in Figure 3-21.

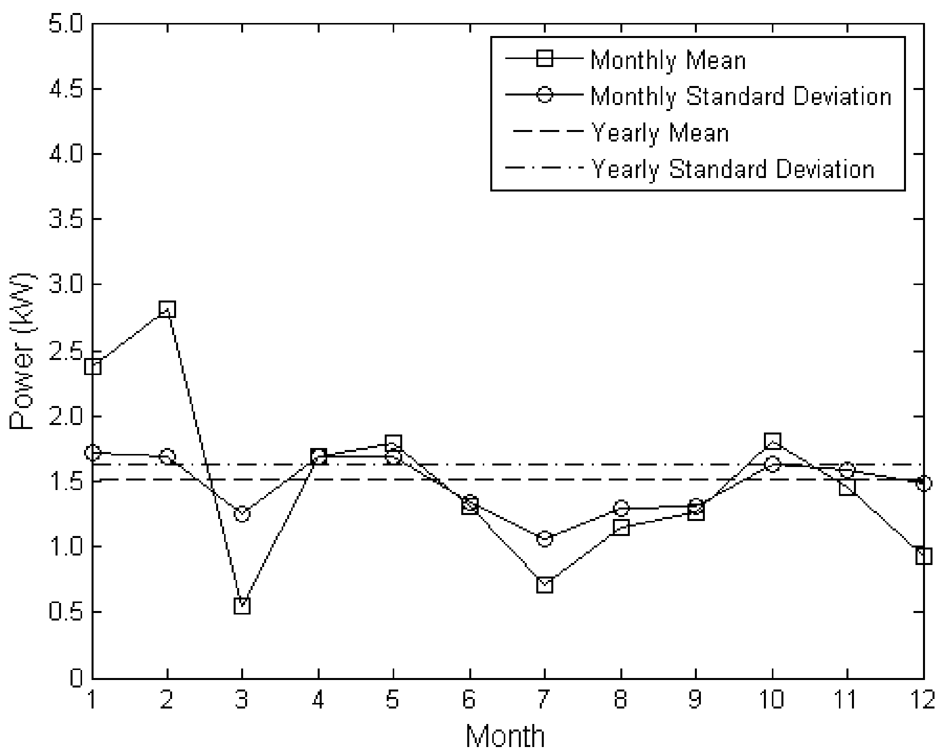

Figure 3-21: Monthly power variation

3.3.2.2 Power Curve during Turbine Performance Campaign

The raw power data was filtered for values from the undisturbed sector and used to obtain the bin-averaged power outputs. Concurrent hub height wind estimates were limited using a range of shear exponents between -0.05 and 1 to constrain extreme values and the resulting measured power curve is shown in Figure 3-22. For each time period that a 1-minute average value was calculated, maximum, minimum, and standard deviation was also calculated and is shown in Figure 3-22 as well.

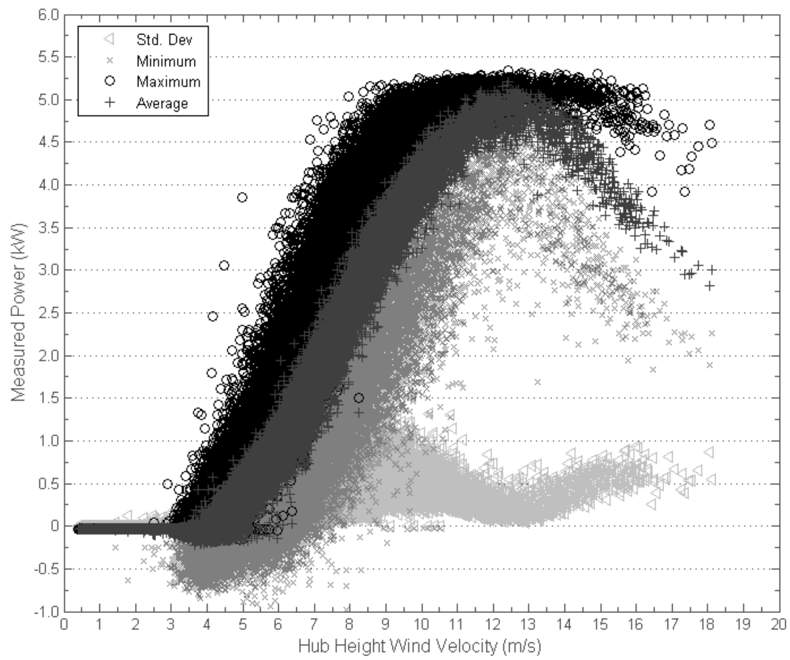

Figure 3-22: Scatter plot of mean, standard deviation, minimum and maximum power data. 1 Hz samples with 1 minute averaging

The raw data from the test shows a number of interesting trends. The 1 minute average values do not show a significant visual spread at any region point in the plot, although standard deviation appears to minimize around the highest power outputs of the turbine in the wind velocities in the range of 12m/s. Negative 1 minute minimum power values are present near the cut-in wind velocity of 3.1m/s as the turbine draws from the grid in order to reach rotational velocity necessary to generate grid-frequency energy. Negative 1 minute minimum values are present as high as 9m/s, demonstrating how quickly wind velocity can change and necessitate turbine motor up. Unlike many other test sites and turbine performance tests, turbine values at wind velocities higher than the rated wind velocity do not show any more spread than those below the rated wind velocity. This behavior can be interpreted as the composed behavior of a well designed stall-regulated turbine, a turbine site wind resource with limited violent high wind velocity behavior, or a combination of the preceding two factors.

Power values were normalized to sea-level air density and the resulting power curve is plotted in Figure 3-23. Binned values are shown overlapping the normalized raw data used to create the bin-averaged power outputs. Open circles represent bins that did not meet the IEC requirement of 10 minutes of data. For the sake of comparison, the Endurance S-343 manufacturer power curve at sea-level air density is plotted alongside the results from Halkirk. A discussion of the standardized raw data and binned power curve from the undisturbed sector and the disturbed sector is conveyed in Section 3.3.2.6.

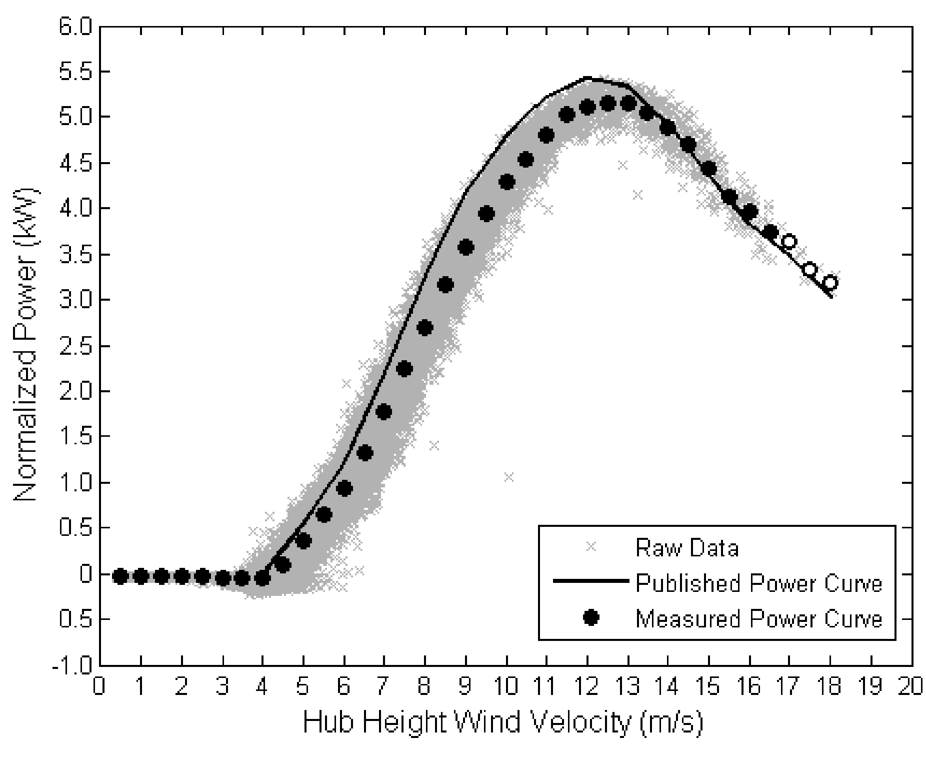

Figure 3-23: Measured power curve, raw and binned data at sea level density, showing manufacturer power data. Open circles represent bins with insufficient data

The purpose of the manufacturer's power curve is to show the expected performance of the turbine in a grid-connected application across a range of wind velocities. The power measurement used during the study was consistent with the standard's requirements, although the test used an alternative wind measurement technique discussed in 61400 which inherently affects the binning method and therefore power curve. Considering this and the fact the turbine at Halkirk was grid-connected, direct comparison of the two power curves is possible. The largest difference in binned power values occurs on the front side of the power curve up to the rated wind velocity of 11m/s, where the manufacture power curve over predicts the binned turbine power output by 0.16 to 0.57kW (8-30%). On the back side of the power curve at wind velocities in excess of the rated wind velocity, the manufacturer power curve is closer to the binned turbine power output up to 14m/s, with binned estimates low by 0.04 to 0.30kW (1-6%). In the wind velocity bins higher than 14m/s, the manufacturer prediction is very close to the binned turbine power output, slightly underpredicting the binned turbine power output by 0.04 to 0.08kW (2-4%).

The results of the power curve uncertainty analysis from Appendix C are shown below in Figure 3-24. The error bars in Figure 3-24 are the 95% level of confidence in the bin means. The manufacturer power curve falls at the high end of the 95% confidence interval in the wind speed bins below cut in at 3.1m/s to the wind speed bin of 11.5m/s. Although the measured power values are closer to the manufacturer power curve in the 12, 12.5, and 13m/s wind speed bins than in the preceding bins, the manufacturer power curve falls outside the 95% confidence interval due to the smaller spread in power data in these bins caused by the upper power limit of the turbine. The manufacturer power values associated with wind speed bins from 13.5 to 18m/s are within the 95% confidence interval and close to the bin means, as discussed in the preceding paragraph. Data pertaining to the 68.27% level of confidence in the bin means is located in Figure H-1 and Table H-1 in Appendix H. Further analysis of uncertainties will be provided in the discussion on AEP estimates.

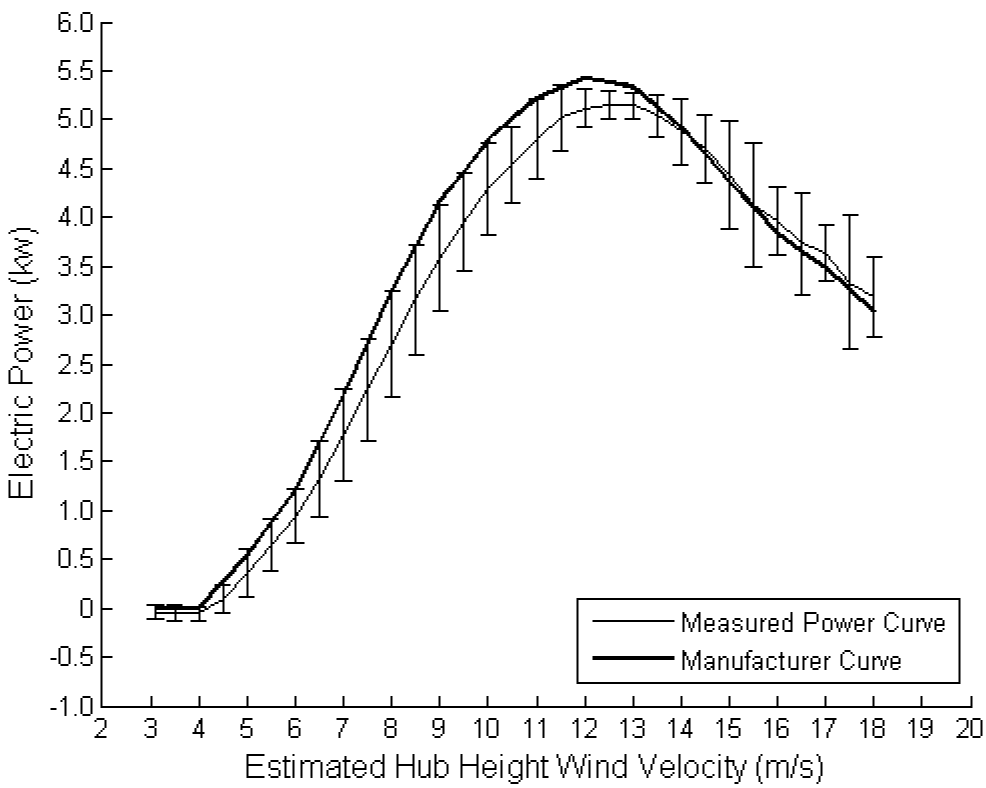

Figure 3-24: Sea level normalized power curve with 95% uncertainty bars along with manufacturer power curve. Uncertainty determined from IEC 61400-12-1 recommendations

3.3.2.3 Productive Capacity

Calculation of the AEP using the normalized sea density power curve and wind distributions of known shape is one way to quantify the difference over a year of production between manufacturer predictions and actual results. In addition, AEP calculation also gives an indication of the effect of wind resource regime on turbine performance. AEP estimates were made using a Rayleigh distribution as explained in Section 3.3.1.3 for sites with average wind velocities of 4 to 11m/s. The results are presented visually in Figure 3-25 and in tabular form in Table 3-6 alongside manufacturer estimates that were available for sites with average wind velocities of 3.5 to 8.5m/s. Additionally, for reference and consistency, the AEP was re-calculated using manufacturer power curve data for average wind velocities of 4 to 11m/s and is shown in Figure 3-26.

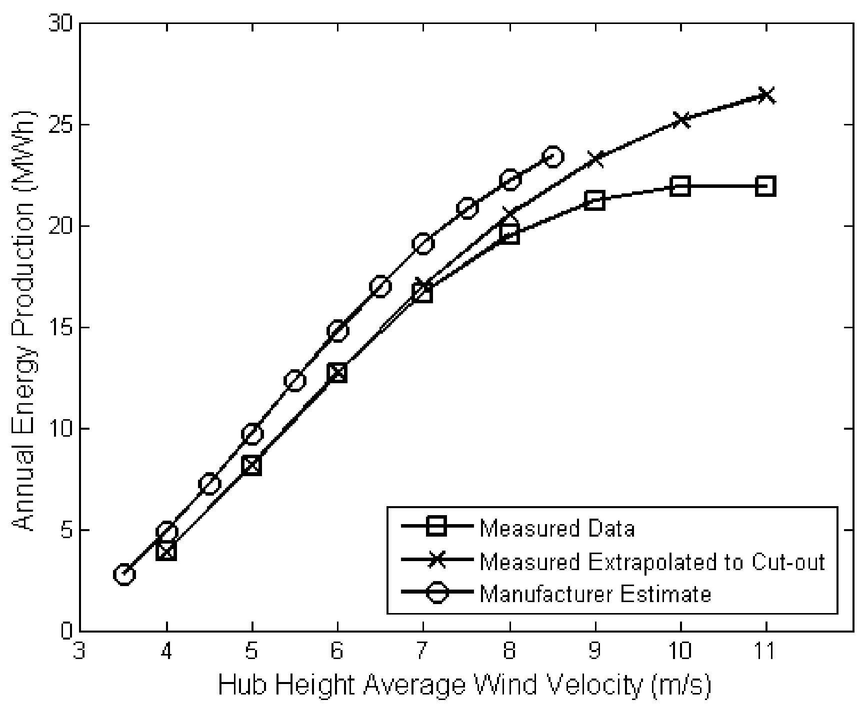

Figure 3-25: Estimated Annual Energy Production, Manufacturer and Measured

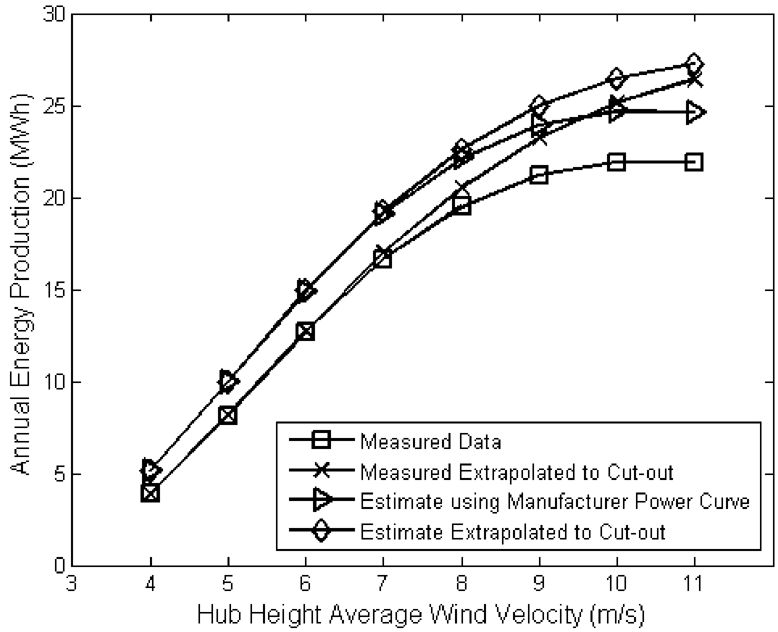

Figure 3-26: Estimated Annual Energy Production, Measured and Estimated from Manufacturer Power Curve

AEP estimates were made using values up to 16.5 m/s, the highest bin meeting the IEC requirements. The AEP that was calculated from the manufacturer data was also estimated using values up to 16.5m/s. Very minor differences were seen between the AEP calculated from manufacturer data and the AEP estimate from the manufacturer, with the calculated value differing from the AEP estimate ranging from 4% high at 4m/s average wind velocity to 0.4% low at 11m/s average wind velocity. This confirmed that the methods used by both the manufacturer and this study were reasonably similar. Using the measured power curve (normalized to sea level air density), AEP estimates were 13 to 21% lower than the manufacturer power curve, with the largest difference in AEP estimate occurring at sites with wind low wind velocities. The difference can be explained as the difference between the manufacturer and measured power curves. The measured power values were slightly lower for bins of 3.5 to 14m/s compared to the manufacturer power curve. In wind regimes with lower average wind velocities, the turbine is able to generate energy a smaller proportion of the time compared to sites with higher average wind velocities. Therefore differences in binned power curves have a larger effect on AEP estimates at lower average wind velocities. A summary of the AEP measured, calculated, and estimates are below in Table 3-6, accompanied by the results of the uncertainty analysis.

Table 3-6: Estimated annual energy production

			Reference air density:		1.225	kg/m^3	
			Cut-out wind velocity:		24	m/s	
Hub height annual average wind velocity (Rayleigh)	AEP-manufacturer estimate	AEP-calculated from manufacturer power curve	AEP-measured	Standard Uncertainty in AEP-measured		AEP-measured extrapolated	Complete if AEP-measured is at least 95% of AEP extrapolated
m/s	kwh		kwh	kwh	%	kwh	
4	4900	5126.4	3862.0	433.4	11.2%	3862.1	Complete
5	9700	9954.9	8130.4	635.6	7.8%	8134.6	Complete
6	14800	14919.6	12679.3	806.7	6.4%	12744.6	Complete
7	19100	19237.3	16632.7	944.7	5.7%	16974.2	Complete
8	22200	22593.2	19506.1	1051.1	5.4%	20491.9	Complete
9	n/a	24970.2	21215.8	1123.4	5.3%	23215.3	Incomplete
10	n/a	26475.5	21926.3	1161.3	5.3%	25168.5	Incomplete
11	n/a	27251.5	21888.2	1169.0	5.3%	26419.5	Incomplete

As expected, combined uncertainty is highest at lower average wind velocities and therefore lower AEP estimates. An AEP-extrapolated value was calculated because a sufficient amount of time with wind velocities above 16.5m/s was not seen during the turbine performance campaign. 61400-12-1 recommends that power values from the highest filled wind velocity bin be used for wind velocities up to cut out wind velocity. In this case, the measured power value from 16.5m/s was used up to the Endurance S-343 cut-out wind velocity of 24m/s. The AEP extrapolated value plotted with the AEP measured value in Figure 3-25.

At lower average wind velocities, extrapolating the AEP to the cut-out wind velocity of the turbine has no effect on the AEP estimate because these sites do not have the probability of the turbine being exposed to high wind velocities to contribute any energy at high wind velocities. The extrapolated AEP gives insight into the estimated production of the turbine at sites with higher average mean wind velocities for bins which the manufacturer does not present power data for. This increased production is noted in both the manufacturer power curve extrapolated curve and the measured power curve extrapolated curve in Figure 3-25. Interestingly, the AEP estimate from the manufacturer follows the trend of the extrapolated curve for bins 7.5 to 8.5 m/s. Although it is assumed that the manufacturer uses the same process from 61400 for the calculation of AEP, it is possible that the manufacturer used extrapolated values for these bins. It is not known why the re-calculated AEP values using the manufacturer power curve were higher for lower average wind velocities and lower for higher average wind velocities as both calculations were done using the same power curve. A slight difference in method could create this discrepancy; for instance, the addition of a loss factor such as blade icing or downtime losses would reduce output estimates.

3.3.2.4 Power Coefficient Curve

Figure 3-27 and Figure 3-28 depict the measured relationship between wind velocity and turbine power output. The 1 minute average estimated wind velocity (U_{hub}) was used to calculate the power coefficient for each data point. Power coefficient is plotted as a function of estimated hub height wind velocity in Figure 3-27 as a function of λ in Figure 3-28.

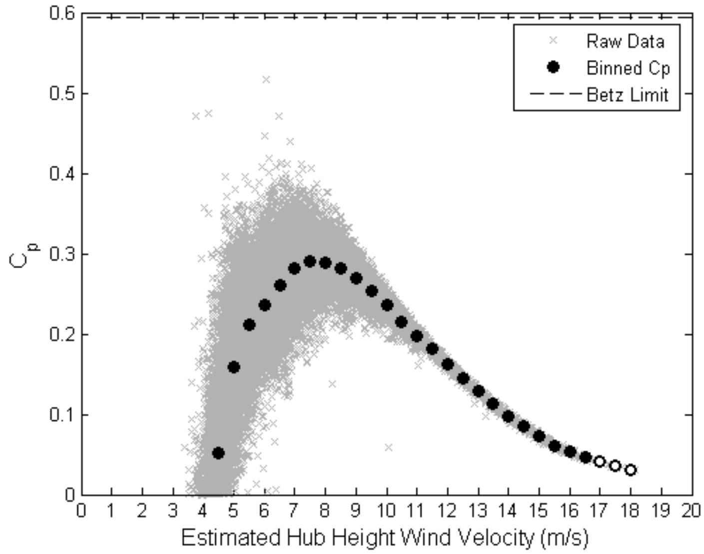

Figure 3-27: Coefficient of performance, raw and binned data at sea level density versus hub height wind velocity, showing Betz limit. Open circle represents insufficient data.

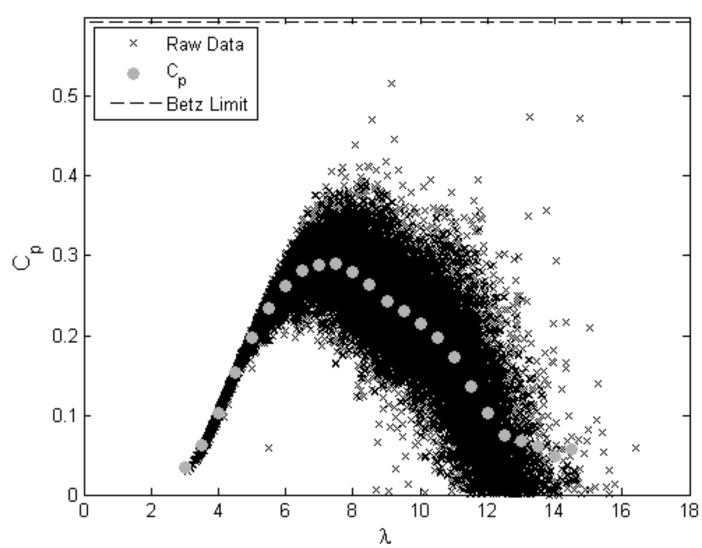

Figure 3-28: Coefficient of performance versus tip velocity ratio

Both Figure 3-27 and Figure 3-28 confirm that the turbine was operating as designed and at a high level across its operating range for a stall regulated three-bladed turbine. The spread of values below the rated wind velocity of 11m/s is due to power train dampening, which occurs during fluctuating winds in order to maintain a constant RPM. This is normal design behavior for stall regulated turbines. The coefficient of performance had very little spread at values above the rated wind velocity of 11m/s. This is also typical design behavior of a stall regulated turbine as the system strives to capture the energy from the less turbulent high wind velocities. This behavior is likely magnified by the fact that the site had extremely low turbulence intensity or the wind velocity range which is analyzed in the next section.

The Category A and Category B uncertainty in the C_p value was calculated and plotted as error bars in the coefficient of performance curve in Figure 3-29. The process used to calculate this uncertainty is detailed in Appendix C.

.

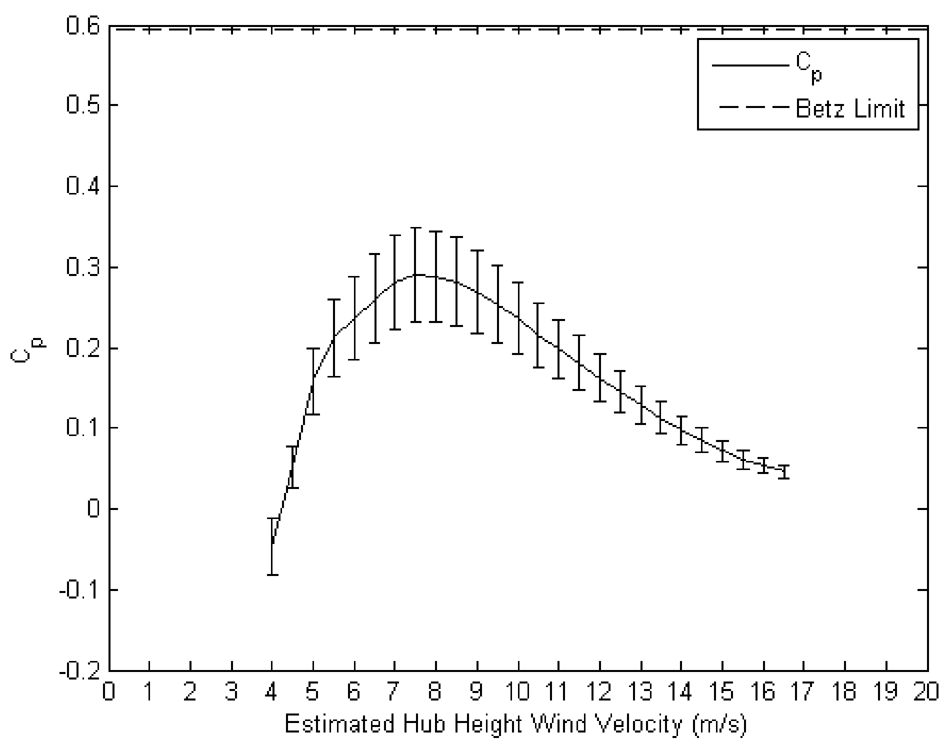

Figure 3-29: Coefficient of performance with error bars indicating a 68.27% confidence interval created from Category A and B uncertainty

The special stall regulated coefficient of performance value, K_p, suggested by Burton was calculated and plotted against concurrent values for $1/\lambda$. In addition, the typical coefficient of performance values, C_p, was calculated, binned and plotted against $1/\lambda$ for reference. Initially, it is noted that there is less spread in K_p compared to C_p in the range of 0.05 to 0.2 for $1/\lambda$. It is noted in Figure 3-30 that the same high wind velocity trend present in the example plot of Figure 3-19 is not present. Unfortunately, high enough wind velocities necessary to see this behaviour were not encountered during the test period. This increase in the K_p indicates that passive stall is working to control the rotor's rotational velocity. According to Equation (3.13), one would expect power outputs to slightly increase at wind velocities in the range 18-24m/s for K_p to follow the same positive linear pattern as seen in Figure 3-19 at corresponding high $1/\lambda$ values.

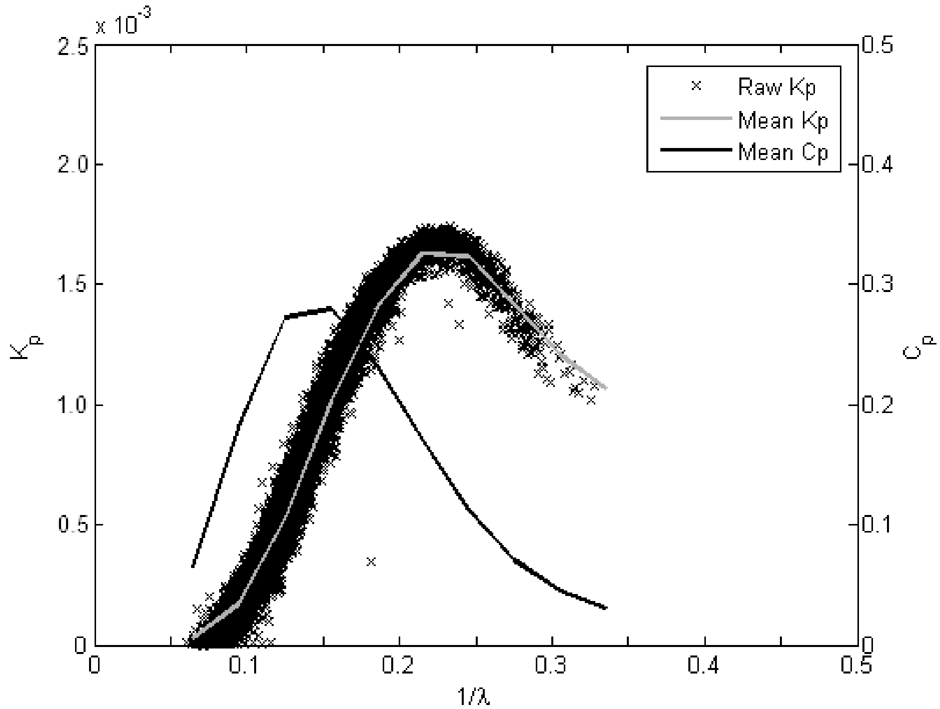

Figure 3-30: Non-dimensional stall regulated and typical performance curves

3.3.2.5 Site Turbulence Intensity during Turbine Performance Campaign

Site turbulence intensity is another requirement for the test reporting mandated under IEC 61400-12-1. Hub height turbulence intensity and wind velocity were estimated using 1 minute values from the undisturbed sector and plotted in Figure 3-31. The dashed line indicates the lower wind velocity boundary of 3.1m/s used in the power performance and wind velocity data analysis. The turbulence intensity categories are defined by curves that cover the wind velocity range (IEC 2005b). The solid black lines in Figure 3-31 indicate the boundaries of these turbulence categories which are labeled to the right of the lines. It is clear that the average turbulence intensities as well as a large majority of the raw data are in the 'C' turbulence category. Sites with low turbulence intensities values like those seen here are highly sought after as the winds are less damaging to wind turbine blades and power trains.

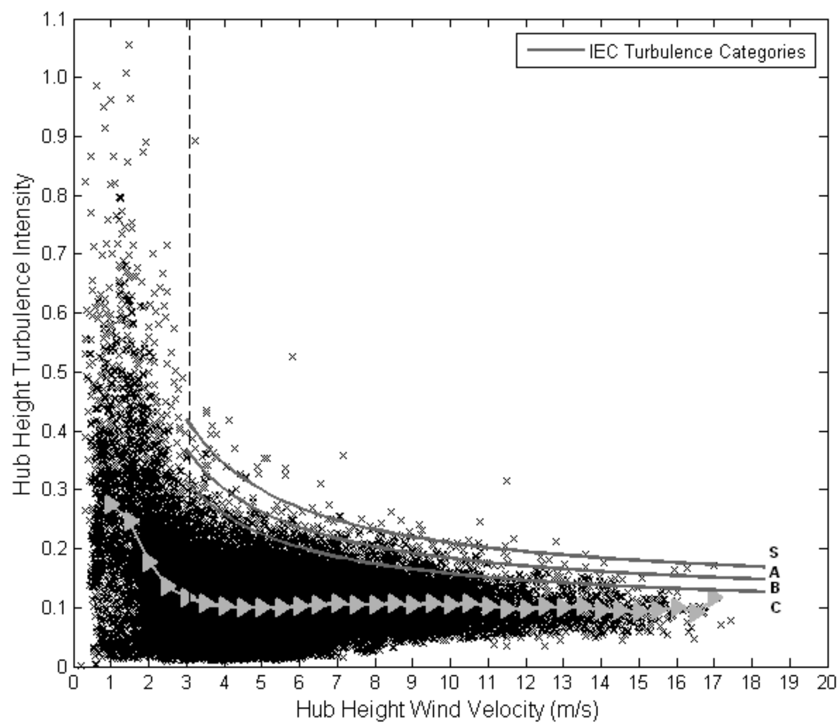

Figure 3-31: Wind turbulence intensity as a function of wind velocity

In addition, hub height turbulence intensity was plotted against the wind direction in Figure 3-32. Only values from the undisturbed sector are required in the test report. Values from all sectors were included, including those affected by tower shading in the 110° to 130° range. Interestingly, average turbulence intensity values binned by 10° direction sector for disturbed sectors (filtered for the region affected by tower shading) ranged from 0.082 to 0.113, which was slightly lower than undisturbed sectors which ranged from 0.111 to 0.127. Filtering the data for wind velocities less 10m/s did not change this trend of lower TI from the undisturbed sectors, which indicates that the lower TI was not only because these regions had higher average wind velocities. This demonstrates that the turbine was installed high enough to be unaffected by the wake of the disturbances in these sectors.

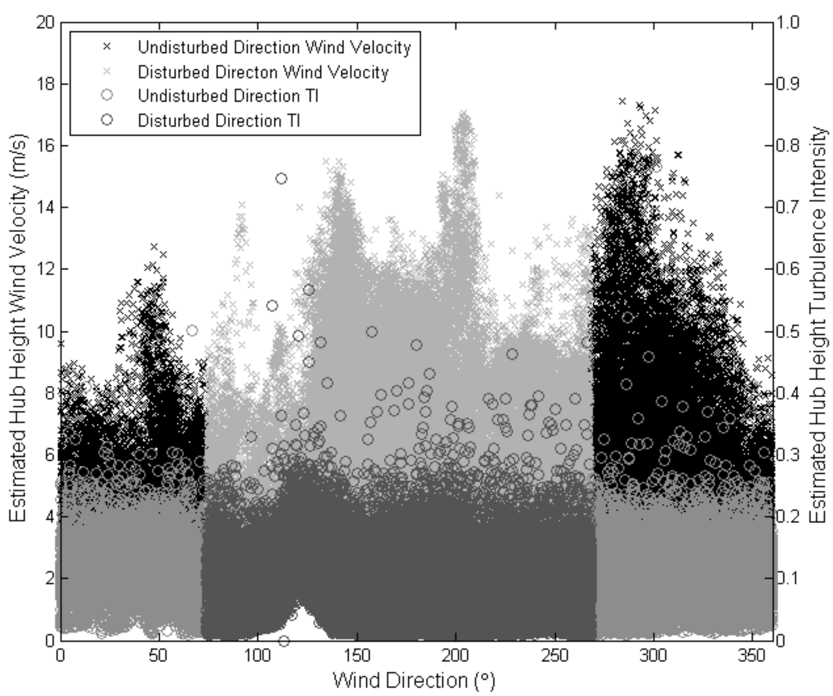

Figure 3-32: Extrapolated hub height wind velocity and estimated turbulence intensity

3.3.2.6 Comparison of undisturbed and disturbed sector power curves

For comparison, the measured power values from the test sector (undisturbed) and non-test sector (disturbed) were standardized to sea level air density and binned by 0.5m/s estimated hub height. Raw data and binned values from both sectors are displayed below in Figure 3-33, as well as the power curve given by the manufacturer for reference. A minimum of 10 minutes of wind data was available up to 16.5m/s in the undisturbed test sector and 17m/s in the disturbed test sector.

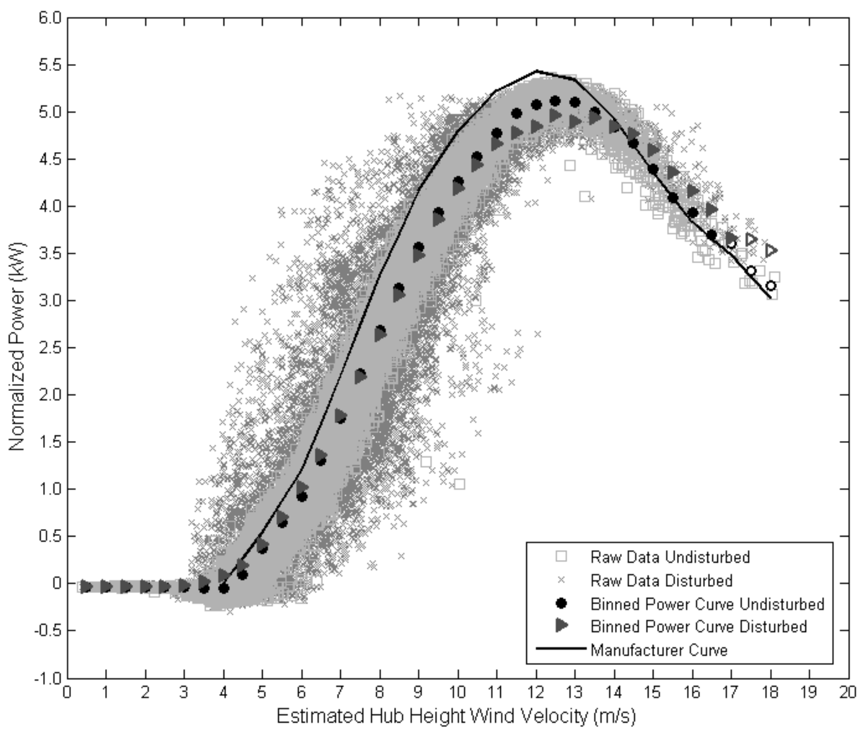

Figure 3-33: One-minute averaged measured power curve, undisturbed and disturbed raw data, binned by. Open circles denote bins with less than 10 minutes of data.

Several interesting observations can be made from Figure 3-33. The spread of the raw data from the non-test sector at all wind velocities is quite evident, caused by upstream disturbances which increase turbulence in the wind. This spread causes several differences between the disturbed and undisturbed power curves, noted by the three intersections between the two binned power curves. These differences have been previously noted in studies discussing the effect of turbulence intensity on power production (Kaiser et al. 2007; Rareshide et al. 2009). At wind velocities from turbine cut-in to 7m/s, the non-test sector power curve is drawn higher by

0.02 to 0.13kW from the wider range of power values in each wind velocity bin. At wind velocities from 7 m/s to 14 m/s, the increased range in the non-test sector power values limited by the maximum generator output cause the binned non-test sector values to be 0.01 to 0.24kW lower than the test-sector power values. At wind velocities above 14m/s, the wide spread in the non-test sector power values are beneficial, with the non-test sector power values being 0.10 to 0.26kW higher than the values from the test-sector. In summary, the power production from the disturbed sector compared to the undisturbed sector is increased in concave regions in the curve, and decreased in convex regions of the curve. To put these differences in perspective, AEP was calculated using each curve. The results are shown below in Table 3-7.

Table 3-7: AEP estimates using binned power curve from undisturbed and disturbed sectors

	Undisturbed			Disturbed		
Hub height annual averaged wind velocity (Rayleigh)	AEP-measured	AEP-extrapolated	Complete if AEP-measured is at least 95% of AEP extrapolated	AEP-measured	AEP-extrapolated	Complete if AEP-measured is at least 95% of AEP extrapolated
m/s	kWh	kWh		kWh	kWh	
4	3825.6	3825.7	Complete	4143.8	4143.8	Complete
5	8058.3	8064.6	Complete	8277.4	8281.0	Complete
6	12548.2	12633.5	Complete	12655.2	12713.5	Complete
7	16397.8	16807.2	Complete	16470.4	16778.5	Complete
8	19128.6	20248.3	Incomplete	19259.0	20153.5	Incomplete
9	20686.5	22878.0	Incomplete	20929.4	22749.8	Incomplete
10	21263.0	24731.2	Incomplete	21630.7	24588.5	Incomplete
11	21122.3	25887.5	Incomplete	21600.6	25740.2	Incomplete
Highest measured wind velocity bin (m/s)	16.5	24		17	24	

From Table 3-7, it is seen that the power curve derived from the disturbed sector data gives a higher estimate at all average wind velocities compared to the undisturbed sector data. The difference between the measured AEP ranges from 8% higher at 4m/s to 1.2% higher at 10m/s. The extrapolated AEP derived from the disturbed sector curve is also 8% higher at 4m/s and within 0.6% of the undisturbed estimate at wind velocities higher than 6m/s. The extrapolation method is more effective in comparing the two as the highest measured wind velocity is different for the two sectors. The high estimates at low annual average wind velocities is due to the higher disturbed power curve values up to 7m/s. The higher undisturbed power curve values from the 7 to 14m/s bins make up the difference at annual average wind velocities higher than 6m/s. The higher disturbed power curve values after 14m/s do not affect the estimates due to the small amount of time spent at these wind velocities compared to the other bins. The difference in the AEP extrapolated estimates between the two methods remained within 1% when changing the highest measured wind velocity bin to be 16.5m/s for both sectors.

This study outlined a comparison of small wind turbine behavior in disturbed and undisturbed sectors at one site. The variability of the wind and therefore power curve created by upstream obstacles was shown. The effects of this variability on AEP estimates at different annual average wind velocities were discussed. Although variability in the power curve at disturbed sites will possibly slightly improve AEP at low average annual wind velocities, the stresses on wind energy conversion machines caused by this variability is a more important factor to consider when siting small wind turbines at these sites.

3.3.2.7 Temperature Performance

The energy output of the turbine was again calculated during the 68 days of the turbine performance period using temperature bins of 2°C and filtered for disturbed wind from 74° to 268° and undisturbed wind from 268° to 360° and 0° to 74°. Bins with at least 10 minutes of valid data were considered for analysis. In addition to the data collected during the turbine performance testing, the energy output of the turbine was calculated during the longer stretch of turbine and instrument availability from July 28th 2010 to July 1st 2011 using the 2° temperature bins. These two time periods will be referred to turbine performance directional study and turbine performance non-directional study. Relations between temperature, turbine production, and wind characteristics were studied.

The results from the turbine performance directional study are shown in the stacked histogram plot in Figure 3-34(a). The height of the bar represents all data, and the black bar represents wind from the undisturbed wind direction. The white bar represents wind from the disturbed wind direction. The data from Figure 3-34(a) and Figure 3-34(b) were used to calculate an average power value across regions where more than 10 minutes of data were present. The results are shown in Figure 3-34(c). It is noted that 26% of the time steps from the turbine performance directional study contained wind from the undisturbed section. From Figure 3-34(a) and (c), it is seen that 17.5% of the energy during this time was produced from wind from the undisturbed section.

(a)

(b)

(c)

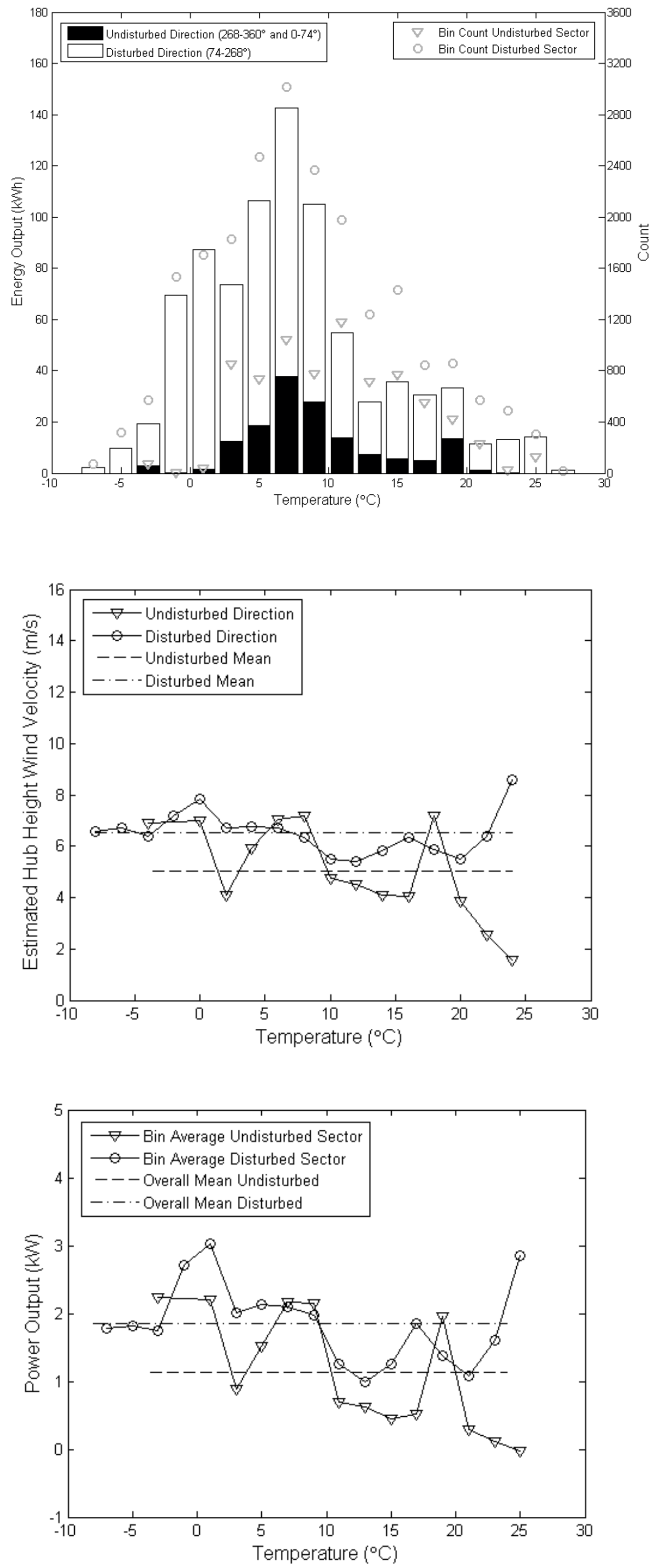

Figure 3-34: Data binned from direction and temperature (a) Energy production binned by temperature (b) Estimated average hub height wind velocity (c) Average power output

From Figure 3-34 (c), it is seen that energy production was very consistent across each temperature and direction bin. During the turbine testing period where direction was available, a correlation coefficient of 0.85 relating the proportion of overall time and energy production for the disturbed direction and a correlation coefficient of 0.73 relating the proportion of overall time and energy production for the undisturbed direction. This difference could be explained by the higher overall average wind velocity from the disturbed direction of 6.41m/s compared to 5.46m/s m/s from the undisturbed direction, as seen in Figure 3-34(b). This translated to a higher average power output of 2.01kW from the disturbed direction compared to 1.18kW from the undisturbed direction, as seen in Figure 3-34 (c).

Further investigations into wind characteristics during the turbine performance study period were necessary to provide additional conclusions. One minute turbulence intensity values were calculated. Correlation coefficients between wind velocity, power production, TI, and temperature were studied. The most clear relationship exhibited were between temperature and TI, with an r = 0.85 for the undisturbed direction and 0.97 for the disturbed direction. Other notable r values include the obvious relationship between wind and power with an r value of 0.94 for the disturbed direction and 0.96 for the undisturbed direction. The r-value between wind and temperature was 0.68 for the undisturbed direction and 0.60 for the disturbed direction. Correlation coefficients between wind velocity and turbulence intensity were not high with -0.54 for the undisturbed direction and -0.62 for the disturbed direction. A reason for this could be that turbulence intensity values is already Category C, the lowest turbulence category, for all temperature bins of both disturbed and undisturbed sectors.

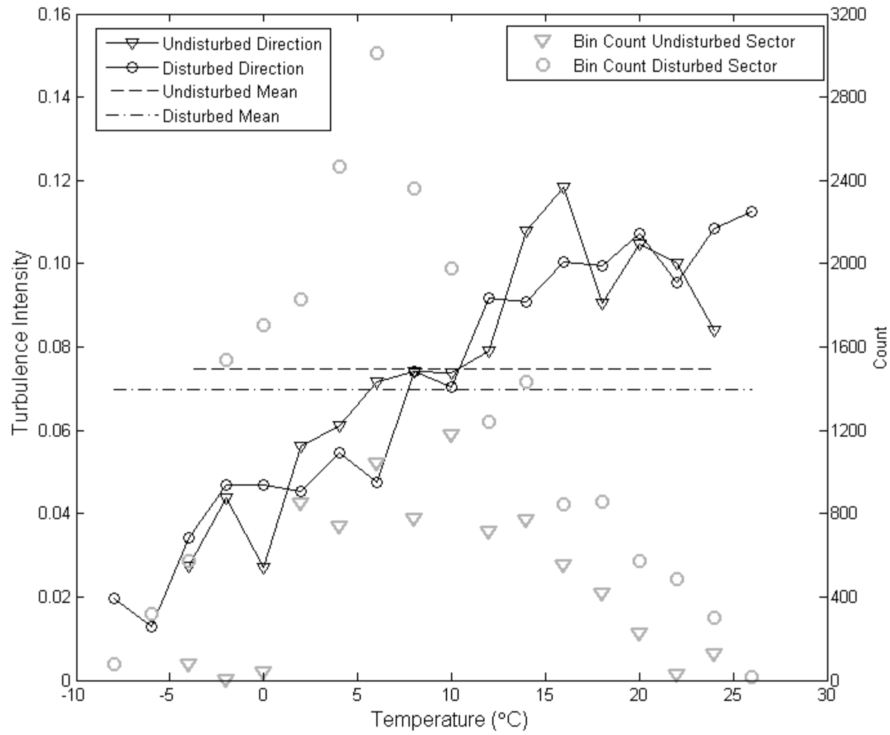

Figure 3-35: Turbulence intensity versus temperature during turbine performance study

Turbine energy production was binned in terms of temperature from the longest stretch of good data from July 28th 2010 to July 1st 2011 and is displayed in Figure 3-36 (a) along with number of counts in each bin. During this period, a correlation coefficient of 0.93 related the proportion of overall time in each bin and energy production. An observation that can be made from this is that energy production was consistent at all temperatures. Average values for estimated hub height wind velocity and turbine power output were calculated and binned by temperature and shown in Figure 3-36 (b) and (c). The hub height wind velocity was very consistent across the temperature bins. The most positive deviation from the average occurred in the 1°C bin at 31% higher and the most negative deviation from the average occurred in the 27°C bin at 31% lower. Because of the cubic relationship between wind and power, the power deviation from the average is 82% higher in the 1°C bin and 69% lower in the 27°C bin.

(a)

(b)

(c)

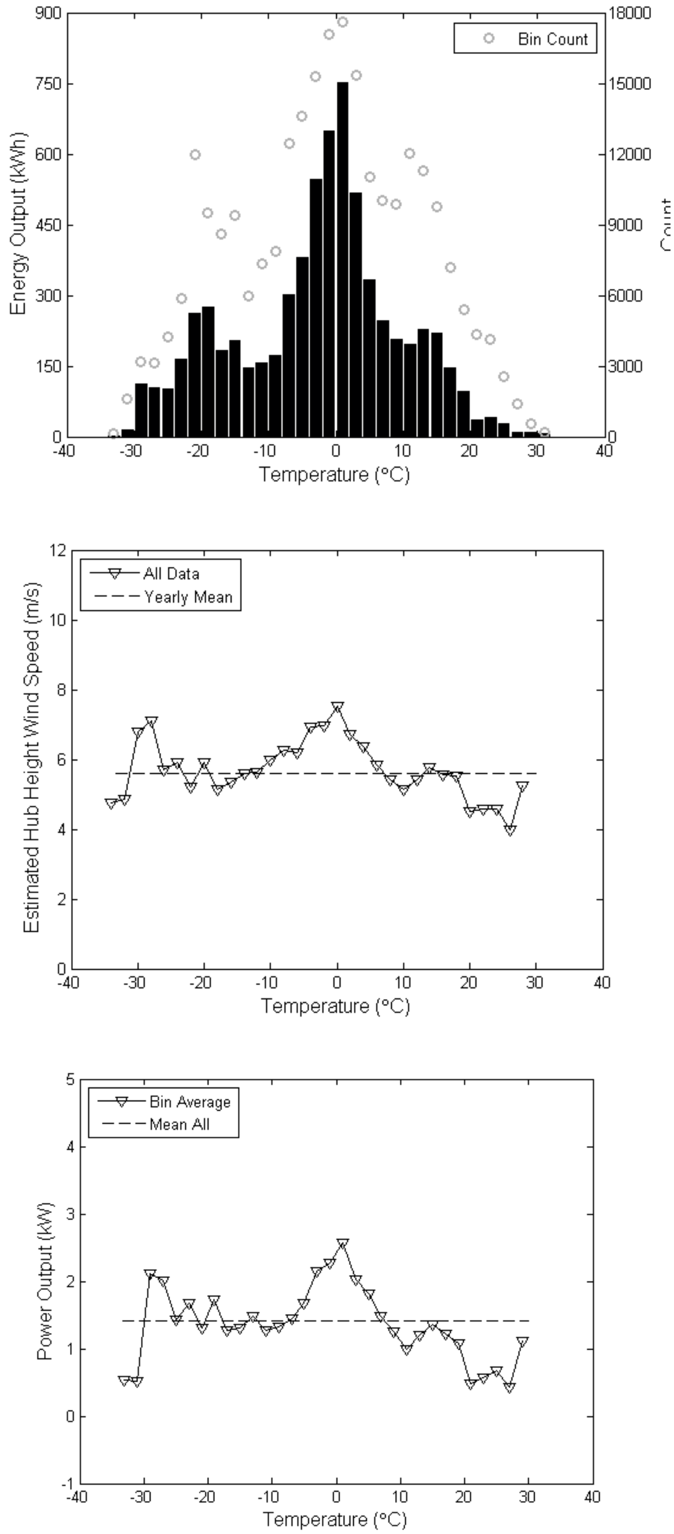

Figure 3-36: Data binned by temperature (a) Energy production binned by temperature (b) Estimated average hub height wind velocity (c) Average power output

Additional statistics were calculated in order to study environmental characteristics that affected turbine performance during the 11 month span. Values for turbulence intensity were calculated and binned by temperature and shown in Figure 3-37. Turbulence intensity was lowest at low temperatures, ranging from 0.02 to 0.07 below freezing and 0.05 to 0.12 above freezing. The overall mean TI during the 11 month span was 0.07.

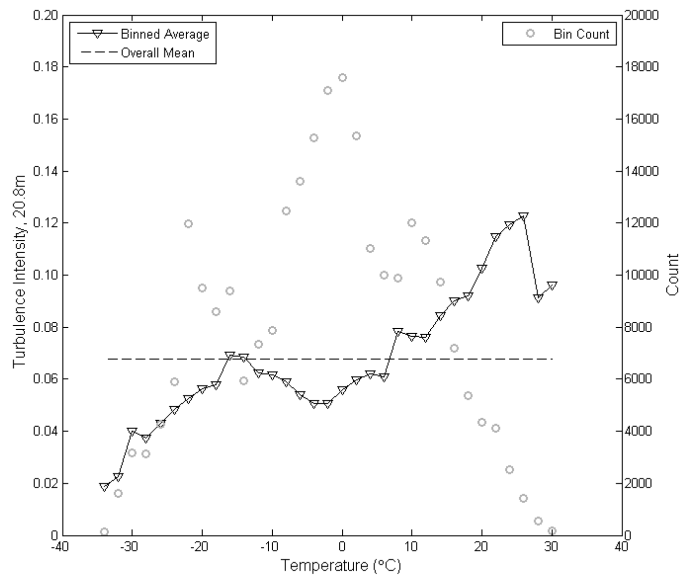

Figure 3-37: Turbulence intensity binned by temperature over the 11 month turbine non-direction study

Correlation coefficients between wind velocity, power output, and TI were calculated. Over the longer study period, wind had high correlation coefficients with TI and power values with an r-value of -0.78 and 0.96, respectively. Power had high correlation coefficients with TI with an r-value of -0.82. Other notable correlation coefficients include r=-0.5 between wind and temperature and -0.57 between power and temperature.

3.3.2.8 Time averaged sampling interval

Wind power curves developed from testing are highly dependent on the time averaging sampling interval. According to 61400-12-1 Annex H, the power curve for a small wind turbine should be based on 1 minute averages. Various studies have been presented on the topic of time averaging sampling interval (de Paz et al. 2004; Klemen 1998; Makkawi et al. 2009). Data from the turbine performance study was averaged into 10 second, 60 second, 10 minute, and hourly datasets and corrected using concurrent sea level air density values. The method of bins and filtering for wind shear values between 0.05 and 1 was performed in the same manner as previously. Bins with more than 10 minutes of data were applied to generic Rayleigh wind distributions of average wind velocities varying from 4 to 11m/s. Measured AEP as well as AEP-extrapolated estimates for the four different averaging intervals are shown in Table 3-8.

Due to the small averaging interval, 10 second shear exponent values were more likely that the longer averaging intervals to fall outside the range of 0.05 to 1, with 80% of the values falling within this range. This compared to 88% for the 1 minute averaging interval, 93% for the 10 minute averaging interval, and 96% for 1 hour averaging intervals. The hub height estimate does not affect the averaged power value, but does affect where the data point is located in the binned power curve. An additional consideration in creating different time averaged power curves is that it is likely for power values from shorter averaging schemes to give a better estimate of the actual power harvested from the wind because the shorter time scale captures more of the power fluctuations. These two variables affect the form of a power curve and a balance must be reached between the two.

The different averaging time scales created different numbers of data in each bin. Because of this, the highest bin filled with 10 minutes of data was different for each averaging. This inherently caused a difference in the measured AEP values. Therefore the AEP estimate that was extrapolated to the power curve cutout of 24m/s was the best to compare between datasets. For reference, the four resulting power curves are in Appendix I.

Table 3-8: Averaging case study for AEP estimation

	10 second average			1 minute average			10 minute average			60 minute average		
Hub height annual averaged wind velocity (Rayleigh)	AEP-measured	AEP-extrapolated	Complete if AEP-measured is at least 95% of AEP extrapolated	AEP-measured	AEP-extrapolated	Complete if AEP-measured is at least 95% of AEP extrapolated	AEP-measured	AEP-extrapolated	Complete if AEP-measured is at least 95% of AEP extrapolated	AEP-measured	AEP-extrapolated	Complete if AEP-measured is at least 95% of AEP extrapolated
m/s	kWh	kWh		kWh	kWh		kWh	kWh				
4	3687.5	3687.6	Complete	3825.6	3825.7	Complete	3921.8	3922.0	Complete	4022.7	4086.0	Complete
5	7814.9	7821.2	Complete	8058.3	8064.6	Complete	8110.5	8129.5	Complete	7619.1	8273.8	Incomplete
6	12250.9	12336.8	Complete	12548.2	12633.4	Complete	12434.9	12625.8	Complete	10428.0	12758.0	Incomplete
7	16105.4	16518.3	Complete	16397.8	16807.2	Complete	15981.5	16745.3	Complete	11938.6	16944.5	Incomplete
8	18878.0	20007.2	Incomplete	19128.6	20248.3	Incomplete	18333.5	20194.7	Incomplete	12365.8	20564.1	Incomplete
9	20490.8	22701.0	Incomplete	20686.5	22878.0	Incomplete	19522.8	22900.0	Incomplete	12098.5	23517.1	Incomplete
10	21120.7	24618.5	Incomplete	21263.0	24731.2	Incomplete	19797.9	24874.8	Incomplete	11455.3	25771.5	Incomplete
11	21025.8	25831.7	Incomplete	21122.3	25887.5	Incomplete	19442.4	26171.3	Incomplete	10644.5	27338.2	Incomplete
Highest measured wind velocity bin	16.5 m/s	24m/s		16	24m/s		15.5m/s	24m/s		14m/s	24m/s	

All datasets were compared to the 1 minute averaging method, the current industry standard for small wind turbine testing. The 10 second averaging method predicted an extrapolated AEP differed from the 1 minute AEP which differed the most at 4 m/s where it was 4% lower. The 10 second estimates for sites with hub height annual averaged wind velocities of 7 to 11m/s differed from the 1 minute average by 0.02% to 2.3%, with the smallest differences occurring at the highest average wind velocity. This is because the largest differences between the two binned power curves occurred at wind velocities lower than the rated wind velocity.

The 10 minute averaging method differed from the 1 minute averaging method by 2.5% at 4m/s. For hub height averages of 5 to 11m/s, the difference between the two methods were no more than 1%. The largest differences came between the 60 minute AEP estimates and the 1 minute averaging method. The 60 minute averages overpredicted the AEP estimate by 1 to 7%, with the largest differences between at the highest and lowest average wind velocities. This is because the differences between the two power curves are at the extremes of the power curve – the 60 minute averaged power curve is higher at low wind velocities and has a cut-off at a power level closer to the rated wind velocity compared to the 1 minute averaged power curve.

The results of this study are by no means a word of support for 10 minute averages. The use of a 1 minute averaging interval is appropriate for small wind turbine testing as these machines are highly sensitive to changes in wind direction and velocity. This study has shown that the turbine's constant velocity design is appropriate for the application and is correctly installed on a tall enough tower to enable it to harvest the Prairie wind regime's consistent winds.

3.3.3 Summary and Conclusions

Results from the in-situ testing of an Endurance S-343 turbine as outlined by IEC Standard 61400-12-1were presented in the form of a measured power curve, AEP prediction tables, coefficient of performance curve, and test sector turbulence intensity plots. The measured power curve was found to agree well with the manufacturer power curve. AEP predictions from the testing results were low compared to manufacturer estimates, largely due to differences between the measured and manufacturer power curve from wind velocities coinciding with turbine cut-in to maximum turbine power output. The coefficient of performance curve showed that the turbine was operating at a high efficiency over the operating range. Test sector turbulence intensity results demonstrated that the turbine was installed in an excellent wind regime well suited to turbine testing.

Several variables affecting turbine performance were studied including the relationship between wind velocity, temperature, and turbulence intensity. These variables were studied during the turbine testing period as well as during the 16 months of operation. It was confirmed that turbulence intensity correlates to temperature, which is likely due to the effect of solar heating on convective atmospheric eddies. Power curves from the non-test sector and test sector were compared and it was confirmed that upstream disturbances change the shape of the curve due to higher turbulence, resulting in differences in AEP predictions. Time averaged sampling intervals of 10 second, 1 minute, 10 minute, and one hour were studied in the form of power curve creation and AEP estimates. The choice of one minute averaging intervals for small wind turbine testing in 61400 were confirmed, as this sampling interval captures the variability the wind without allowing estimates to be affected by small scale turbulence.

3.4 Use of Vertical Extrapolation for Power Performance Testing

3.4.1 Introduction and Methodology

Vertical extrapolation of wind velocities using power or log law methods is a widely accepted method in the wind industry. No official standard exists for the installation of anemometers on the tower of an operating wind turbine. As discussed in Section 1.1.4, several guidelines have been presented in literature. Several works recommend mounting the topmost anemometer at one rotor diameter from hub height (Ziter 2010; Gipe 2004). Using this guideline, the bottom three anemometers are outside the region of influence, with the top anemometer being inside the affected zone. This section looks to study the accuracy of wind estimates within these regions using the bottom two anemometers and power and log law methods.

3.4.1.1 Uncertainty

A summary of error estimation techniques used in this section are presented here. All estimates of extrapolated wind velocities to levels at which instruments existed were compared on the basis of mean error, ME:

$$ME = \frac{\sum_{i=1}^{n}(U_{est,i} - U_{true,i})}{n} \tag{3.21}$$

where $U_{est,i}$ is any estimate of a wind velocity for a 1 minute averaged data point and $U_{true,i}$ is the corresponding wind velocity measurement at the estimate level and n is the number of data points in the sample. It is noted that a positive mean error is an over-prediction and a negative mean error is an under-prediction.

Sample standard deviation σ was calculated in addition to mean error and is calculated as:

$$\sigma = \sqrt{\frac{1}{n-1}\sum_{i=1}^{n}(E_i - ME)^2} \tag{3.22}$$

where E_i is the error associated with each points i. This gives a measure of variability of the estimates about their mean error.

An uncertainty μ can be created from combining the ME and standard deviation as follows:

$$\mu = ME \pm \sigma \tag{3.23}$$

In some areas, mean absolute error (MAE) is used to visualize the magnitude of the error associated with the application of certain methods. *MAE* is calculated as:

$$MAE = \frac{\sum_{i=1}^{n} \left| U_{est,i} - U_{true,i} \right|}{n} \tag{3.24}$$

For further details on error analysis, interested individuals are referred to Appendix C.

3.4.2 Vertical Extrapolation Methods

One minute averaged data was filtered for tower shading and binned into 10° bins. Wind velocity values for the horizontal component of sonic at height 31.5m and the top cup anemometer output at height 33.8m were estimated using four different algorithms used in a previous study (Ray et al. n.d.). Only estimates were made for values above the lower wind cut-off velocity of 3.1m/s. They include:

- Power Law 1 – Each one minute shear parameter calculated from the lower two cup anemometers was used to extrapolate a wind velocity time series from U_2 to the upper two heights and compared to actual concurrent values.
- Power Law 2 – Each one minute wind velocity taken from the lower two cup anemometers was averaged and a single overall shear parameter was calculated from these values. This value was used to extrapolate a wind velocity time series from U_2 to the upper two heights and compared to actual concurrent values.
- Power law 3 – Each one minute shear parameter calculated from the lower two cup anemometers was averaged and a single overall shear parameter was used to extrapolate a wind velocity time series from U_2 to the upper two heights and compared to actual concurrent values.
- Log law – Each one minute wind velocity taken from the lower two cup anemometers is used to solve for the best-fit surface roughness (z_o). This

value is then used to extrapolate a wind velocity time series from U_2 to the upper two heights and compared to actual concurrent values.

3.5 Results and Discussion

The accuracy of the four vertical extrapolation methods was assessed in the context of the sonic anemometer and the top cup anemometer from 10° bins. Resulting ME and MAE from each method for predicting the top cup anemometer wind velocity, U_1, are displayed in Figure 3-38 and Figure 3-39, respectively. Resulting mean error and mean absolute error from each method for predicting the sonic anemometer wind velocity, U_{son}, are displayed in Figure 3-40 and Figure 3-41, respectively. The mean error and mean absolute error for the estimate and the closest anemometer wind velocity, U_2, was also plotted for reference.

As expected, the greatest error occurred when no extrapolation was used. Any of the vertical extrapolation methods outlined here improved the estimate of a wind velocity at a higher point. The direction that the largest differences between U_1 and U_2 and U_{son} and U_1 occurred was to the south where the largest upwind disturbances were located. The smallest differences between these instruments occurred across the test sector.

Interestingly, the test sector in the direction of the instrument boom was where both power law 1 and log law overpredicted the wind velocity at U_{son} and U_1. It is possible that this is due to the effects of upstream wake expansion resulting from the operating wind turbine directly above the instruments. This wake expansion is one of the reasons why met tower installers typically use multiple anemometers at each height and install them at a right angle to each other and at an angle of 60 degrees to the tower, as the tower causes a slowdown of the stream velocity (King et al. 2005).

All four methods utilized here resulted in comparable mean prediction errors, agreeing with findings from previous studies (Elkinton et al. 2006; Ziter 2010). Interestingly, log law resulted in similar errors to power law, with resulting accuracies within 0.2m/s from the test sector. It was previously thought that power law was more accurate than log law over short temporal averaging periods (Ziter 2010). A slightly different application of log law than previously used was utilized which uses concurrent wind velocities from two heights and a line of best fit in order to estimate the best U_* and z_o values. It is clear from Figure 3-38 to Figure 3-41 that this method has improved estimates.

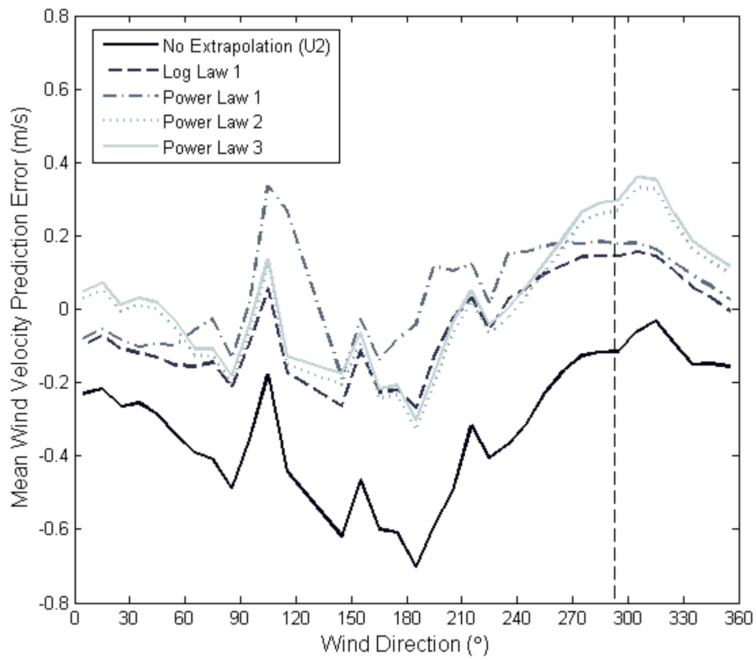

Figure 3-38: U_1 mean estimation error resulting from tower mounted anemometers and different vertical extrapolation methods. The vertical dashed line indicates the instrument boom direction.

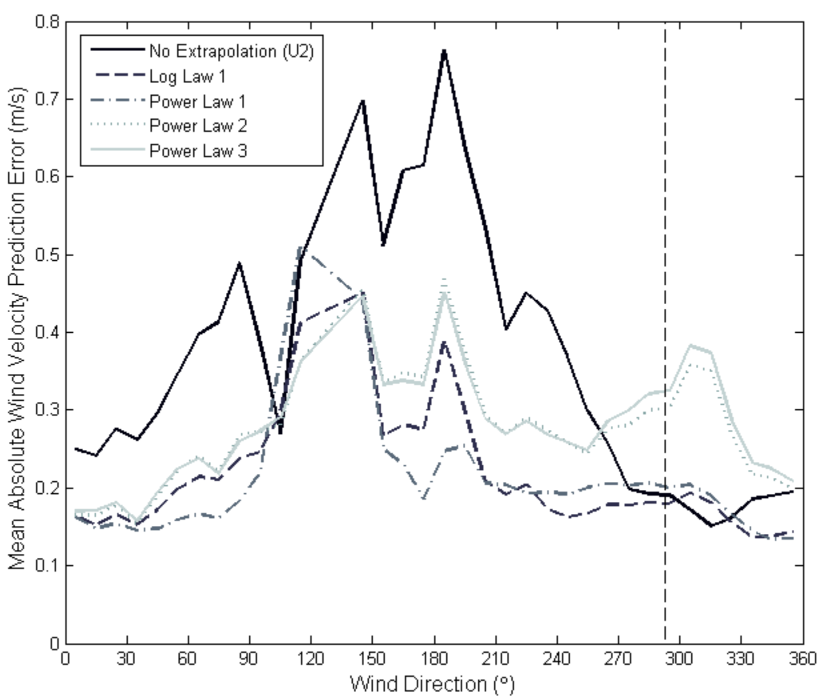

Figure 3-39: U_1 mean absolute estimation error resulting from tower mounted anemometers and different vertical extrapolation methods

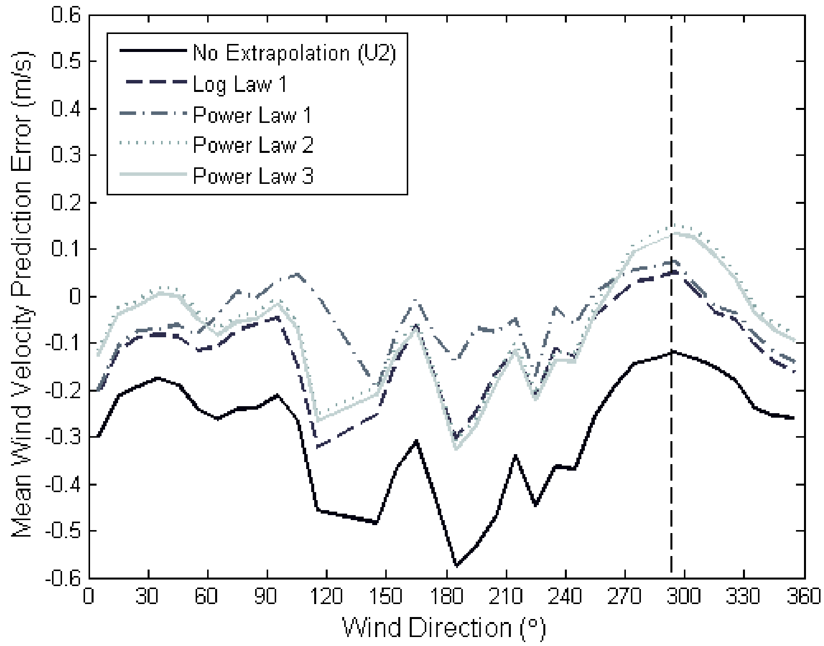

Figure 3-40: Sonic horizontal component mean estimation error resulting from tower mounted anemometers and different vertical extrapolation methods

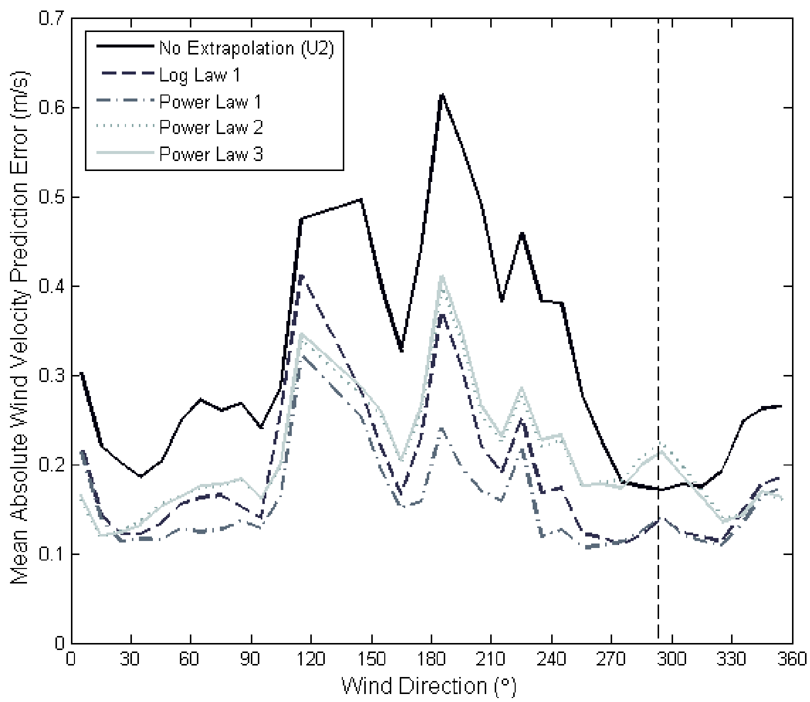

Figure 3-41: Sonic horizontal component mean absolute error resulting from tower mounted anemometers and different vertical extrapolation methods

Vertical extrapolation methods were less accurate when instruments were affected by nearby obstacles (tower) and near vicinity obstacles (trees and other disturbances). Elimination of tower shadow was attempted by filtering. An increase in magnitude of error in the directions of 110° to 240° direction is likely mostly from upstream obstacles. Because only one instrument was installed at each height and all were installed on booms mounted in the same direction, it is impossible to differentiate between error from the tower and obstacles farther upstream. That being said, this installation method is the best option with one instrument at each height as the most important region, the test sector, was not affected by tower shadow.

Uncertainties and errors derived from the application of the four methods on U_1 and U_{son} estimates from the test sector only are summarized in Table 3-9 and Table 3-10. As expected, the use of U_2 with no extrapolation was the least accurate estimate. Interestingly, the mean error, standard deviation, and MAE of using the U_2 to estimate U_{son} was larger than using U_2 to estimate U_1. All vertical extrapolation methods resulted in reasonably low ME and MAE at each height. As well, all methods produced similar standard deviations at each height. The two methods calculated in each time step, log law and power law, resulted in lower ME and MAE for both anemometer heights compared to power law 2 and 3. Often power law 2 and 3 are used in practice because they are the least computationally intensive along with resulting in reasonable accurate estimates (Ziter 2010), although often the best choice is site specific (Elkinton et al. 2006). Overall lower uncertainty was found when estimating the sonic wind velocity compared to the top cup anemometer, although slightly higher standard deviation resulted in this estimation. A margin wide enough to consider the top cup anemometer severely affected by the operating wind turbine was not found.

Table 3-9: Tower-Mounted Anemometer Measurement Errors and Vertical Extrapolation Prediction Errors when compared with U_1 Data at 33.8m (Test Sector Data Only)

Method	Uncertainty, m/s	MAE, m/s
U_2	-0.147±0.228	0.211
Log Law	0.069±0.208	0.175
Power Law 1	0.103±0.199	0.181
Power Law 2	0.192±0.273	0.273
Power Law 3	0.217±0.278	0.289

Table 3-10: Tower-Mounted Anemometer Measurement Errors and Vertical Extrapolation Prediction Errors when compared with Sonic Data at 31.5m (Test Sector Data Only)

Method	Uncertainty, m/s	MAE, m/s
U_2	-0.172±0.320	0.320
Log Law	-0.030±0.316	0.134
Power Law 1	-0.008±0.313	0.129
Power Law 2	0.067±0.341	0.180
Power Law 3	0.051±0.339	0.174

In order to study the directional dependence on extrapolation accuracy, the wind velocity estimates for U_1 and U_{son} were studied in terms of four direction sectors that were derived from the findings of the site survey. Wind velocity estimates were made using the two methods calculated in each step, power law 1 and log law. The uncertainty and MAE were calculated for each of the sectors using the concurrent wind velocities from the instruments at the two heights and are presented in Table 3-11 and Table 3-12 alongside relevant data set statistics.

Table 3-11: Directional Case Studies for Vertical Extrapolation – U_1 at 33.8m

			Power Law Method 1		Log Law	
Direction Sector	Data Points	Mean, m/s	Uncertainty, m/s	MAE, m/s	Uncertainty, m/s	MAE, m/s
Test Sector (74°-268°)	31339	5.98	0.103±0.200	0.181	0.069±0.208	0.175
Railroad ties (74°-106°)	2770	5.32	0.017±0.312	0.238	-0.099±0.283	0.225
SE Windrow (117°-203°)	31919	7.11	-0.154±0.444	0.346	-0.276±0.425	0.390
SW Shrubs (212°-268°)	14509	6.16	0.138±0.209	0.198	0.0474±0.220	0.177

Table 3-12: Directional Case Studies for Vertical Extrapolation - U_{son} at 31.5m

			Power Law Method 1		Log Law	
Direction Sector	Data Points	Mean, m/s	Uncertainty, m/s	MAE,m/s	Uncertainty	MAE
Test Sector (74°-268°)	31339	6.00	-0.008±0.313	0.128	-0.030±0.316	0.134
Railroad ties (74°-106°)	2770	5.22	0.013±0.320	0.134	-0.068±0.339	0.161
SE Windrow (117°-203°)	31919	7.03	-0.233±0.420	0.315	-0.322±0.428	0.372
SW Shrubs (212°-268°)	14509	6.18	-0.043±0.175	0.136	-0.105±0.194	0.169

The highest average wind velocities were seen from the disturbed SE windrow sector to the south. The uncertainty and MAE were also the highest in this sector for both methods compared to the other 3 sectors. Neither extrapolation method performed consistently better than the other at either one of the heights. For the most part, the U_{son} estimates had a slightly lower MAE and ME compared to the U_1 estimates. Method standard deviations for each sector were similar at the two heights. Power law 1 and log law had the lowest uncertainty and MAE when estimating wind velocities in the test sector at both heights compared to non-test sectors.

To study what wind velocities that the highest extrapolation error was occurring at, the mean wind velocity prediction error from using the power law extrapolation method was calculated for each height and binned by the instrument wind velocity being estimated. The results are shown in Figure 3-42 and Figure 3-43. Error bars represent one standard deviation from the bin mean in these figures and the number of points in each wind velocity bin is shown for reference.

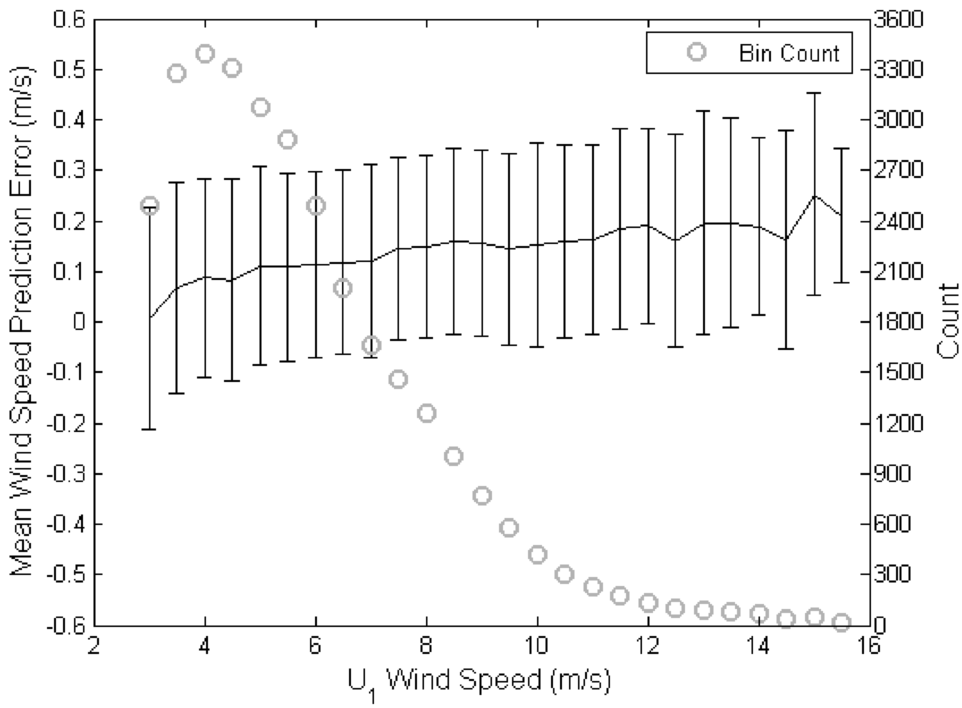

Figure 3-42: U_1 mean wind velocity prediction error, binned by U_1 wind velocity

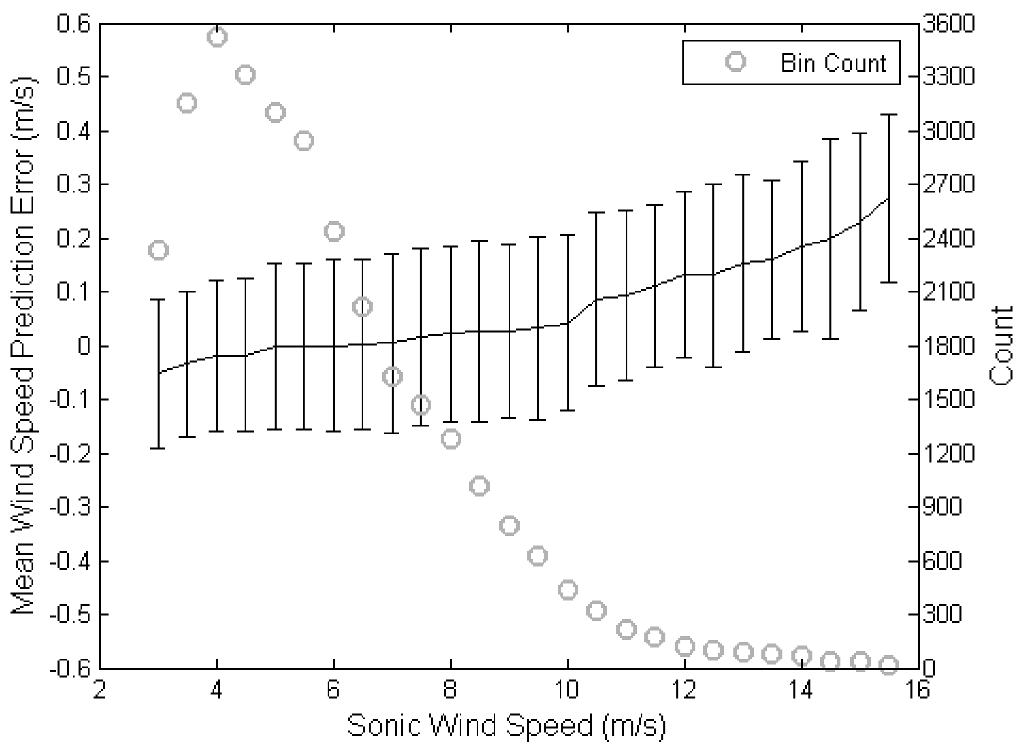

Figure 3-43: Sonic mean wind velocity prediction error, binned by sonic wind velocity

The wind velocity prediction errors at both heights show a slight increase in error as the binned wind velocity increases. No significant increase in standard deviation was present at either height. The wind velocity prediction error of U_{son} remains very close to 0 up until 11m/s, where it increases up to 0.25m/s at the 15.5m/s bin. This compares to the wind velocity prediction error of U_1 which is slightly 0.09m/s at 4m/s and has a slight increase to 0.15m/s at 15.5m/s. It is possible that the upstream wake expansion from the operating wind turbine which causes the over predictions at U_1 for all of the wind velocity bins does not affect the sonic until wind velocities above 11m/s.

The mean wind velocity prediction error as well as the mean absolute wind velocity prediction error for both heights was further filtered into 2° bins defined by elevation angle outputted by the sonic anemometer. The ME and MAE of U_1 wind velocity estimates are shown below in Figure 3-44 and Figure 3-45 and the ME and MAE of U_{son} wind velocity estimates are shown below in Figure 3-46 and Figure 3-47. All bins plotted have a minimum of 10 minutes of data.

Apparent trends include the relationship between over predicting wind velocities and low elevation angles at both heights. Mean wind velocity prediction errors of U_1 estimates appear to be less dependent on the elevation angle than U_{son} estimates. From 3m/s to 8m/s, sonic over estimates are typically related to more positive elevation angles and underestimates are related to more negative elevation angles. In contrast, far more U_1 binned estimates are over predictions no matter what elevation bin. Both heights have an increase in absolute mean wind velocity error as the estimated wind velocity bin increases.

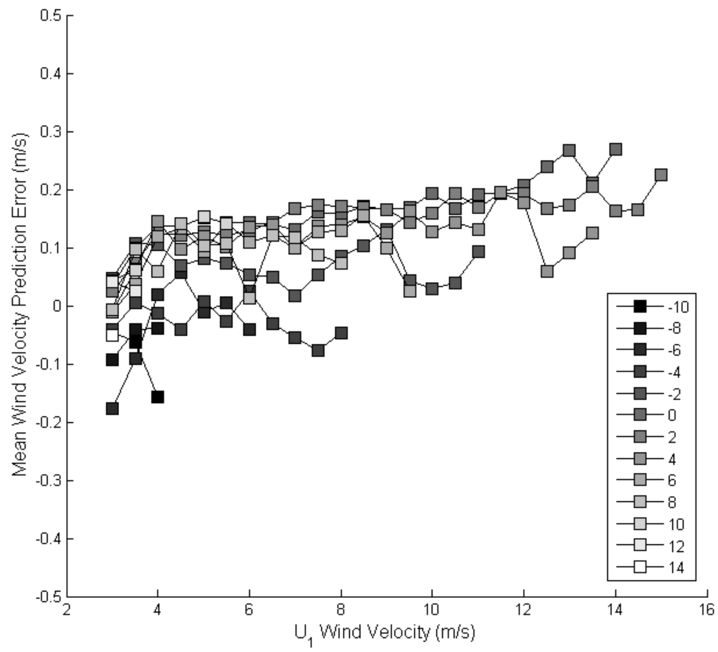

Figure 3-44: U_1 mean wind velocity prediction error, binned by sonic elevation angle

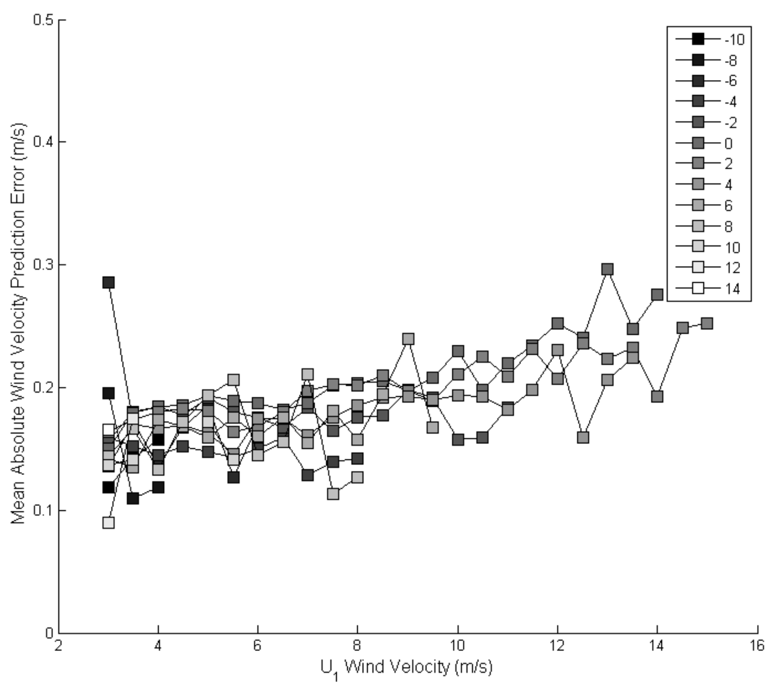

Figure 3-45: U_1 Mean absolute wind velocity prediction error, binned by sonic elevation angle

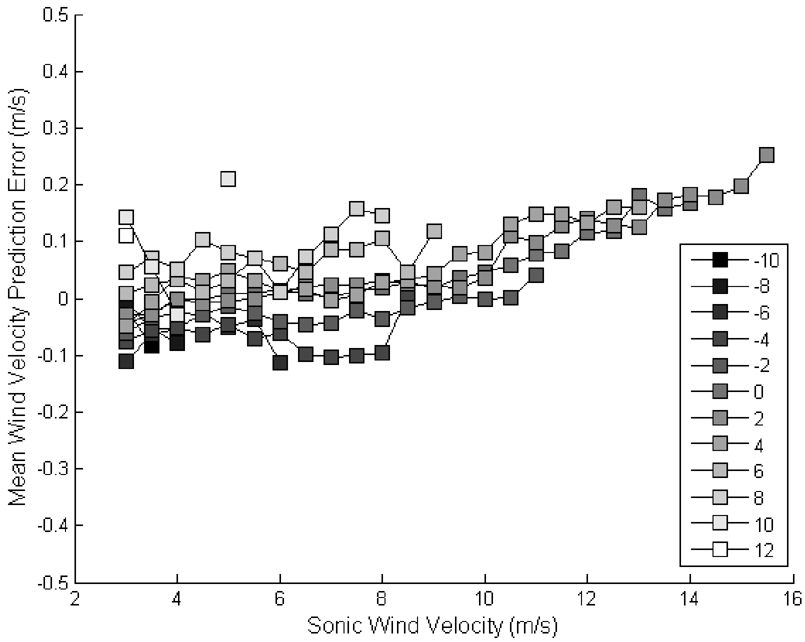

Figure 3-46: 2-D sonic mean wind velocity prediction error, binned by sonic elevation angle

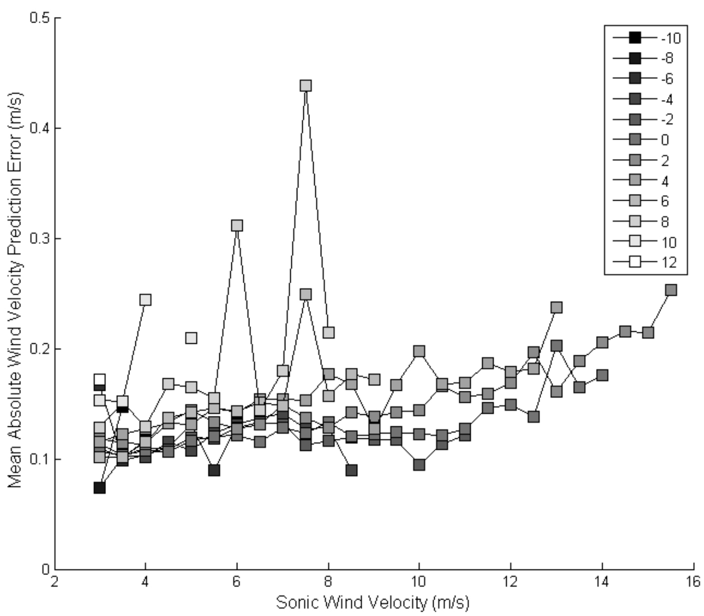

Figure 3-47: 2-D sonic mean wind velocity prediction error, binned by sonic elevation angle

3.6 Summary and Conclusions

The goal of this section was to quantify the extent of the interference zone below a constant RPM operating wind turbine. Although the use of tower mounted anemometers is an accepted practice for confirming the performance of small wind turbines, no firm standard exists for the placement of anemometers below a small wind turbine for prediction of hub height wind velocity. Literature recommends that no anemometer be installed within one rotor diameter of hub height.

In order to test this recommendation, the accuracy of several vertical extrapolation methods for prediction of wind velocities below an operating wind turbine was analyzed. These methods include log law and several variation of power law which were applied to wind velocity measurements at two heights below an operating wind turbine in order to estimate the wind velocity at two upper heights. The instruments at the two upper heights included a sonic anemometer installed outside the recommended one rotor diameter from hub height and a cup anemometer installed within the one rotor diameter.

It was concluded that use of vertical extrapolation improves wind velocity predictions of upper heights when compared to instruments mounted at lower heights. Power law and log law with parameters calculated within each time step performed well and similar to each other. These methods performed slightly better than using methods which used one parameter for all estimates.

Mean error and mean average error were slightly less for U_{son} estimates compared to U_1 estimates, especially at wind velocities below 11m/s. It is unknown whether this improvement was because of the smaller distance to the sonic anemometer height, instrument differences, or because the top cup anemometer was installed within the interference region of the turbine.

Directional case studies confirmed the value of using an undisturbed test sector when confirming small wind turbine performance testing. The lowest mean error and mean average error for power law and log law calculated in each step was from values estimated from the test sector. The highest mean error and mean average error for both heights was from the sector with the most significant disturbances.

Elevation angle of the three-dimensional wind profile appeared to have more of an obvious trend with the sonic estimate mean error than the U_1 estimate mean error. Although the turbine appears to have some effect on the estimates at the U_1 location, effects were less notable than anticipated.

4 Conclusion

4.1 Summary

The goal of this thesis was to explore various elements pertaining to the application of small wind turbines for power generation. This work is part of growing interest in small wind turbine research in the Mechanical Engineering department at the University of Alberta.

Chapter 2 presented the results of a life cycle assessment performed on three sizes of small wind turbines. Using applicable standards as well as previous works in the area of wind turbine life cycle assessment, the environmental effect of a small wind turbine installed in a typical rural east-central Alberta wind regime was discussed. Each array of 5, 20, and 100kW turbines studied were rated for 100kW of nameplate power and analyzed on a consistent unit of impact per kilowatt-hour produced. The following conclusions were made from the study:

- The unit processes with the largest affect on the life cycle energy and emission impact of the small wind turbine arrays were those encompassing the manufacturing of the turbine systems as well as transportation and installation.
- The financial performance of any of the configurations is not currently attractive from an investor's standpoint in the current economic environment. Government subsidies and incentives in support of small wind would need to be great to make such energy systems attractive from a purely revenue based perspective.
- The economy of scale concept was shown to govern the environmental, energy, and economic impact of small wind turbines. Although all arrays of turbines produced close to the same amount of energy in the same wind resource over their lifespan, the array comprised of one 100kW wind turbine had the fastest return on the environmental, energy, and economic input necessary to manufacture, install, and maintain the arrays.
- The results of this study were discussed with regards to the current Alberta Microgeneration Law, which limits the size of generators that private individuals in Alberta can connect to the grid to only produce enough energy to offset the owner's energy use. Therefore it was concluded from the results of

the study that in order to improve the emissions intensity of the Alberta power grid, the constraining variable limiting connection of clean sources of power such as wind turbines must be the local power grid.

Chapter 3 discussed the results of a wind resource and turbine performance analysis conducted on data collected over 17 months from a grid-connected 5kW turbine installed in East-Central Alberta. Application of relevant standards and previous works were used to analyze the wind resource and factors affecting the performance of the wind turbine over the period. The utilization of tower mounted anemometers for prediction of hub height wind velocities was also studied. The following conclusions were made from the results of this study:

- The wind resource at Halkirk was that of a typical open Canadian Prairie environment with low overall turbulence intensity, large diurnal and monthly temperature extremes, consistent monthly wind velocities, and mixed long Prairie grass/short tree surface roughness.
- An excellent correlation was found between wind velocity and direction data estimated at 10m from Halkirk and the nearest Environment Canada meteorological station. Parameters calculated include Weibull statistics as well as monthly, diurnal, and direction roses.
- An experimental power curve following recommendations from the SWT testing standard and power law predictions based on tower mounted anemometers was created and closely matched the manufacturer power curve. Compared to the manufacturer's power curve, the binned curve was lower at wind velocities less than the rated wind velocity by 0.16 to 0.57kW (8-30%). In contrast, the binned power curve was slightly higher at winds higher than the wind velocity, higher than the manufacturer's curve by 0.04 to 0.08kW (2-4%). The manufacturer's power curve fell within a 95% confidence interval of the normalized experimental power curve in all wind speed bins but three at 12, 12.5, and 13m/s.
- Wind and power statistics from the direction and non-direction study periods were studied in terms of temperature behavior. A clear relationship between turbulence intensity and temperature was apparent. It was found that overall turbine energy production was not affected by temperature as total energy

produced at each temperature was strongly related to proportion of time in each bin.

- Annual Energy Production estimates were created using 10 second, 1 minute, 10 minute, and 60 minute time averaged data sets. Due to the temporally sensitive nature of turbulence and how it affects wind and turbine power production, 1 minute averages captured the best estimates of hub height wind velocity estimates and turbine production
- Vertical extrapolation was used to estimate wind velocity at heights inside and outside the 'influence region' of the turbine. Slow down of the wind from the region in line with the boom due to stream tube expansion was noticeable and more apparent at the higher wind velocities where increased sonic wind velocity elevations were evident.

4.2 Recommendations for Future Research and Development

The broad work performed in this study identified many areas of future work. Possible areas for work in the life cycle assessment area are detailed below:

- In the life cycle assessment study, the emissions intensity used throughout was limited to the current Alberta grid emissions factor. Recently introduced laws restricting coal-fired generating stations will dramatically affect the future grid emissions factor. Sensitivity analysis into different future grid scenarios would provide insight into the effect of grid emissions on small wind turbine return on emissions, energy, and economic investment.
- With the closure of coal-fired generating stations, the economic environment will change around grid energy production in Alberta. An economic sensitivity analysis would provide insight into ways to encourage the growth of small-scale distributed renewable generation in Alberta.
- The intermittency of the wind resource was not considered in the life cycle assessment. A discussion on intermittency of wind power and backup power options would be a good follow up to the LCA portion of this study.
- The turbine performance study assumed that wind direction at hub height was the same as that at the height of the tower mounted direction sensor. Effects of yaw could be studied by installation of a yaw sensor on the yaw bearing of the turbine.

- The turbine site used within the turbine performance study had extremely low turbulence, even in areas considered disturbed. Analysis of the S-343 model's performance at a site with higher turbulence would provide a better understanding of the constant velocity rotor's capabilities in this type of flow.
- In this study, a single sensor for wind velocity and direction was installed at each height on the turbine tower. Because of this, some tower shading occurred and affected certain sectors of the wind profile. The use of multiple sensors at each height is very common in utility wind resource assessment and its usefulness could be easily studied for in-situ wind turbine testing.
- The use of systems identification would provide a more concrete idea of the magnitude of factors affecting small wind turbine performance. This work would provide potential turbine owners a better idea of which generator to select for their specific site and wind resource.
- The application of earth based optical remote sensing technology such as LIDAR or SODAR for in-situ turbine testing would be an interesting study. Highly accurate sensors are available with this technology and in the future this technology may become financially viable.
- Further testing of real world grid-connected small wind turbines to a common standard will only increase the effectiveness of the testing standard in small scale wind applications. Additional studies will provide further information for future research. As well, public results of more turbine testing will increase consumer confidence and encourage the growth of the small wind industry on a provincial, national, and global level.

4.3 References

Bailey, B., McDonald, S., Bernadett, D., Markus, M. & Elsholz, K., 1997. *Wind resource assessment handbook: Fundamentals for conducting a successful monitoring program*, SAGE Publications. Available at: http://www.osti.gov/energycitations/product.biblio.jsp?osti_id=486127 [Accessed February 16, 2011].

Bailey, D.T., 2000. *Meteorological monitoring guidance for regulatory modeling applications*, DIANE Publishing. Available at: http://www.epa.gov/scram001/guidance/met/mmgrma.pdf [Accessed July 26, 2011].

Burton, T., Sharpe, D., Jenkins, N. & Bossanyi, E., 2001. *Wind energy handbook*, John Wiley and Sons.

Elkinton, M.R., Rogers, a L. & McGowan, J.G., 2006. An Investigation of Wind-shear Models and Experimental Data Trends for Different Terrains. *Wind Engineering*, 30(4), pp.341-350.

Endurance Wind Power, 2011. S-343 Specification Sheet. Available at: http://www.endurancewindpower.com/s343.html pdf [Accessed August 26, 2011].

Environment Canada, 2011a. Canadian Wind Energy Atlas. Available at: http://www.windatlas.ca/en/nav.php?no=44&field=E1&height=50&season=ANU [Accessed March 2011].

Environment Canada, 2011b. National Climate Data and Information Archive. Available at: http://climate.weatheroffice.gc.ca/Welcome_e.html [Accessed June 2011].

Gipe, P., 2004. *Wind power: renewable energy for home, farm, and business* 2nd ed., Chelsea Green Publishing.

Google Maps, 2011. Halkirk Turbine Site. Available at: http://g.co/maps/yvd4a [Accessed June 2011].

IEC, 2005a. *61400-12-1: Power performance measurements of electricity producing wind turbines*,

IEC, 2005b. 61400-1: Wind turbine generator systems - Part 1: Design requirements.

Kaiser, K., Langreder, W., Hohlen, H. & Højstrup, J., 2007. Turbulence Correction for Power Curves. *Wind Energy*, pp.159-162.

King, B., Cobden, L. & Hoopes, T., 2005. The How and Why of Wind Sensor Mounting. (October). Available at: http://www.nrgsystems.com/TechSupport/~/media/Files/PDFs/The How and Why.ashx.

Klemen, M., 1998. Wind Speed Data and its Application to Wind Generated Power. *Home Power*, (January), pp.34-38.

Makkawi, a, Celik, a & Muneer, T., 2009. Evaluation of micro-wind turbine aerodynamics, wind speed sampling interval and its spatial variation. *Building Services Engineering Research and Technology*, 30(1), pp.7-14.

Mathworks, 2009. MATLAB Software Package Version 7.9.0.529.

Microsoft, 2007. Microsoft Visual Basic 6.5 Version 1053.

Mistaya Engineering Inc., 2011. Windographer Profession Edition Version 2.4.0.

Montgomery, D.C. & Runger, G.C., 2007. *Applied Statistics and Probability for Engineers* 4th ed., John Wiley and Sons.

Ohio Semitronics Incorporated, 1998. Operation and Calibration Manual. , 5.

de Paz, L.A., Avia, F., Cano, L., Cruz, I. & Soria, E., 2004. Power Performance Testing of Small Wind Turbines: Experiences and findings obtained testing the Bornay 1500 Inclin Neo Wind Turbine. In *2004ewec.info*. Available at: http://www.2004ewec.info/files/23_1400_felixavia_01.pdf [Accessed February 16, 2011].

Peterson, T.C. & Parton, W.J., 1983. Diurnal variations of wind speeds at a shortgrass prairie site–a model. *Agricultural Meteorology*, 28(4), pp.365–374.

Rareshide, E., Tindal, A., Johnson, C., Graves, A., Simpson, E., Bleeg, J., Harris, T. & Schoborg, D., 2009. Effects of Complex Wind Regimes on Turbine Performance. In *AWEA Windpower*. pp. 1-15. Available at: http://www.gl-garradhassan.com/assets/technical/Effects_of_complex_wind_regimes_on_turbine_performance_14May09_final.pdf.

Ray, M.L., Rogers, A.L. & Mcgowan, J.G., Analysis of wind shear models and trends in different terrains. *Renewable Energy*, pp.1-14.

Turner, D.B., 1986. Comparison of three methods for calculating the standard deviation of the wind direction. *Journal of climate and applied meteorology*, 25(5), pp.703–707.

Weis, T., Doukas, A., Anderson, K. & Howell, G., 2010. *Landowners' Guide to Wind Energy in Alberta*, Available at: http://pubs.pembina.org/reports/alberta-landowners-guide-web.pdf. [Accessed July 16, 2011].

Wood, D., 2011. *Small Wind Turbines: Analysis, Design, and Application*, Springer.

Ziter, B., 2010. *Alternative Methods of Estimating Hub-height Wind Speed for Small Wind Turbine Performance Evaluation*. Master's Thesis, University of Guelph.

Appendix A: Electrical Diagram of System

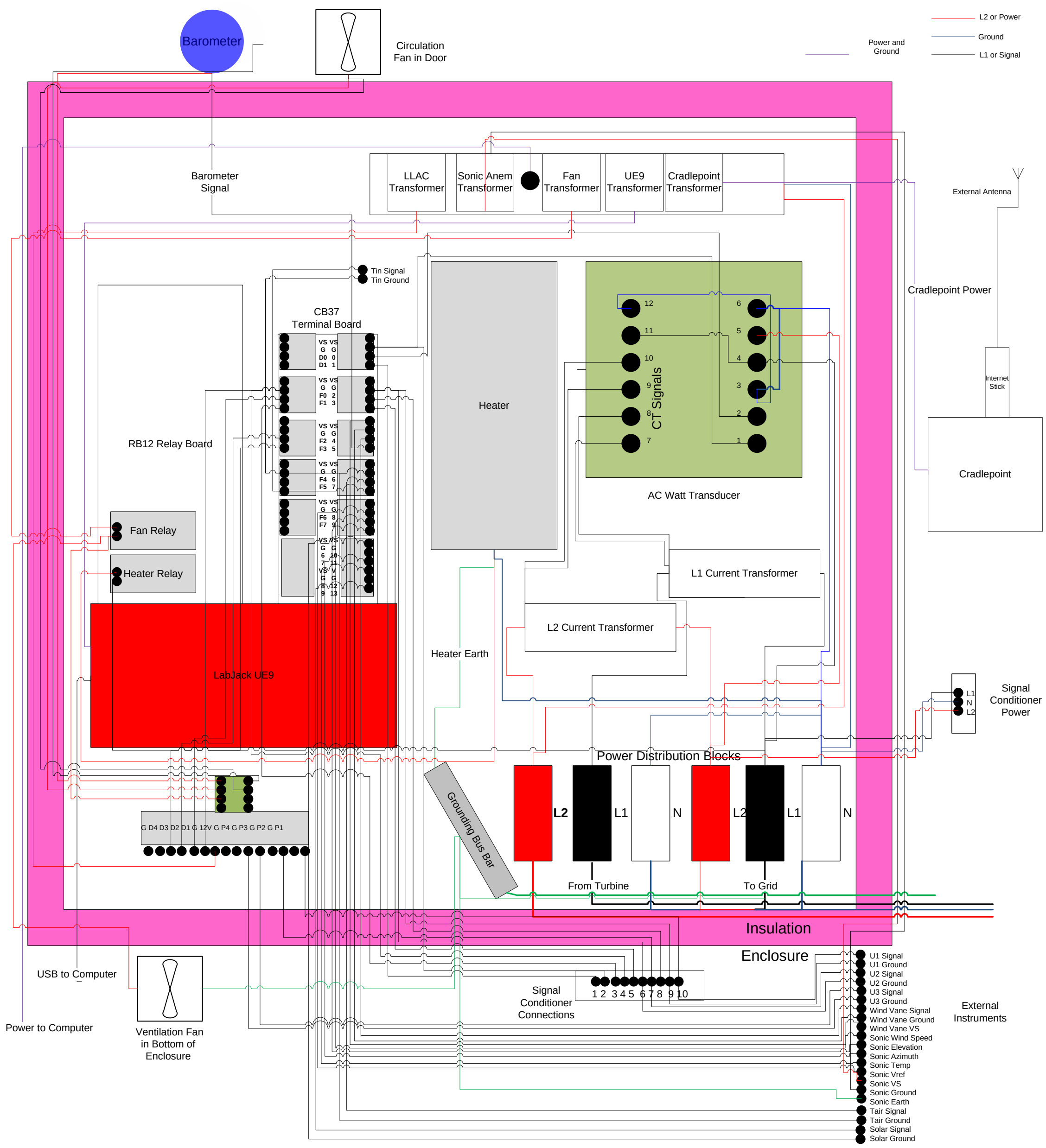

Figure A-1: Detailed Electrical Diagram of Enclosure Data Acquisition System

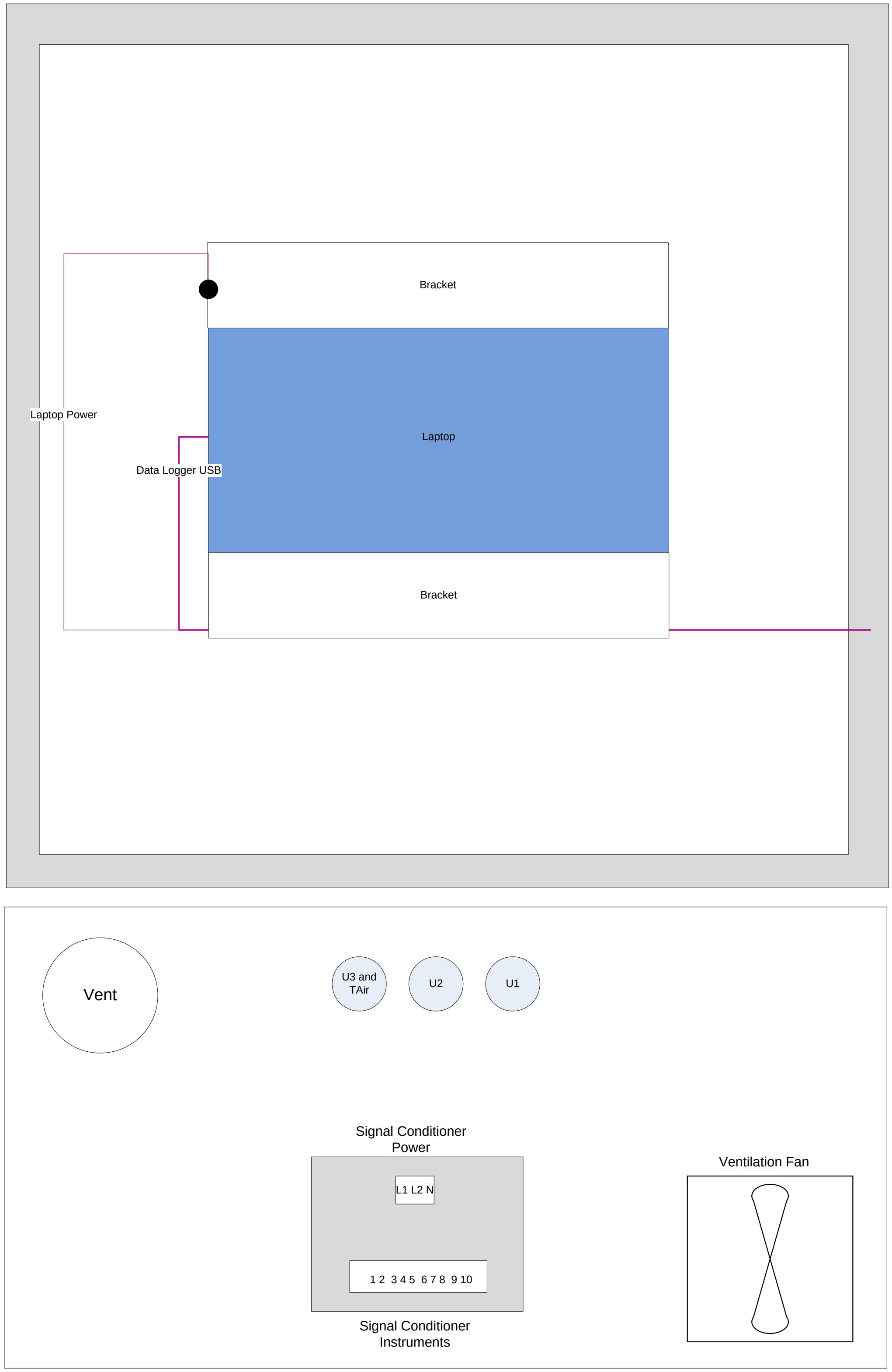

Figure A-2: Detailed Electrical Diagram of Enclosure Door and Bottom

Appendix B: Instrument Details

Table B-1: Field instrument details

Instrument	Make, Model	Serial Number	Logging Method/Channel	Range		Accuracy	Further Info Available at:	Conversion (V to Native Units)
Logging Equipment								
Data Logger	LabJack, UE9 v1.1	278954133					http://labjack.com/catalog/ue9	
Terminal Board	LabJack, CB37 rev 2.1	379814					http://labjack.com/catalog/cb37-terminal-board-rev-21	
Relay Board	LabJack, RB12 rev 1.2	23/09 SEPL					http://labjack.com/catalog/rb12-relay-board	
LLAC to TTL Pulse Converter	Campbell Scientific, LLAC4	2200					http://www.campbellsci.com/llac4	
Sensors								
Cup Anemometer (3)	NRG, #40C	179500125435	Digital/D1	0-50m/s		±0.1m/s (5m/s to 25m/s)	http://www.nrgsystems.com/sitecore/content/Products/1900.aspx?pf=StandardSensors	(750000/V)*0.759+0.34
		179500125441	Digital/D2					(750000/V)*0.759+0.37
		179500125447	Digital/D34					(750000/V)*0.759+0.38
Sonic Anemometer	Campbell Scientific, 81000	2614	Analog/A8-A11	Wind Velocity	0-40m/s	±0.05m/s (0-30m/s) and ±0.15m/s (30-40m/s)	http://www.campbellsci.ca/Catalogue/81000.html	((100/5)*V)-60
				Azimuth	360deg	±2 degrees (0-30m/s) and ±5 degrees (30-40m/s)		(540/5)*V

				Elevation	±60deg	±2 degrees (0-30m/s) and ±5 degrees (30-40m/s)		((120/5)*V)*60
				Temperature	-50degC to +50degC	±2 degrees C (0-30m/s)		((100/5)*V)+220
Wind Direction Vane	NRG, #200P	309	Analog/A4	360 degrees		potentiometer linearity within 1% (wind velocity >1m/s)	http://www.nrgsystems.com/sitecore/content/Products/1904.aspx?pf=StandardSensors	(V+0.01)*70.5
Temperature Sensors (2)	IC, LM335Z	N/A	Analog/A6-A7	minus 40 degrees to 100 degrees C		assumed 1.5°K from relevant literature	http://ca.digikey.com/1/1/358139-ic-sensor-precision-temp-92-lm335z.html	(V-2.7316)*100 (V-2.7316)*101
Watt Transducer	OSI, PC5 061X5	9100581	Analog/A1	0-15kW F.S.		± 0.5% F.S.	https://www.ohiosemitronics.com/pdf/catalog/ac_watt_transducer_modelPC5.pdf	V*2
Pressure Transducer	NRG, BP-20	1805 9806	Analog/A5	150 mbar to 1150 mbar		±15mbar	http://www.nrgsystems.com/sitecore/content/Products/2046.aspx	217.9*V+105.5
Solar Pyranometer	NRG, Li-Cor #LI-200SZ	PY66558	Analog/A12	0-3000 W/m^2		1% for sensor range	http://www.nrgsystems.com/sitecore/content/Products/1948.aspx	(V-0.392)*(7373/5)

Appendix C: Additional Uncertainty Considerations

Wind Velocity, Electric Power, AEP, and Coefficient of Performance Uncertainty

There are two types of errors that were accounted for in the power performance study: design stage uncertainty and data reduction uncertainty. IEC 61400-12-1 classifies data reduction uncertainty as Category A uncertainty and design stage uncertainty as Category B uncertainty. Data reduction uncertainty is the error in data due to the random scatter of data. Design stage uncertainty includes the instrument resolution and the analog to digital converter error. These precision errors were calculated for electrical power and AEP as outlined in 61400-12-1 as well as for coefficient of performance calculations included in the analysis.

In the cases of hub height wind velocity and C_p, multiple uncertain quantities are used in the calculation. In this occurrence, the uncertainties of the component quantities result in a total uncertainty in the parameter. This uncertainty can be determined using the "root-sum-square" (RSS) technique which is used for combining the individual components to determine the Category A uncertainty results for a calculated value as well as the overall uncertainty which combines the Category A and Category B uncertainty (J. R. Taylor 1997).

For some parameter f that is a function of several variables, $f=f(x_1,\ldots,\ x_n)$, the uncertainties of the components, $u_{x1},\ldots,u_{xn}$, are combined to result in an overall uncertainty u_f. u_f is determined by the following, assuming the uncertainties are independent and normally distributed:

$$u_f = \sqrt{\left(\frac{\partial f}{\partial x_1} u_{x_1}\right)^2 + \ldots + \left(\frac{\partial f}{\partial x_n} u_{x_n}\right)^2} \qquad \text{(C.1)}$$

Wind Measurement Uncertainty

As in other measurement error, wind measurement uncertainty is directly dependent on the instrument used. Error propagation in vertical extrapolation for prediction of hub height wind velocity propagates error via the method, be it power or logarithmic law. In the analysis, a number of methods for vertical extrapolation were used. Estimating the wind velocity using vertical extrapolation methods calculated within each time step must be treated differently than those using methods which use an average value.

It will be discussed here the uncertainty in the hub height wind velocity calculated within each time step. Uncertainty analysis of hub height wind velocity estimation has been treated before in the prediction of hub height wind velocities for utility scale wind turbines (M. Lackner & A. Rogers 2007; M. Taylor et al. 2004). The error in values calculated in each time step for power law or log law are dependent on Equations (1.2) or (1.4), respectively. As a review, with respect to power law the hub height wind velocity is calculated as follows:

$$U_{hub} = U_2 \left(\frac{h_{hub}}{h_2} \right)^{\left[\frac{\ln\left(\frac{U_2}{U_3} \right)}{\ln\left(\frac{h_2}{h_3} \right)} \right]} \tag{C.2}$$

Major sources of uncertainty for calculation of hub height wind velocity are the measurement uncertainty in U_2 and U_3. Uncertainties in the instrument heights h_2 and h_3 as well as hub height h_{hub} have significantly less impact and are neglected here. Measurement uncertainty arises when measuring the actual wind velocity at the site for each anemometer and is defined here as:

$$u_M = \sqrt{\left(u_{WS,i}\right)^2 + \left(u_{TE,i}\right)^2 + \left(u_{ME,i}\right)^2 + \left(u_{DA,i}\right)^2} \tag{C.3}$$

where u_{ws} is the uncertainty in the instrument reading in bin i, u_{TE} is the uncertainty caused by terrain effects, u_{ME} is the uncertainty caused by mounting effects, and u_{DA} is the uncertainty caused by data acquisition. All values used in the analysis are presented in Table C-1.

The hub height mean wind velocity uncertainty is defined here as the measurement uncertainty combined with the sensitivity factor of the measurement as follows:

$$u_{hub} = \sqrt{\left(c_M u_M\right)^2} \tag{C.4}$$

The sensitivity factor can be defined as follows. Assuming the calculation of predicted mean wind velocity is calculated using the following equation:

$$\bar{U}_{hub} = \bar{U}_2 \left(\frac{h_{hub}}{h_2} \right)^{\left[\frac{\ln\left(\frac{\bar{U}_2}{\bar{U}_3}\right)}{\ln\left(\frac{h_2}{h_3}\right)} \right]} \tag{C.5}$$

where variables with an over-bar indicate overall means. The data reduction of the predicted mean hub height wind velocity $\bar{U}_{hub}$ is defined as:

$$u^*_{\bar{U}_{hub}} = \pm\sqrt{\left(\frac{\partial \bar{U}_{hub}}{\partial \bar{U}_2} u^*_{\bar{U}_{M2}} \right)^2 + \left(\frac{\partial \bar{U}_{hub}}{\partial \bar{U}_3} u^*_{\bar{U}_{M3}} \right)^2} \tag{C.6}$$

Assuming the measurement uncertainties at each height are the same:

$$u_M = u_{\bar{U}_2} = u_{\bar{U}_3} = \frac{u^*_{\bar{U}_2}}{\bar{U}_2} = \frac{u^*_{\bar{U}_3}}{\bar{U}_3} \tag{C.7}$$

Submitting Equation (C.7) into Equation (C.6), the ratio of fractional uncertainty in the predicted mean wind at hub height, $u_{\bar{U}_{hub}}$, to the fractional standard measurement uncertainty, u_m, is written as follows and is the sensitivity factor for the measurement uncertainty, c_M:

$$c_M = \frac{u_{\bar{U}_{hub}}}{u_M} = \sqrt{\left(\frac{\partial \bar{U}_{hub}}{\partial \bar{U}_2} \frac{\bar{U}_3}{\bar{U}_2} \right)^2 + \left(\frac{\partial \bar{U}_{hub}}{\partial \bar{U}_3} \frac{\bar{U}_{hub}}{\bar{U}_2} \right)^2} \cdot \left(\frac{\bar{U}_2}{\bar{U}_{hub}} \right) \tag{C.8}$$

Partial derivatives and ratios of mean velocities are calculated using Equation (C.5). After substitution and simplification, the equation for measurement sensitivity factor becomes a function of the three heights. The final result for the sensitivity factor c_M is:

$$c_M = \sqrt{\frac{2\left(\ln\left(\frac{h_{hub}}{h_2}\right)\right)^2 + \left(\ln\left(\frac{h_2}{h_3}\right)\right)^2 + 2\ln\left(\frac{h_2}{h_3}\right)\ln\left(\frac{h_{hub}}{h_2}\right)}{\left(\ln\left(\frac{h_2}{h_3}\right)\right)^2}} \tag{C.9}$$

Substituting the wind velocity heights used at Halkirk, the measurement uncertainty of the hub height wind velocity result is:

$$u_{hub} = \sqrt{\left(2.54 u_M\right)^2} \tag{C.10}$$

Substituting the results of Equation (C.3) into (C.10), the measurement uncertainty for hub height wind velocity u_{hub} in each bin i can be estimated.

Electric Power Uncertainty

IEC 61400-12-1 outlines the procedure for estimating the standard uncertainty of the normalized and averaged power in each wind velocity bin using the following equation:

$$s_i = s_{P,i} = \frac{\sigma_{P,i}}{\sqrt{N_i}} \tag{C.11}$$

where $s_{P,i}$ is the category A standard uncertainty of power in bin i, $\sigma_{P,i}$ is the standard deviation of the normalized power data in bin i, and N_i is the number of 1 minute data sets in bin i.

Category B uncertainties in each bin are determined by combining the uncertainties from each data stage which include data acquisition system, electric power, wind velocity, and density. Category B uncertainty values were combined with individual sensitivity factors as displayed in Table C-1 and are found for each bin using the following equation:

$$u_i = \sqrt{u_{P,i}^2 + c_{V,i}^2 u_{hub,i}^2 + c_{T,i}^2 u_{T,i}^2 + c_{B,i}^2 u_{B,i}^2} \tag{C.12}$$

where $u_{P,i}$ is the standard uncertainty for electric power in each bin i, $c_{V,i}$ is the sensitivity factor for the wind velocity measurement, $u_{hub,i}$ is the uncertainty of each wind velocity bin, $c_{T,i}$ is the sensitivity factor for the temperature measurement, $u_{T,i}$ is the uncertainty in measured air temperature for each bin, $c_{B,i}$ is the sensitivity factor for measured air pressure for each bin, and $u_{B,i}$ is the uncertainty in measured air pressure for each bin.

Table C-1: Uncertainty values used in analysis

Component	Uncertainty	Units	Source	Sensitivity Factor
Power				
Power Transducer	37.5	W	Specs	n/a
Data Acquisition	0.1	% of FS	Assumption	
Wind Velocity				
Anemometer	0.1*	m/s	Specs (see above)	$c_{V,i} = \left\lvert \frac{P_i - P_{i-1}}{V_i - V_{i-1}} \right\rvert$
Mounting Effects	1	% of WS	IEC method	
Terrain Effects	2	% of WS	IEC method	
Data Acquisition	0.1	% of FS	Assumption	
Temperature				
Temperature Sensor	1.5	K	Assumption	$c_{T,i} = \frac{P_i}{288.15}$
Radiation Shielding	2	K	Assumption	
Mounting effects	1	K	Assumption	
Data Acquisition	0.1	% of FS	Assumption	
Air Pressure				
Pressure Sensor	15	mbar	Specs	$c_{B,i} = \frac{P_i}{1013}$
Pressure Correction	4.52	mbar	IEC method	
Data Acquisition	0.1	% of FS	Assumption	

Using the standard A uncertainty from the data collection process and standard B uncertainty from the instrument specifications and various assumptions and recommendations, the combined standard uncertainty of each bin, $u_{c,i}$, was performed as follows:

$$u_{c,i} = \sqrt{s_i^2 + u_i^2} \tag{C.13}$$

Assuming a normal distribution of uncertainty, the combined standard uncertainty resulting from this analysis has a 68.27% level of confidence. In order to expand the confidence interval, the combined standard uncertainty can be multiplied by certain coverage factors. These coverage factors are shown below in Table C-2.

Table C-2: Expanded uncertainties (IEC 2005a)

Level of Confidence (%)	Coverage Factor
68.27	1
90	1.645
95	1.960
95.45	2
99	2.576
99.73	3

AEP Uncertainty

The combined standard uncertainty of annual energy production, u_{AEP}, was found by combining the category A and B uncertainties with the wind frequency distribution from the AEP calculation applied as follows:

$$u_{AEP} = N_h \sqrt{\sum_{i=1}^{N} f_i^{\,2} s_i^2 + (\sum_{i=1}^{N} f_i u_i)^2} \qquad \text{(C.14)}$$

Where the average probability of wind velocity in bin *i*, f_i, is defined as:

$$f_i = \frac{((F_{i+1} - F_i) + (F_i - F_{i-1}))}{2} \qquad \text{(C.15)}$$

Coefficient of Performance Uncertainty

The Category B uncertainty (total design stage uncertainty) of the coefficient of performance calculation was calculated by combining the data acquisition and instrument errors with the individual parameter sensitivity. For the calculated value C_P, the sensitivity factor is defined as the partial derivative of each parameter within the final equation. The Category B uncertainty of C_P was determined by the following equation:

$$u_{C_p,i} = \pm\sqrt{\left(\frac{\partial C_p}{\partial P_i} u_{P_i}\right)^2 + \left(\frac{\partial C_p}{\partial B_i} u_{B_i}\right)^2 + \left(\frac{\partial C_p}{\partial T_i} u_{T_i}\right)^2 + \left(\frac{\partial C_p}{\partial U_i} u_{V_i}\right)^2} \qquad \text{(C.16)}$$

Following the same method as the power curve and AEP uncertainty procedures, the total uncertainty for the coefficient of performance is determined by combining the Category B and Category A (data reduction uncertainty) as below:

$$u_{C_p,c,i} = \sqrt{s_i^2 + u_i^2} \qquad \text{(C.17)}$$

References

IEC, 2005. *61400-12-1: Power performance measurements of electricity producing wind turbines*.

Lackner, M. & Rogers, A., 2007. Uncertainty analysis in wind resource assessment and wind energy production estimation. *45th AIAA Aerospace*, pp.1-16. Available at: http://www.crm.umontreal.ca/probindustriels2011/pdf/ASME07_2.1.pdf [Accessed September 15, 2011].

Taylor, J.R., 1997. *An introduction to error analysis: the study of uncertainties in physical measurements* 2nd Ed., University Science Books.

Taylor, M., Brower, M.C., Markus, M., Meteorologist, S. & Truewind, A.W.S., 2004. An Analysis of Wind Resource Uncertainty in Energy Production Estimates. In *European Wind Energy Conference*. pp. 1-11. Available at: http://www.2004ewec.info/files/23_1400_marktaylor_01.pdf.

Appendix D: Cup Anemometer Calibration Sheets

Wind velocity measurements for each cup anemometer were verified against a pitot tube in the University of Alberta low-velocity wind tunnel. The purpose of anemometer calibration was not to recalibrate the instrument but to confirm the manufacturer calibration curve. Calibration curves certified to National Institute of Standards and Technology (NIST) standards were provided for each NRG cup anemometer. A generic offset for the sonic anemometer from the manufacturer which was used in the wind tunnel verification.

Up until very recently, NRG supplied all of their cup anemometers with default offsets and slopes, like the Campbell Scientific does with their sonic anemometer. NRG now gives the option of supplying each anemometer with a custom default and slope derived from a wind tunnel experiment. The cup anemometer used with the S-343 turbine control system for low wind velocity motoring and braking as well as cut-out braking used the NRG default slope and offset of 0.765 and 0.35. This cup was not available for post-test calibration, as it was still installed in the field operating in the wind turbine control system. This was not deemed an issue in the performance analysis of the turbine as the anemometer had a limited purpose in the operation of the turbine.

Each cup anemometer was positioned in the center of the wind tunnel and the wind tunnel was run at a constant velocity while data was recorded and compared to concurrent measurements from the pitot tube. The experiment was repeated at several different wind velocities, from 4 to 16 m/s and the results are summarized in Figure D-1. For all instruments, a linear best fit curve with intercept was used to reproduce the linear calibration equations. *r*-squared values were also calculated for the linear fit of each anemometer.

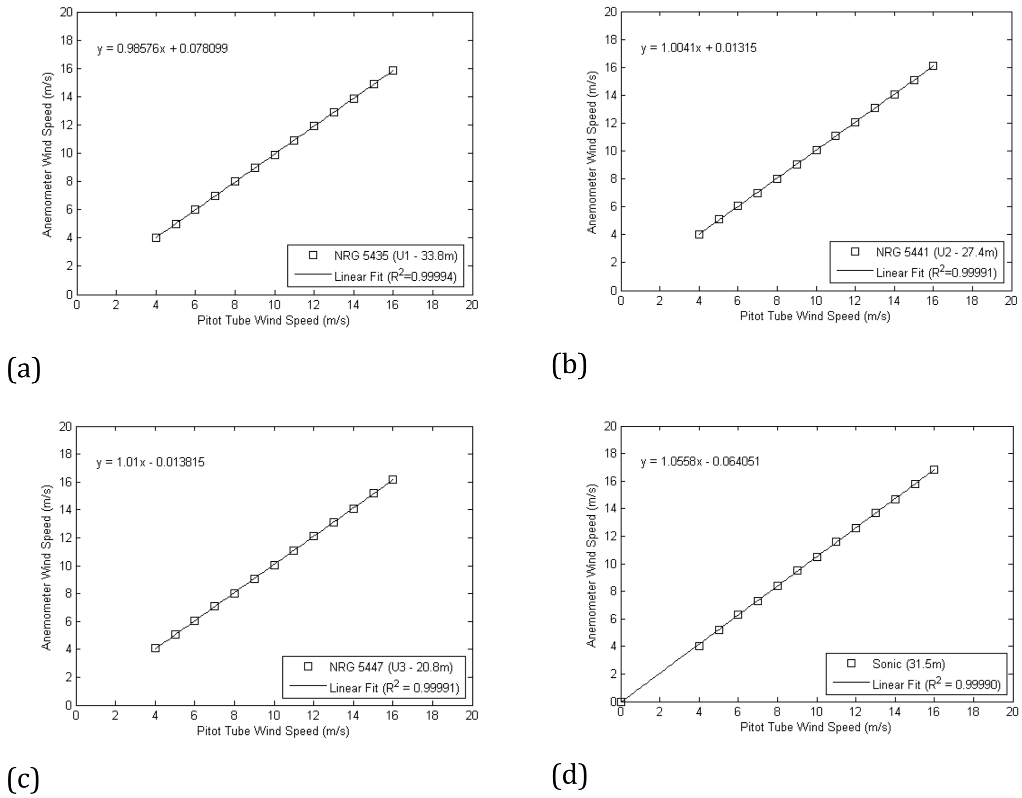

Figure D-1: Anemometer wind velocities plotted against reference pitot tube wind velocities during wind tunnel verification of calibration curves, 4-6 July 2011

From Figure D-1, it is clear that the NRG cup anemometers were consistent with the pitot tube wind velocities and with each other. 61400-12-1 Annex F deals with cup anemometer calibration procedure and states that acceptable value for correlation coefficient is over 0.99995. Until this value can be achieved, calibration should be repeated and if not possible, either the wind tunnel facility is inadequate or the anemometer is excessively non-linear. The NRG 40C is a high quality cup anemometer but not of Class 1A rating that 61400-12-1 recommends. Considering the different factors going into the results, it was concluded that correlation coefficient determined for each instrument was sufficient.

Regression lines for the anemometers have been left as determined experimentally. This is because standard cup anemometers calibration values are allowed offsets to account for a slight non-linearity in anemometer response at low wind velocities, meaning it is not appropriate to force each line through the origin. For the sonic anemometer, this is not an issue and the reading obtained from the instrument at the start of calibration was used at the origin.

As seen in Figure D-1 (d), the sonic anemometer did not perform well in reference to the pitot wind velocity at which the three cup anemometers performed very well. The sonic was not factory calibrated in a wind tunnel and the manufacturer supplied data sheet showed that the instrument was only tested for azimuth accuracy at one wind tunnel velocity. This justified a calibration correction correcting the default offset and slope provided by the manufacturer by a slope of 1.05 derived from the calibration in order to achieve consistency between the instruments. This conclusion was taken into consideration in further experiments utilizing the sonic anemometer. The results of this regression analysis after correction are shown in Figure D-2.

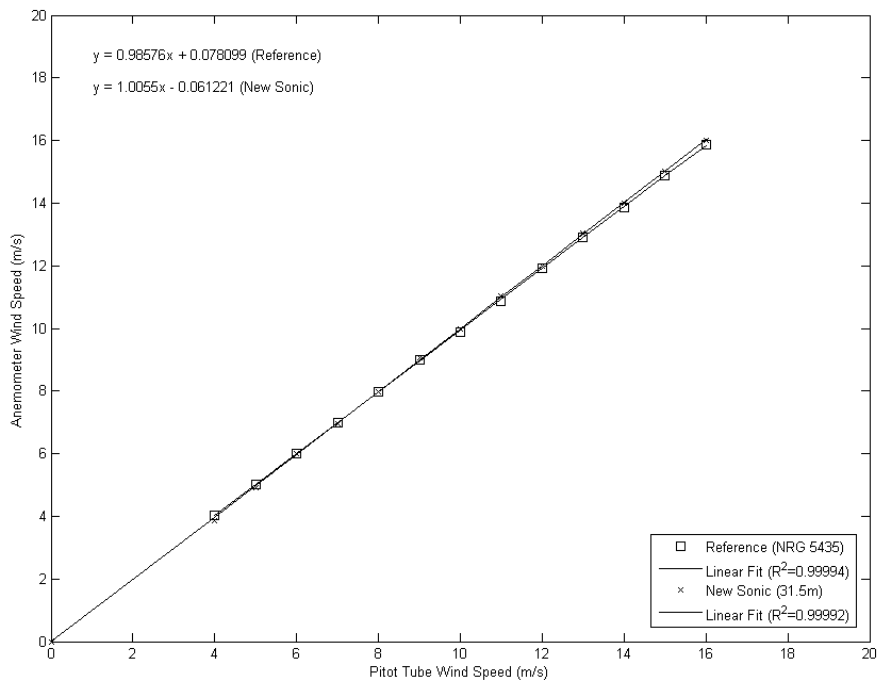

Figure D-2: Results of linear regression to sonic anemometer measurements obtained in wind tunnel with correction factor applied

Appendix E: Power Transducer Calibration

Power measurements for the power transducer were verified against a power source in the University of Alberta Electrical Engineering Power Systems lab. As with the cup anemometers, the purpose of power transducer calibration was not to recalibrate the instrument but to confirm the manufacturer calibration curve. The power transducer was factory calibrated using calibrated instruments traceable to N.I.S.T. (National Institute of Standards and Technology). Calibration sheets from this calibration process were available from the manufacturer at time of purchase but a miscommunication led to the sheets not being purchased. In order to confirm the accuracy of power measurements under 61400-12-1, it was decided that it was necessary to confirm the calibration.

Calibration was performed using an adjustable single-phase voltage source and a resistor bank of known resistance. Voltage from the continuously variable voltage auto transformer and current across the resistor load bank was monitored simultaneously using two digital multimeters. This method is called the two-meter wattmeter method and was utilized to calculate power values across the range of the transducer and compared to measured values from the power transducer. Ideally, the transducer would be energized using a precision instrument calibrator or a single-phase wattmeter standard. As the purpose of the exercise was only to confirm the calibration, this setup was considered adequate. As recommended by the manufacturer, ampere turns through the current transducer were used to simulate the current outputs necessary to create power values across the majority of the transducer range at which the power measurement device was originally calibrated. This process is summarized in Equation (E.1). Results of the process are shown below in Figure E-1.

$$P_{calculated} = 2n_{amp}IV \tag{E.1}$$

where $P_{calculated}$ is the power calculated from current and voltage measurements, I is the measured power, V is the measured voltage, and n_{amp} is the number of ampere turns through the current transformer window. The factor of 2 is used as the supplied current was passed through both current transducer windows.

Measured power values were slightly lower than the calculated supply power in all readings but the lowest. Across the transducer range, measured power values were below the calculated source power values by an average of 1.8%, which is slightly outside the instrument's full scale accuracy of 0.5%. This inaccuracy could be propagated from a number of places: resistor load bank heating, digital multimeter accuracy, data logger accuracy. Considering these areas in which slight inaccuracies could be generated and subsequently multiplied through several levels of calculations, it was concluded that the power measurement device was performing sufficiently post-experiment and the use of a factory calibrated device was justified.

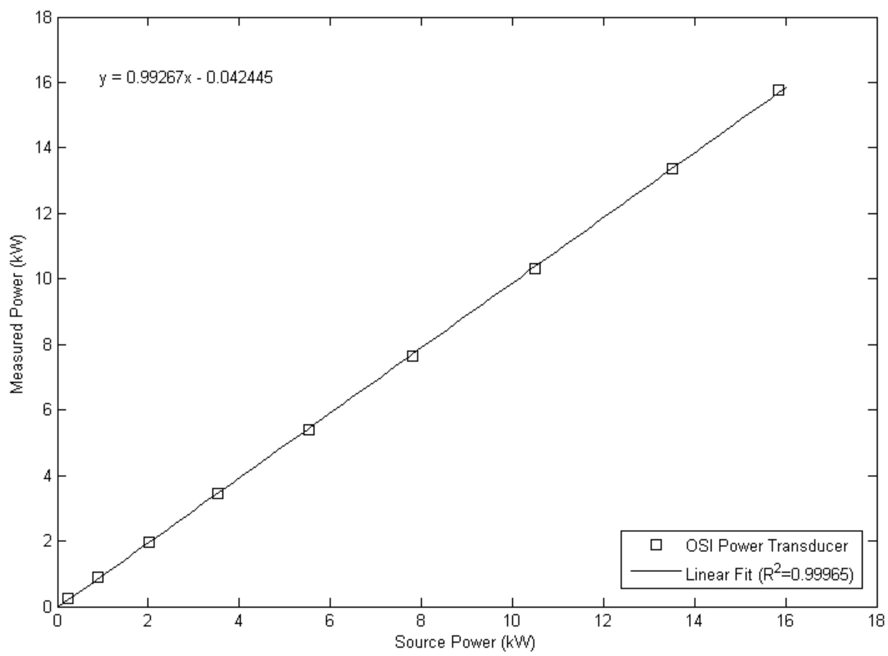

Figure E-1: Power transducer plotted against reference power during verification of power calibration curve, 12 July 2011

Appendix F: Drawings of turbine and instrument arrangement

Arrangement of various instruments on the tower and relevant turbine, tower, and instrument dimensions are documented in this section.

(a)

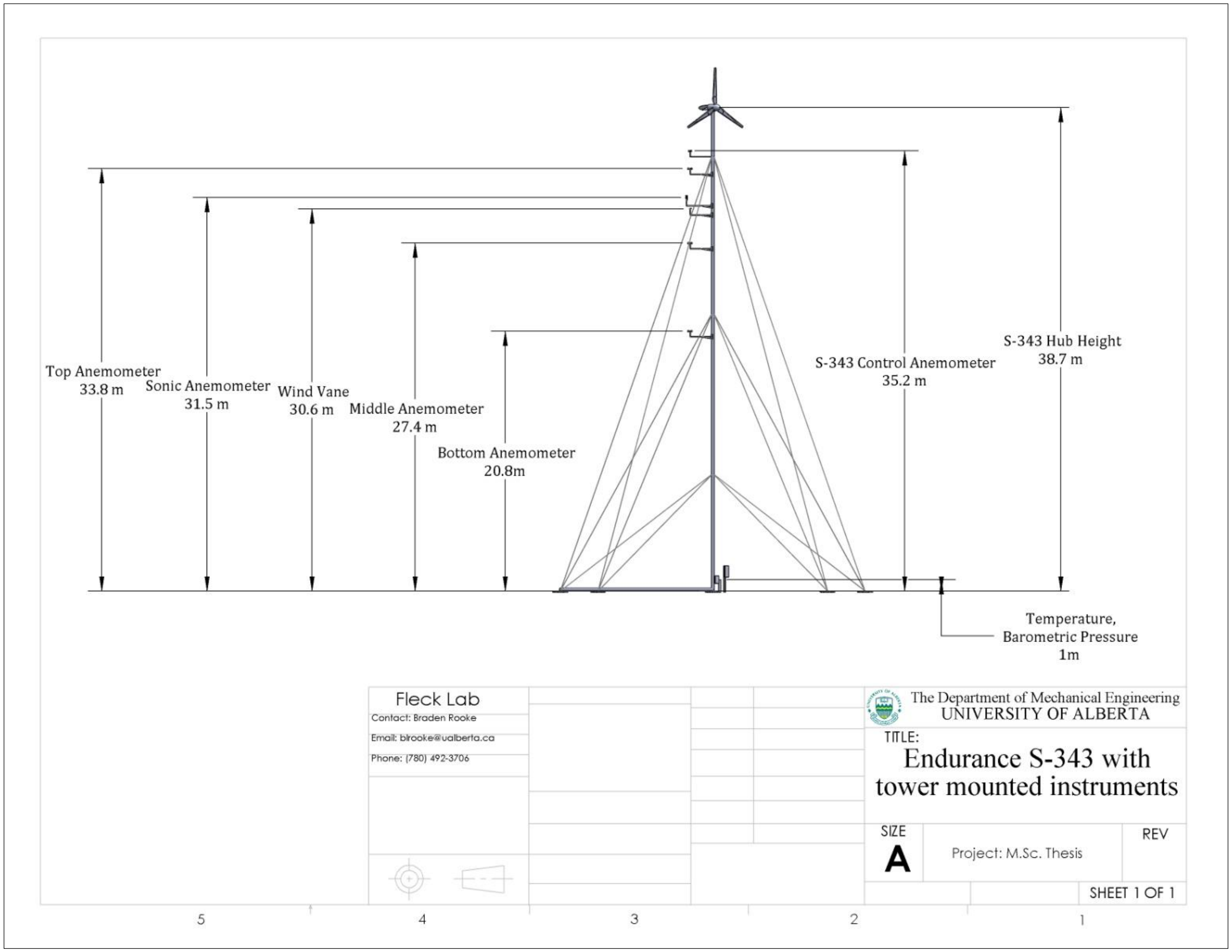
Top Anemometer
33.8 m
Sonic Anemometer
31.5 m
Wind Vane
30.6 m
Middle Anemometer
27.4 m
Bottom Anemometer
20.8m
S-343 Control Anemometer
35.2 m
S-343 Hub Height
38.7 m
Temperature,
Barometric Pressure
1m
Fleck Lab
Contact: Braden Rooke
Email: brooke@ualberta.ca
Phone: (780) 492-3706
The Department of Mechanical Engineering
UNIVERSITY OF ALBERTA
TITLE:
Endurance S-343 with
tower mounted instruments
SIZE
A
Project: M.Sc. Thesis
REV
SHEET 1 OF 1
5
4
3
2
1

(b)

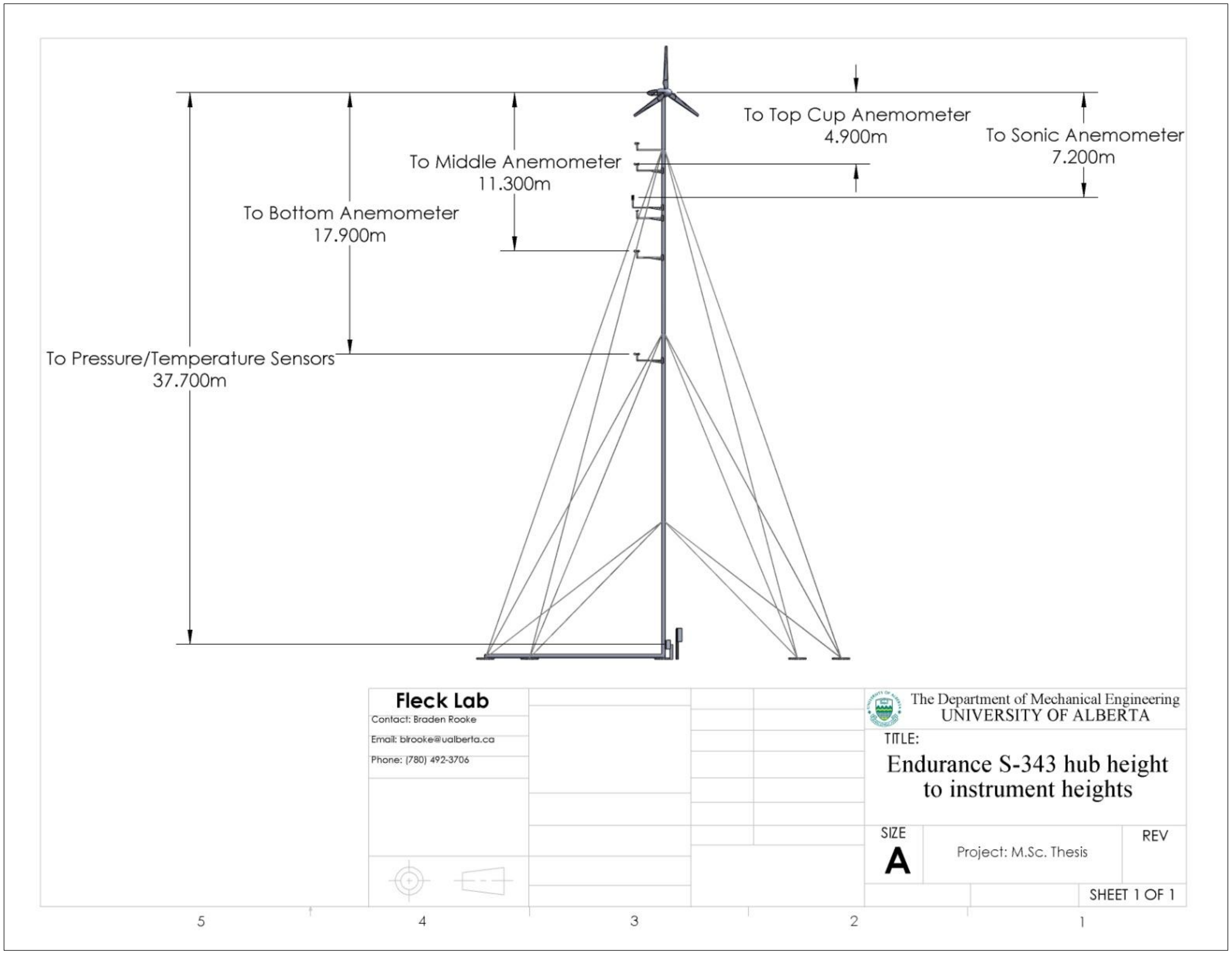

To Top Cup Anemometer
4.900m
To Sonic Anemometer
7.200m
To Middle Anemometer
11.300m
To Bottom Anemometer
17.900m
To Pressure/Temperature Sensors
37.700m
Fleck Lab
Contact: Braden Rooke
Email: blrooke@ualberta.ca
Phone: (780) 492-3706
The Department of Mechanical Engineering
UNIVERSITY OF ALBERTA
TITLE:
Endurance S-343 hub height
to instrument heights
SIZE
A
Project: M.Sc. Thesis
REV
SHEET 1 OF 1
5
4
3
2
1

(c)

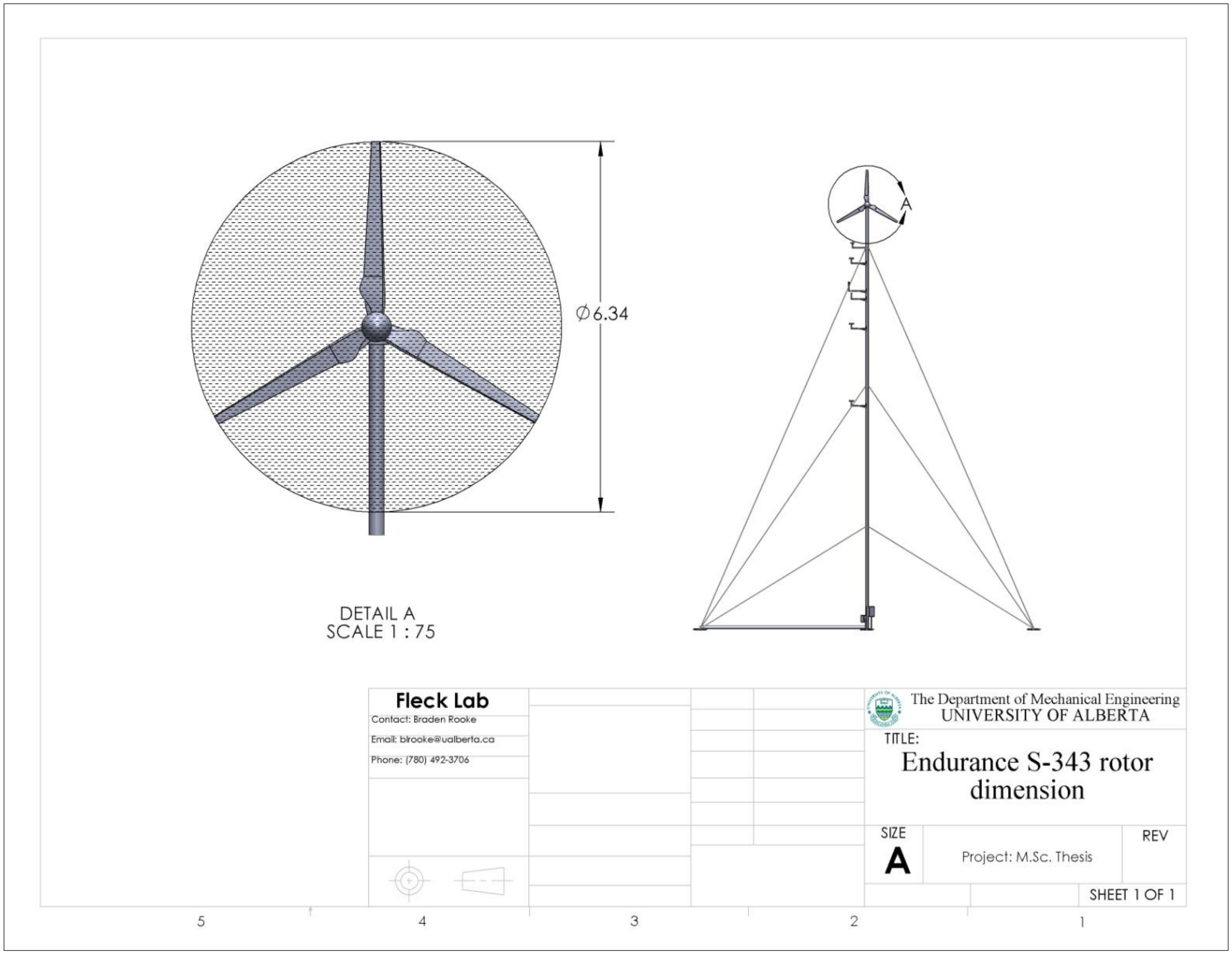

∅6.34
A
DETAIL A
SCALE 1 : 75
Fleck Lab
Contact: Braden Rooke
Email: brooke@ualberta.ca
Phone: (780) 492-3706
The Department of Mechanical Engineering
UNIVERSITY OF ALBERTA
TITLE:
Endurance S-343 rotor dimension
SIZE
A
Project: M.Sc. Thesis
REV
SHEET 1 OF 1
5
4
3
2
1

(d)

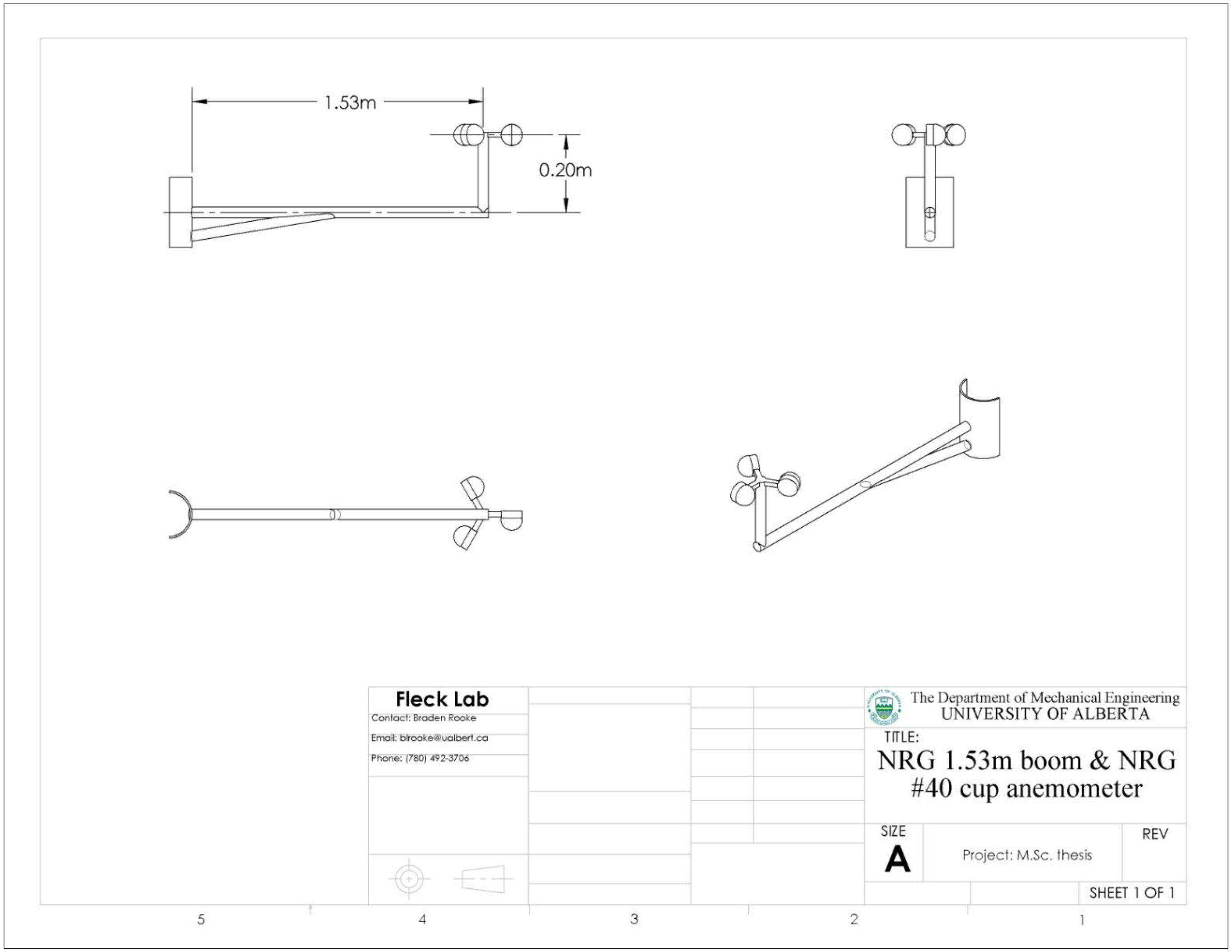
1.53m
0.20m
Fleck Lab
Contact: Braden Rooke
Email: brooke@ualbert.ca
Phone: (780) 492-3706
The Department of Mechanical Engineering
UNIVERSITY OF ALBERTA
TITLE:
NRG 1.53m boom & NRG #40 cup anemometer
SIZE
A
Project: M.Sc. thesis
REV
SHEET 1 OF 1
5
4
3
2
1

(e)

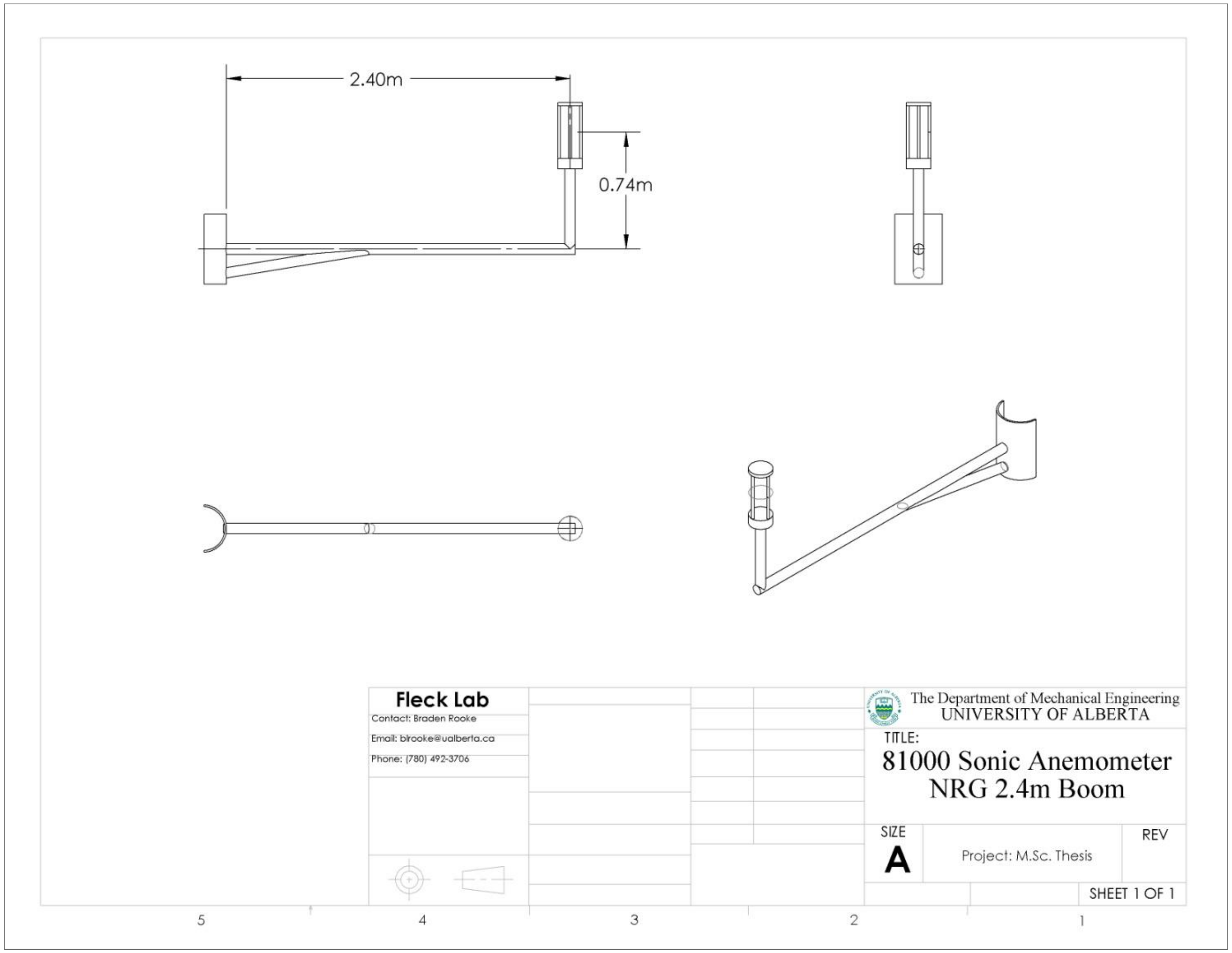

Figure F-1: (a) Instrument heights (b) Hub height to instrument distances (c) Rotor detail (d) Cup anemometer and boom (e) Sonic Anemometer and boom

Appendix G: Wind velocity distributions of datasets

Distributions from raw data

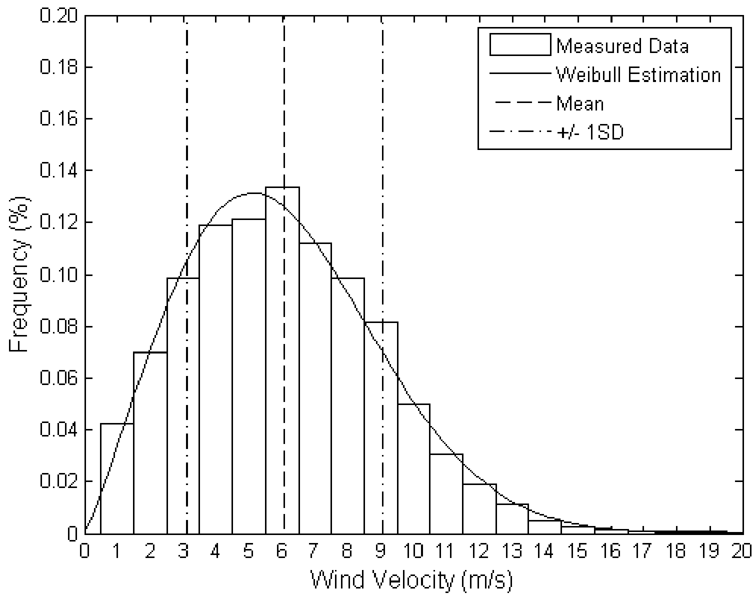

Figure G-1: Wind velocity frequency distribution, Halkirk U_1 (33.8m)

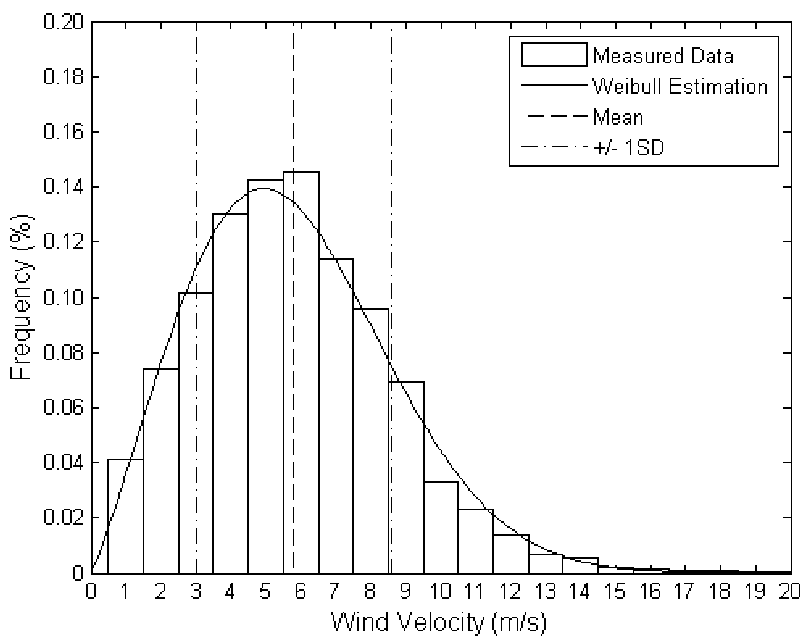

Figure G-2: Wind velocity frequency distribution, Halkirk U_2 (27.4m)

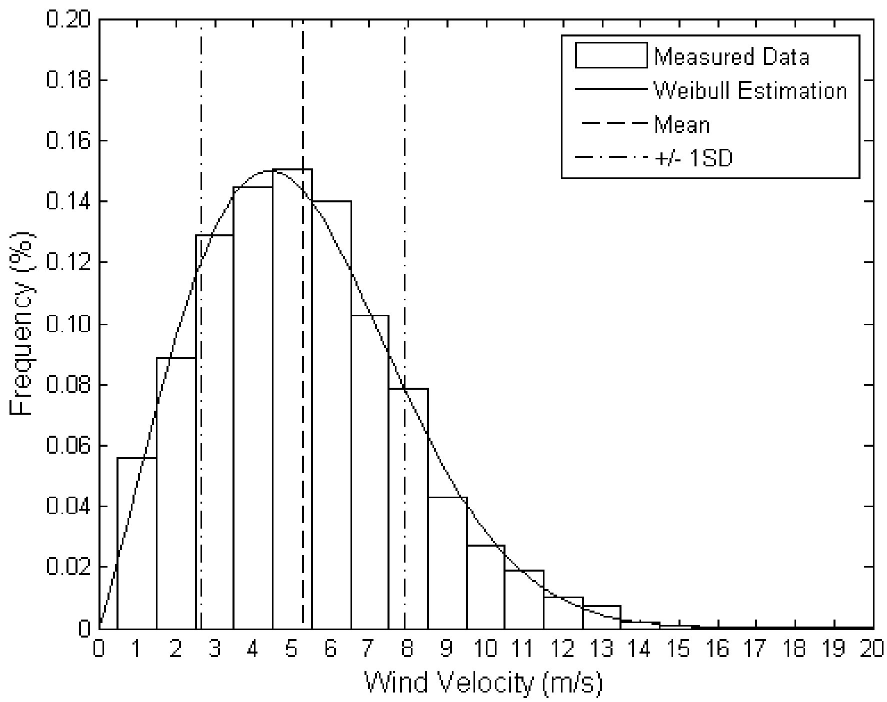

Figure G-3: Wind velocity frequency distribution, Halkirk U_3 (20.8m)

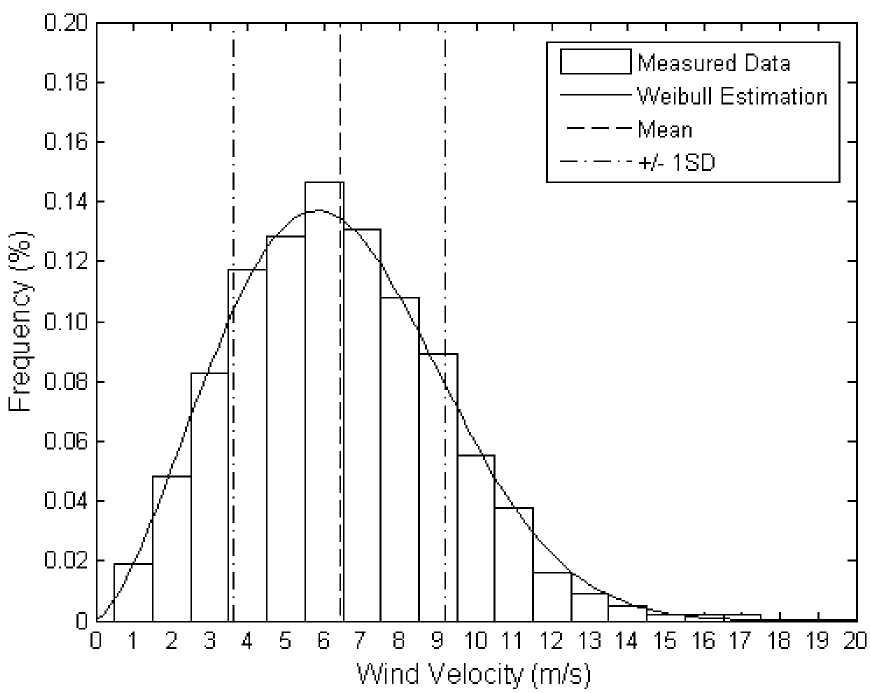

Figure G-4: Wind velocity frequency distribution, Halkirk 2-D sonic (31.5m)

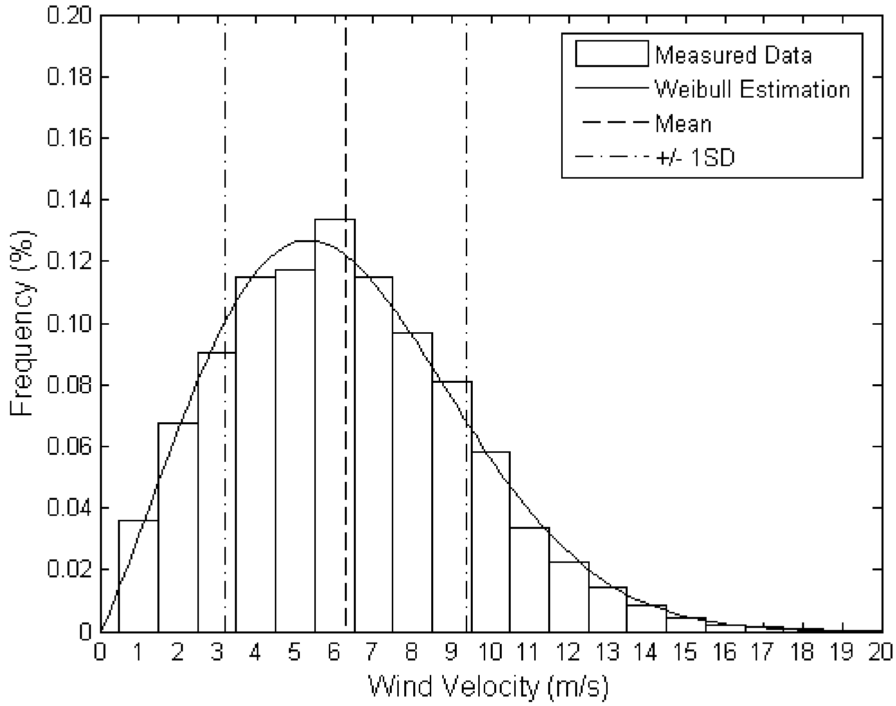

Figure G-5: Wind velocity frequency distribution, Halkirk U_{hub} (38.7m) estimated from U_2 and U_3 values and power law in each time step

Comparative seasonal distributions, Canadian Wind Atlas and Halkirk 30m synthesized

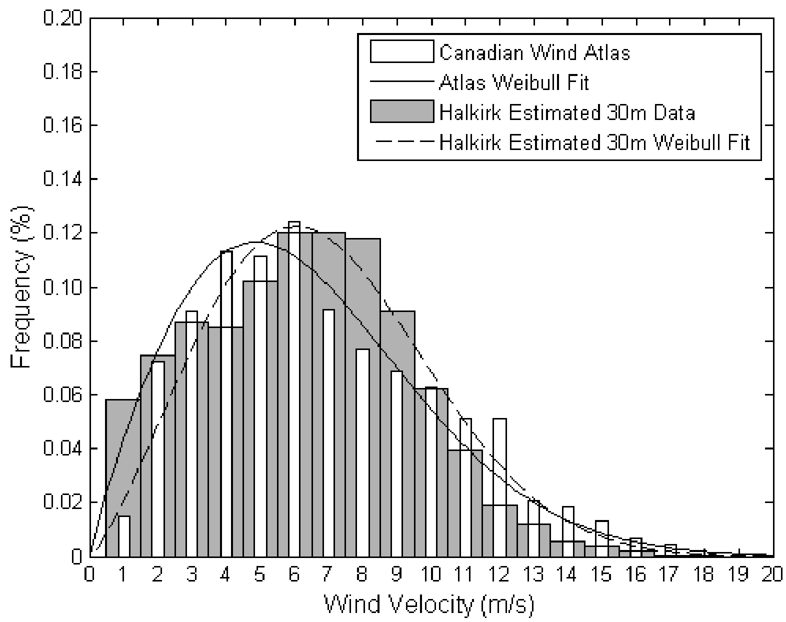

Figure G-6: Frequency distributions, Canada Wind Atlas and Halkirk Synthesized 30m data, winter season (December/January/February)

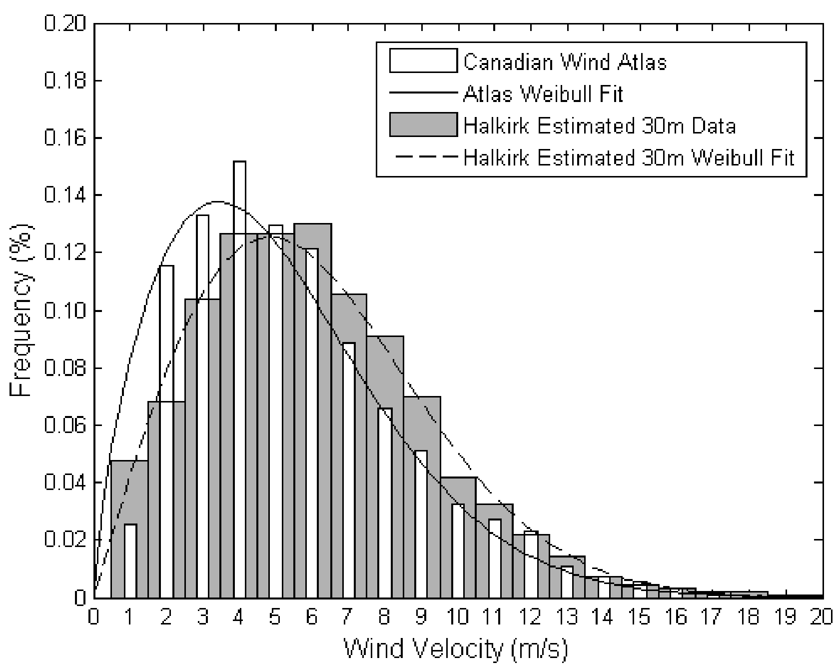

Figure G-7: Frequency distributions, Canada Wind Atlas and Halkirk Synthesized 30m data, spring season (March/April/May)

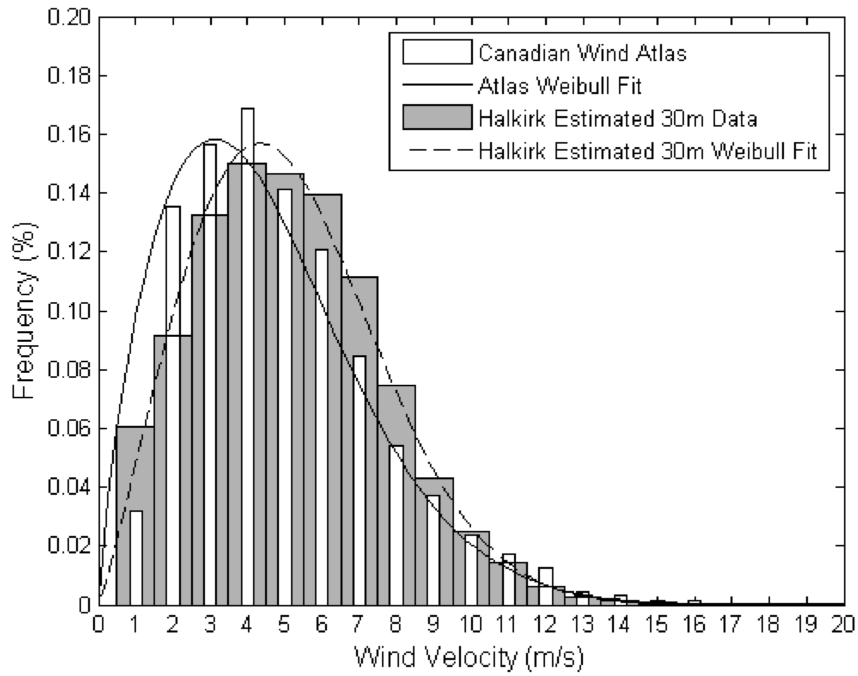

Figure G-8: Frequency distributions, Canada Wind Atlas and Halkirk Synthesized 30m data, summer season (June/July/August)

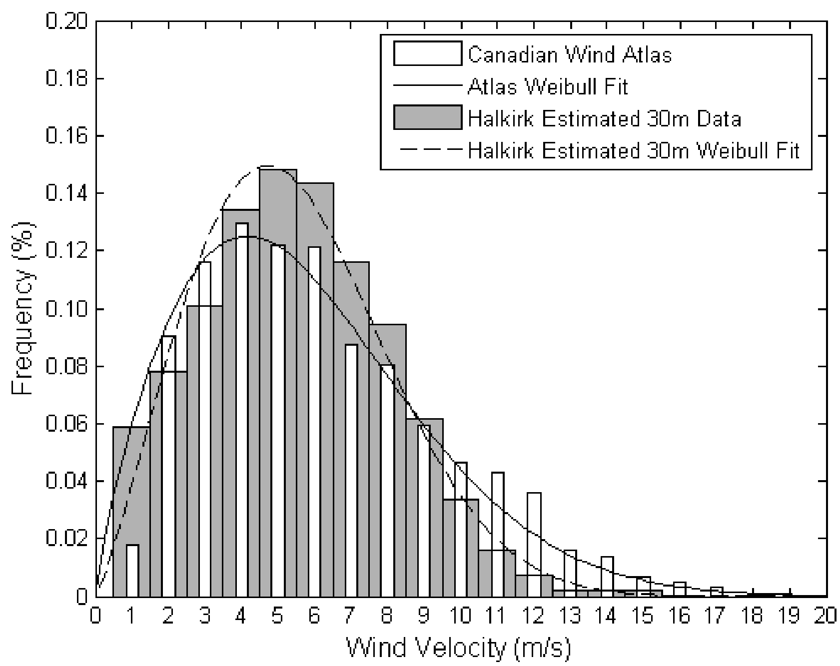

Figure G-9: Frequency distributions, Canada Wind Atlas and Halkirk Synthesized 30m data, fall season (September/October/November)

Appendix H: Measured Power Curve Table

Table H-1: Measured power curve table (standardized to sea level air density, 1.225kg/m^3)

Bin Number	Hub height annual averaged wind velocity (Rayleigh dist.) (m/s)	Power Output (kW)	*Cp*	No. of Data Sets (1min avg,)	Category A Standard uncertainty (kW)	Category B Standard uncertainty (kW)	Combined Standard Uncertainty (kW)
1	3.1	-0.039	-0.067	2037	0.000	0.038	0.038
2	3.5	-0.047	-0.056	2683	0.000	0.038	0.038
3	4	-0.054	-0.043	2898	0.001	0.038	0.038
4	4.5	0.094	0.053	3225	0.003	0.072	0.072
5	5	0.369	0.151	3171	0.003	0.125	0.125
6	5.5	0.653	0.201	2903	0.003	0.135	0.135
7	6	0.939	0.223	2792	0.004	0.143	0.143
8	6.5	1.321	0.246	2540	0.005	0.198	0.198
9	7	1.771	0.264	2087	0.006	0.243	0.243
10	7.5	2.240	0.272	1662	0.007	0.266	0.266
11	8	2.702	0.270	1454	0.008	0.275	0.275
12	8.5	3.163	0.264	1248	0.008	0.287	0.287
13	9	3.583	0.252	1048	0.009	0.274	0.274
14	9.5	3.951	0.236	817	0.011	0.252	0.253
15	10	4.285	0.220	611	0.014	0.240	0.240
16	10.5	4.545	0.201	457	0.017	0.197	0.198
17	11	4.809	0.185	311	0.010	0.208	0.209
18	11.5	5.020	0.169	244	0.008	0.176	0.176
19	12	5.116	0.152	178	0.010	0.099	0.100
20	12.5	5.155	0.135	145	0.012	0.070	0.071
21	13	5.141	0.120	92	0.019	0.063	0.065
22	13.5	5.043	0.105	92	0.017	0.108	0.109
23	14	4.876	0.091	78	0.022	0.166	0.168
24	14.5	4.706	0.079	74	0.023	0.174	0.176
25	15	4.431	0.067	47	0.034	0.279	0.281
26	15.5	4.123	0.057	37	0.033	0.320	0.322
27	16	3.964	0.050	29	0.036	0.176	0.180
28	16.5	3.732	0.043	10	0.069	0.256	0.266
29	17	3.634	0.038	4	0.077	0.120	0.143
30	17.5	3.338	0.032	6	0.059	0.343	0.349
31	18	3.182	0.028	2	0.093	0.189	0.211

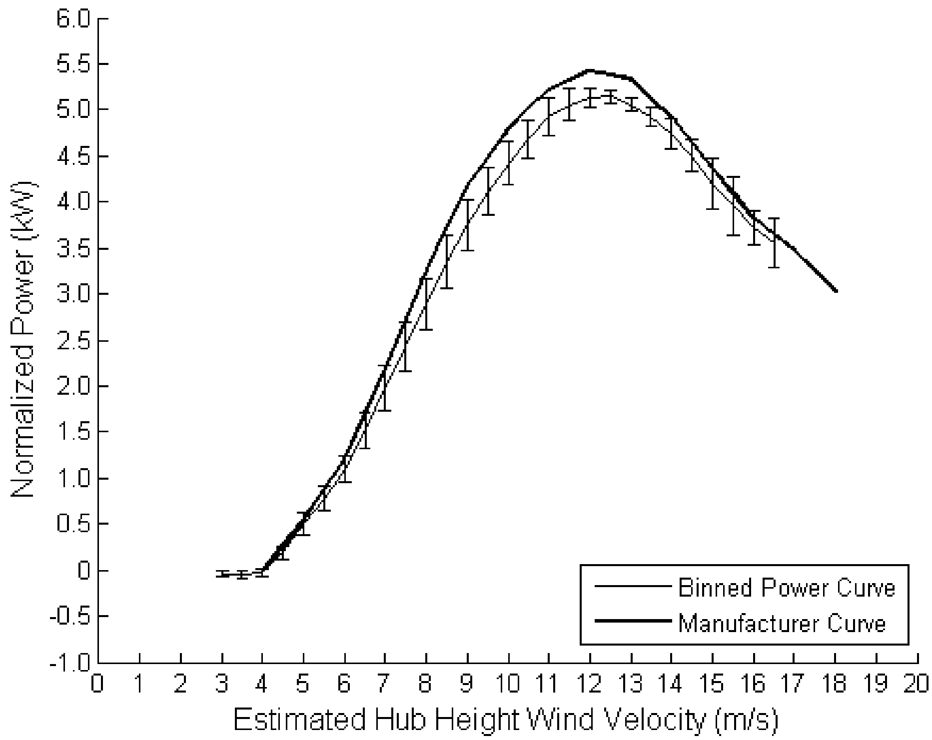

Figure 4-1: Sea level normalized power curve with 68.27% uncertainty bars along with manufacturer power curve. Uncertainty determined from IEC 61400-12-1 recommendations

Appendix I: Power Curves from Using Different Averaging Schemes

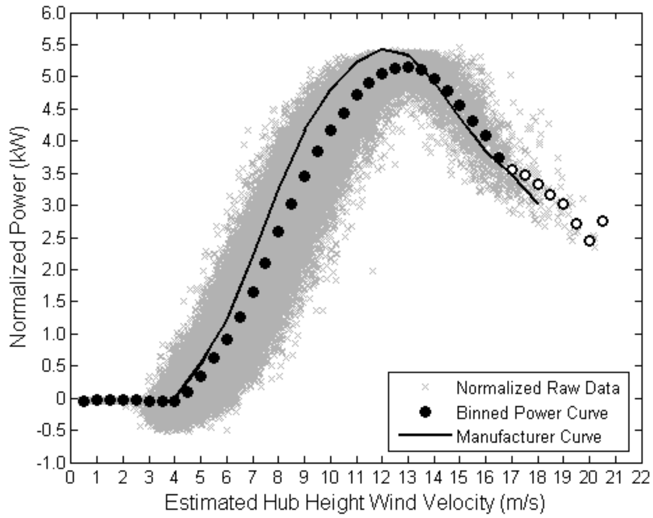

Figure I-1: Ten-second averaged test sector power curve, raw and binned data at sea level density, showing manufacturer power data. Open circles represent bins with less than 10 minutes of data

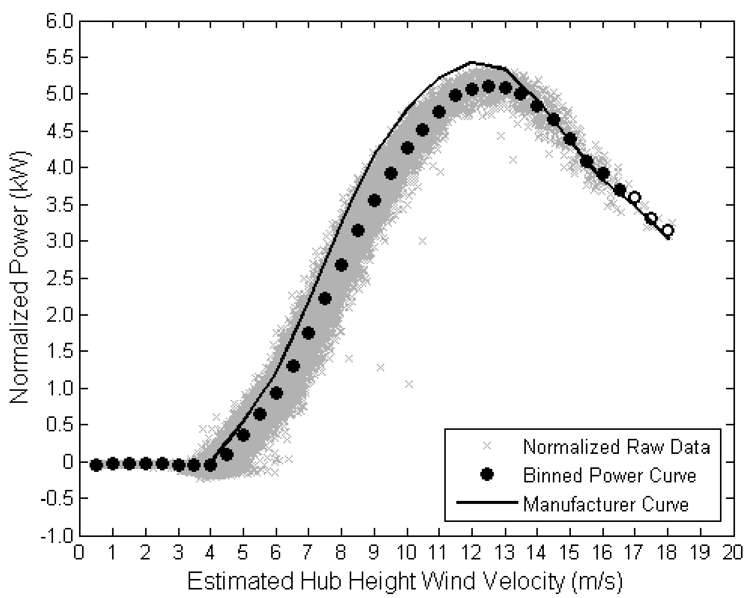

Figure I-2: One-minute averaged test sector power curve, raw and binned data at sea level density, showing manufacturer power data. Open circles represent bins with insufficient data.

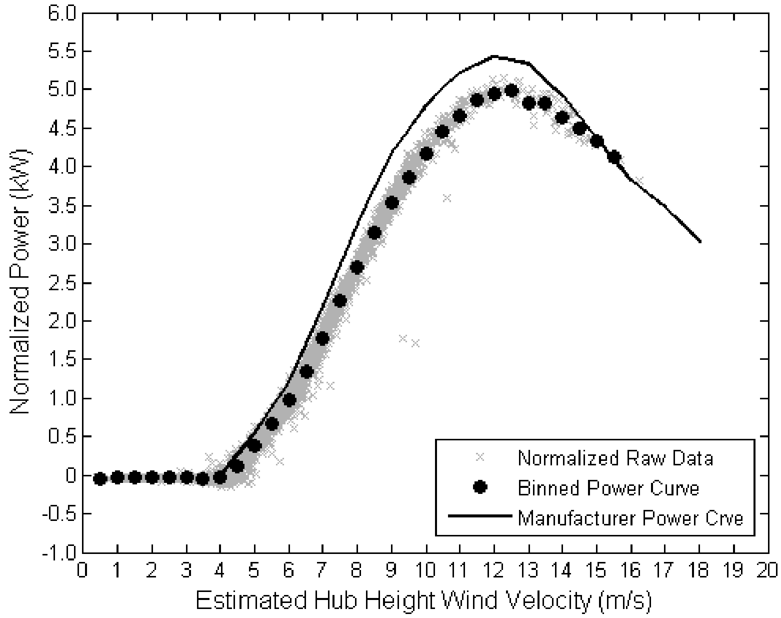

Figure I-3: Ten-minute averaged test sector power curve, raw and binned data at sea level density, showing manufacturer power data. Open circles represent bins with insufficient data.

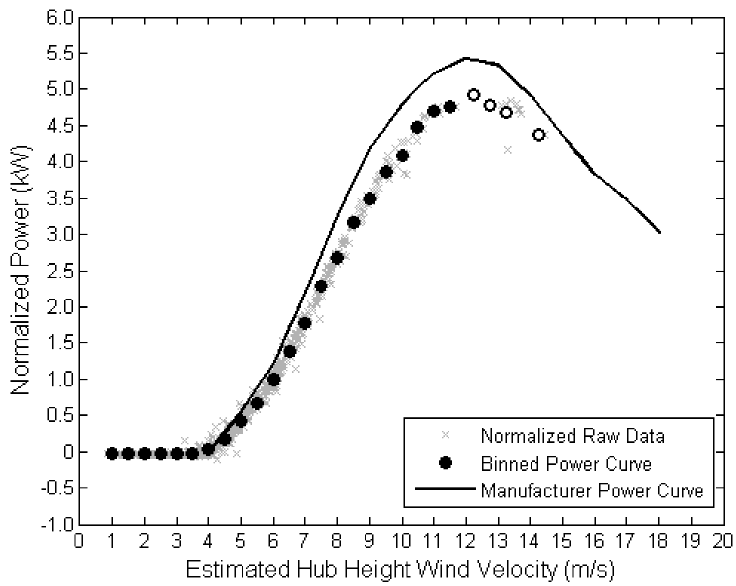

Figure I-4: Hourly averaged test sector power curve, raw and binned data at sea level density, showing manufacturer power data. Open circles represent bins with insufficient data.

Appendix J: Pictures of the Turbine Site with Direction and Disturbance Annotations

Figure J-1: Winter View to the South

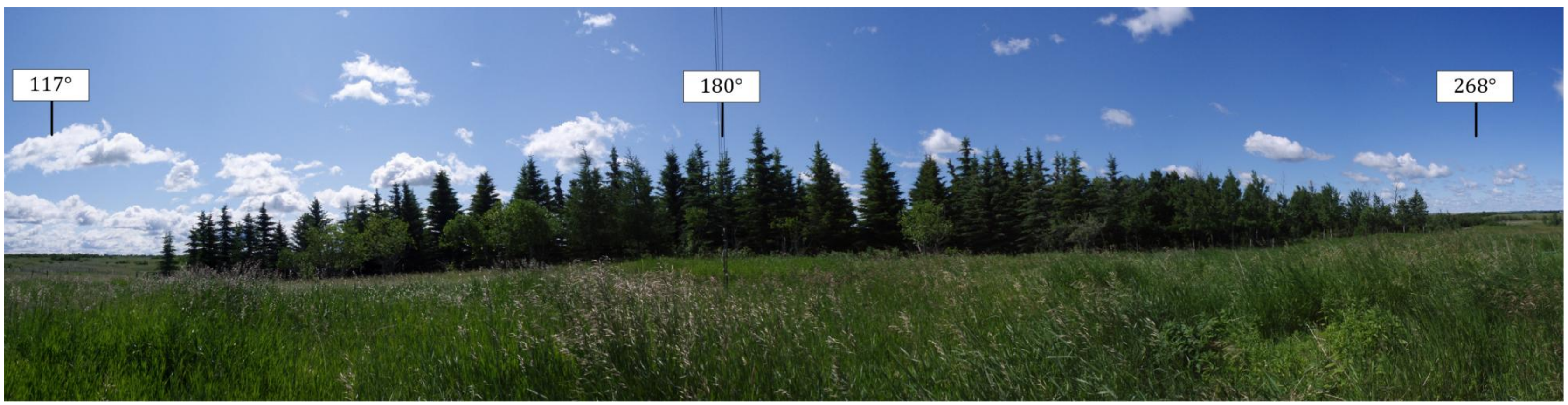

Figure J-2: Summer View to the South

Figure J-3: Winter View to the West

Figure J-4: : Summer View to the West

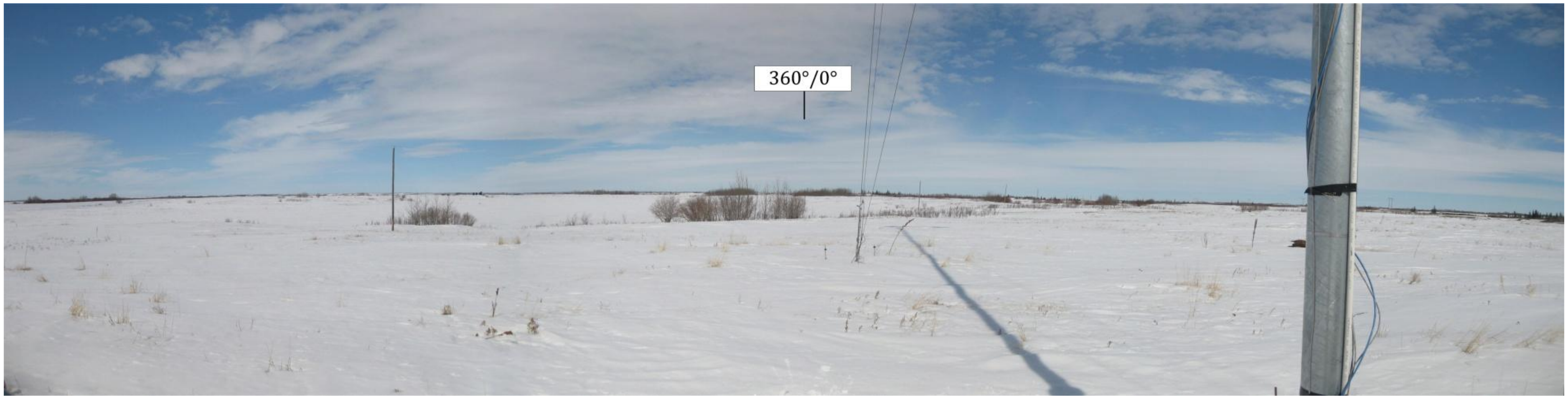

Figure J-5: Winter View to the North

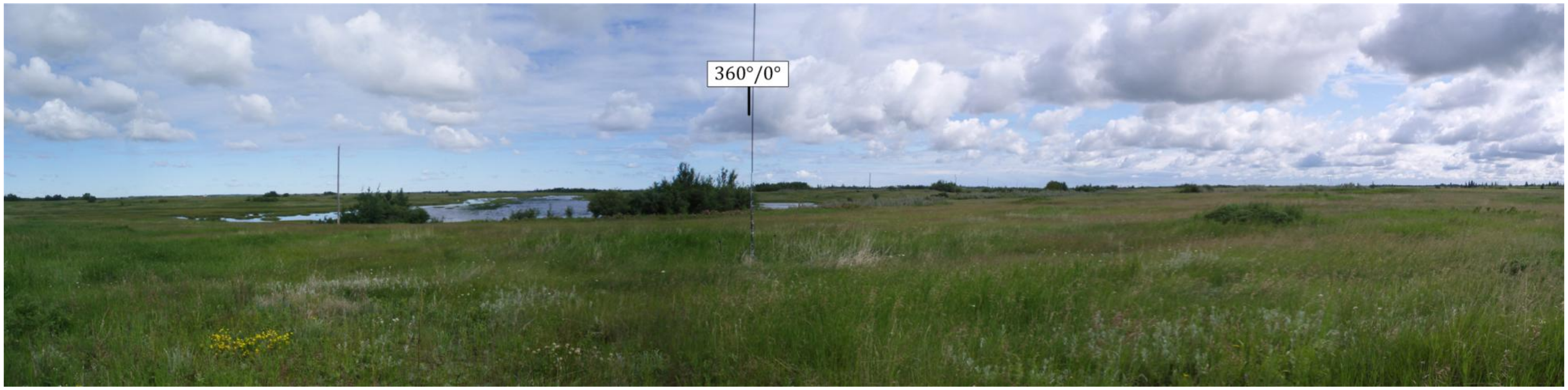

Figure J-6: Summer View to the North

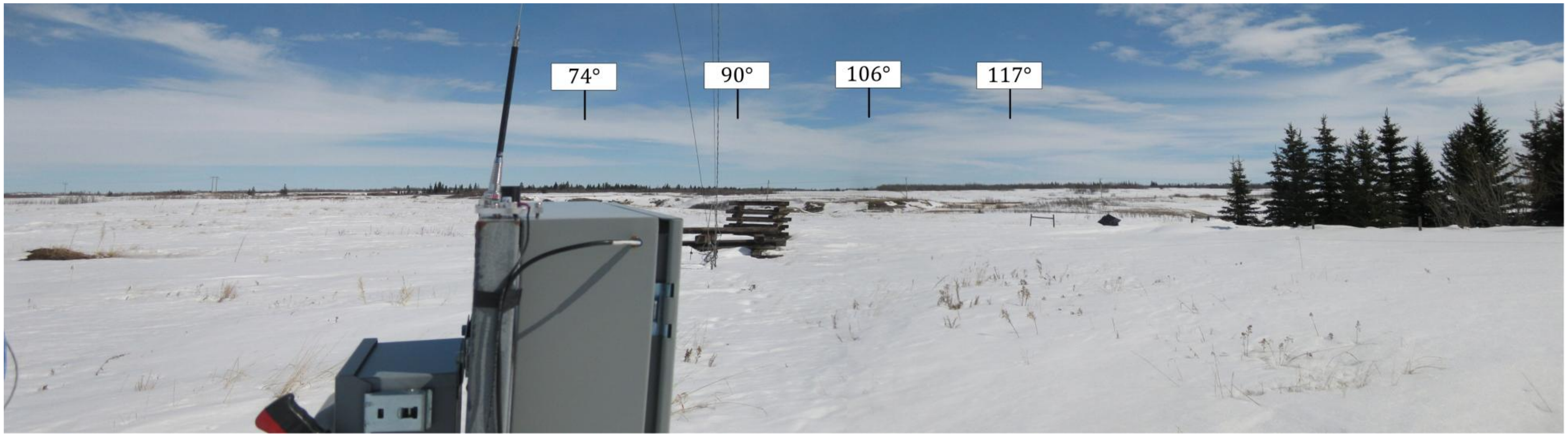

Figure J-7: Winter View to the East

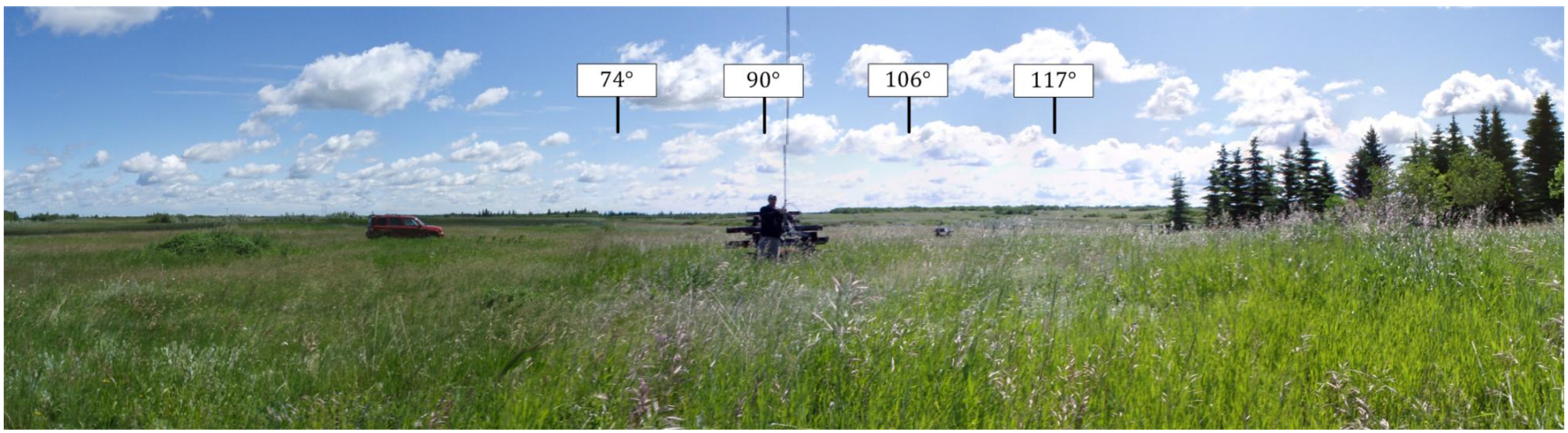

Figure J-8: Summer View to the East